Master's thesis

NTNU
Norwegian University of Science and Technology
Department of Energy and Process Engineering

Muhammad Zahid Saeed

Energy efficient and climate friendly cooling, freezing and heating onboard fishing vessels

Master's thesis in Sustainable Energy

Supervisor: Armin Hafner Co-supervisor: Kristina Norne Widell

June 2020

NTNU
Kunnskap for en bedre verden

NTNU

Norwegian University of Science and Technology

Energy efficient and climate friendly cooling, freezing and heating onboard fishing vessels

Muhammad Zahid Saeed

Master's thesis in Sustainable Energy
Submission date: June 2020
Supervisor: Armin Hafner, EPT
Co-supervisor: Kristina Norne Widell, SINTEF Ocean

Norwegian University of Science and Technology
Department of Energy and Process Engineering

Preface

This report summarizes my master's thesis work at the Norwegian University of Science and Technology, Department of Energy and Process Engineering. The work was in collaboration with SINTEF Ocean. The topic of the master thesis is formulated on the practical challenges of environment and energy efficiency in fishing vessels. An analysis of different energy systems of the fishing vessel is performed to enhance their performance.

I want to express my gratitude to Professor Dr. Armin Hafner and Dr. Kristina Norne Widell for their guidance, encouragement, and supervision. I would also like to thanks Eirik Starheim Svendsen for his great assistance in simulation work and thanks to Tom Ståle Nordtvedt and Yves Ladam for technical help.

Summary

Liquefied natural gas (LNG) fueled vessels are increasing in the fishing industry due to its reduced environmental footprint as compared to vessels applying heavy hydrocarbon fuels. Cryogenic tanks are used to store LNG on ships, and the LNG vaporization can be done with different technology before used for engine fuel. Chilling and freezing onboard are energy consuming process but are necessary to ensure high-quality products. LNG cold from vaporization can be utilized to boost the refrigeration capacity. The natural refrigerant CO_2 is gaining an attraction for fishing vessels due to its compact units, non-toxic behaviour, favourable thermophysical properties and negligible global warming potential (GWP). Cold thermal storage is a smart feature that assists the refrigeration system at peak loads. Heating is also necessary onboard, for hot tap water, space heating, and processing of fish rest raw material (RRM) for fish oil. Currently, the onboard refrigeration system challenges are insufficient capacity at peak loads and performance issues at part load operations.

The aim of this work is to develop simulation models on Dymola/Modelica (software) for optimization of an energy system of fishing vessels. The two independent cases were designed for chilling and freezing vessel. The chilling vessel was optimized with LNG sub-cooler, heat recovery (for space heating), and integration of water/ice thermal storage in refrigeration system. Heat was also recovered from flue gases of engine for hot tap water production. The energy performance of freezing vessel was improved by adding LNG sub-cooler, heat recovery for RRM processing, and integration of CO_2 thermal storage in refrigeration system.

Results for the chilling vessel show that an average coefficient of performance (COP) of the refrigeration system is increased by 15.2 % with LNG sub-cooler compared to simple unit. The mean heat recovery from desuperheater and flue gases is 38 kWh and 114 kWh, respectively. A water/ice thermal storage of size 0.76 m^3 reduced the peak capacity by 30 kW for the designed chilling system.

The results of freezing vessel represent an average increment of COP by 6.4 % with LNG sub-cooler compared with normal freezing system. The mean heating demand for RRM processing is 261 kWh, which is in favourable match with the heat recovery of 298 kWh from freezing system. A 450 liters of fish oil can be produced from an interrelated RRM amount of 150 minutes freezing cycle. A CO_2 thermal storage of size 0.3 m^3 (75 liters) including an internal heat transfer area is an ideal solution to cover the peak loads of designed system. An average 50 kWh stored thermal energy increased the production capacity of equivalent 56 minutes in one day.

Sammendrag

Andelen sjøfartøy som drives av flytende naturgass (LNG) i fiskeindustrien øker på grunn av deres reduserte miljøavtrykk sammenlignet med fartøy som utnytter tunge hydrokarbonbrensler. På skip oppbevares LNG i kryogene tanker, og kan fordampes på flere måter, tidligere brukt for brensel. Kjøling og frysing om bord i båtene er energikrevende prosesser, men er også nødvendige for å sørge for at fiskeproduktet holder høy kvalitet. Kald, fordampet LNG kan brukes til å øke fartøyets kjølekapasitet. Flere fiskeriselskaper får øynene opp for det naturlige kjølemediet CO_2 på grunn av dets kompakte komponenter, ikke-toksisitet, gode termofysiske egenskaper og neglisjerbare globale oppvarmingspotensial (GWP). Kald termisk energilagring er nyttig som støtte når et fartøys kjølesystem fungerer ved topplast. Ombord er det også nødvendig med oppvarming for translatvarmtvann, ovner og for prosessering av fiskerester (RRM) til fiskeolje. De foreløpige utfordringene for båtenes kjølesystem er utilstrekkelig kapasitet ved topplast og ytelsesproblemer ved delbelasting.

Arbeidets mål er å utvikle simulerte modeller i programvarene Dymola/Modelica for å optimalisere energisystemene på fiskefartøy. Det ble utledet to uavhengige design; et for kjøling og et for frysing. Kjølefartøyet ble optimalisert med LNG-underkjøler, varmegjenvinning for oppvarming og innføring av vann/is-basert termisk energilagring i kjølesystemet. Varme fra eksosgasser gjenvinnes for å varme springvann. Frysefartøyets energiytelse ble forbedret ved å tilføre LNG-underkjøler, varmegjenvinning for prosessering av RRM og integrering av CO_2 basert termisk energilagring i kjølesystemet.

Resultatene fra kjølefartøyet viser at den gjennomsnittlige ytelseskoeffisienten (COP) til kjølesystemet med LNG-underkjøling økes med 15.2% sammenlignet med ordinære kjølesystemer. Den gjennomsnittlige varmegjenvinningen fra desuperheateren og eksosgasser er henholdsvis 38 kWh og 114 kWh. Innføring av vann/is-basert termisk energilagring med et volum på 0.76 m^3 reduserte det designede kjølesystemets nødvendige toppkapasitet med 30 kW.

Resultatene fra frysefartøyet representerer en gjennomsnittlig øking av COP på 6.4 % med LNG-underkjøler sammenlignet med ordinære frysesystemer. Den gjennomsnittlige nødvendige varmeenergien for RRM-prosessering er 261 kWh, noe som passer godt med frysesystemets varmegjenvinning på 298 kWh. En frysesyklus på 150 minutter gjenvinner nok varmeenergi til å prosessere 450 liter fiskeolje. CO_2 basert termisk energilagring med et volum på 0.3 m^3 (75 liters) er passende for å støtte frysesystemet ved topplast. I gjennomsnitt vil 50 kWh med lagret energi øke systemets produksjonskapasitet med 56 minutter per dag.

Table of Contents

List of Tables

List of Figures

Abbreviations and Symbols

HCFC	Hydrochlorofluorocarbon
HFC	Hydrofluorocarbon
LNG	Liquefied natural gas
CNG	Compressed natural gas
GWP	Global warming potential
RSW	Refrigerated sea water
RRM	Rest raw material
HT	High temperature
LT	Low temperature
HP	High pressure
LP	Low pressure
HX	Heat exchanger
Ph	Pressure enthalpy
Th	Temperature enthalpy
Ts	Temperature entropy
COP	Coefficient of performance
COP_{COM}	COP combine
COP_{Cac}	COP Carnot cooling
COP_{Cah}	COP Carnot heating
HTC	High temperature circuit
LTC	Low temperature circuit
REF	Refrigeration
VHC	Volumetric heating capacity
VRC	Volumetric cooling capacity
HX	Heat exchanger
PCM	Phase change material
TES	Thermal energy storage
C1	Chilling refrigeration system
C2	Chilling system with LNG sub-cooler
C3	Chilling system with LNG desuperheater
C4	Chilling system with desuperheater and LNG sub-cooler
S1	Freezing refrigeration system
S2	Freezing system with LNG sub-cooler
S3	TES charging analysis and compressor
S4	TES charging with ejector
S5	TES discharging
η_{is}	Isentropic efficiency
Q_o	Evaporator load
Q_c	Condenser load

Chapter 1

Introduction

1.1 Introduction

Fishing vessels are the most significant energy consumer and responsible for emissions from the seafood product value chain (Jafarzadeh et al., 2017). In 2015, the fishing sector was liable for 1.9% of total Norway's emissions (Norwegian ministry of climate and environment, 2018). The physical conditions on the fishing vessels are severe, and refrigerant leakage is quite often. The refrigerants leak from global shipping (refrigerated containers excluded) is estimated at 8,400 tons, which corresponds to around 15 million tons CO_2 equivalent emissions. The refrigerant emissions are 2% of the total GHG emissions from the ships (Hafner et al., 2019). It is not safe to have refrigerants, which are harmful to crew members and the environment as well. Due to the rapid phase-out of HCFC/HFC, natural working fluids like Ammonia and CO_2 are one of the solutions to the future.

The European commission transport white paper (2011) set a target of 60% lower carbon emissions by 2050 compared to 1990 and 70% compared to 2008 with the aim towards zero energy emissions (Sihvonen, 2018). Norway's ambition is to become low emission society by 2050. Several steps are considered in Norway to achieve the target. One effort is increased CO_2 tax (currently 508 NOK/ton) to incentivize businesses towards more sustainable solutions (Norwegian ministry of climate and environment, 2018).

Transportation industry will require a change from heavy hydrocarbon fuels to electric batteries, hydrogen or gas. LNG or gas use in the EU is encouraged by regulations, tax breaks, and subsidies (Sihvonen, 2018). LNG is gaining more attraction in the marine industry due to its high energy density, availability, and fewer emissions. LNG has a higher hydrogen-to-carbon ratio than diesel. LNG-fueled ships emit 90% less NO_x, 25% less CO_2, and almost no SO_x as compared to heavy hydrocarbon fuels (LR, 2015).

The thermal energy system of fishing vessel constitutes of chilling and freezing system for fish, onboard space heating and hot tap water for crew members, and heating for

processing of rest raw material. The short journey fishing vessels store fish in refrigerated seawater (RSW) systems. The long journey vessels who spend weeks in the sea, freeze the fish to have a long shelf life. These vessels often have onboard processing units in which they produce fillets from the whole fish. The fish is processed and frozen after the catch and then stored in low-temperature cargo storage. In this way, the vessels remains at sea until the cargo storage is full. The energy system demands are different for each type of vessel due to its unique requirements making the system complex to generalize (Valentina, 2012). Apart from the propulsion, refrigeration systems are the primary energy consumers on the fishing vessels. The fishing sector is sensitive to the energy price. To make the business more sustainable, highly efficient systems and emissions cut are necessary.

1.2 Objectives

The following tasks are to be considered in this work.

- Review of relevant literature, e.g. maritime refrigeration systems, thermal storage, plate freezers
- Develop skills in the Modelica/Dymola modelling environment
- Describe and develop models representing the energy systems of fishing vessels
- Perform simulations of the different parts of energy system
- Analyse the results in terms of system performance, energy consumption and thermal energy storage potential/demand
- Summary report
- Draft scientific paper related to the findings of the Master Thesis
- Proposals for further work

Chapter 2

Literature Review

2.1 Refrigeration history

Natural ice was the only source of cooling in the ancient time. Ice collected from glaciers and frozen lakes etc. were stored in unique underground spaces. In the mid 19^{th} century, first mechanical refrigeration system invented and patented by Jacob Perkins. The system had a condenser, hand-operated compressor, and expansion device. Natural working fluids like ammonia, CO_2 and isobutene, etc. were utilized at that time. With the advent of synthetic working fluids in 1930, natural fluids phased out due to better operating conditions of their counterparts. Later, the artificial fluids found to be harmful to the Ozone layer and the environment. After the Montreal protocol in 1987, there was a strong emphasis to phase out the high GWP (Global warming potential) refrigerants and increase research on natural working fluids like Ammonia and CO_2 (Eikevik, 2019a).

2.2 Refrigeration principles

Refrigeration is the method of extracting heat from low temperature (LT) and discharge at high temperature (HT) with the help of some external work. The main types of refrigeration cycles are vapor absorption and vapor compression cycle. The vapor compression cycle in the closed-loop is the discussed refrigeration process in this project. The process runs with a working fluid, which is called refrigerant. The refrigerant absorbs heat from the LT side in an evaporator and the evaporation temperature must be lower than the surrounding temperature to initiate the heat transfer. The vapors then compressed to HT and pressure with the help of a compressor, the gas then condensed in the condenser, the condensation temperature must higher than the surrounding to discharge heat. The temperature and pressure again decrease to evaporator conditions by an expansion valve, and the cycle repeats. The refrigeration process in a simple diagram is shown in Figure 2.1 with four thermodynamic state points, which is further explained by the pressure enthalpy (Ph) and temperature entropy (Ts) diagrams.

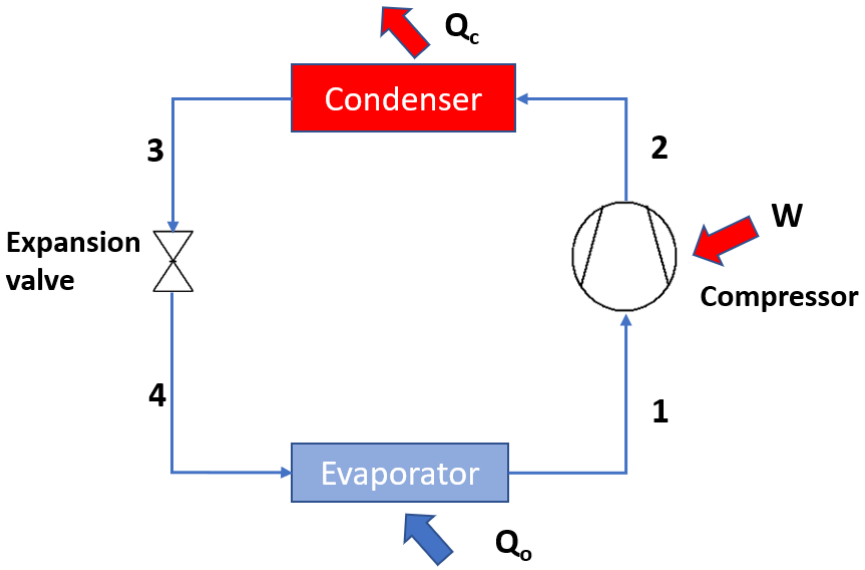

Figure 2.1: Simple refrigeration cycle

The thermodynamic process and their state points are described below:

- **1-2:** Isentropic compression. Ideal work done by the compressor can be expressed as $W_{is} = m_R(h_{2s} - h_1)$. By including the isentropic efficiency the equation can be written as.

$$W = W_{is}/\eta_{is}\ [kW] \tag{2.1}$$

- **2-3:** Isobaric rejection. The heat rejected from the condenser is the sum of evaporation heat and compression heat. This can represented in equation by:

$$Q_c = Q_o + W = m_R.(h_2 - h_3)\ [kW] \tag{2.2}$$

- **2-3:** Isenthalpic expansion. Temperature and pressure of the refrigerant is decrease by expansion valve and the process is constant enthalpy process i.e. $h_3 = h_4$

- **3-4:** Isobaric heat absorption. Heat absorbed from the evaporator surrounding is the evaporation load of the system. This can be calculated by the equation:

$$Q_o = m_R.(h_1 - h_4)\ [kW] \tag{2.3}$$

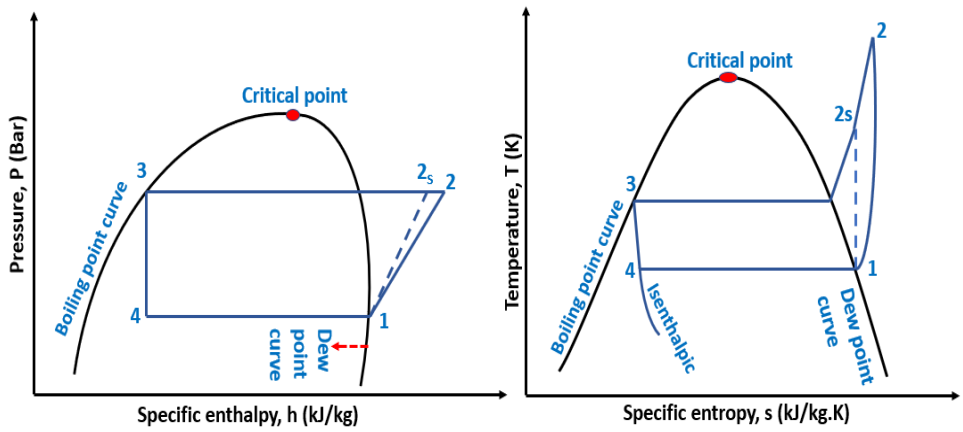

Figure 2.2: Ph and Ts diagrams of refrigeration cycle

The performance of the refrigeration system is expressed by the coefficient of performance (COP), which is the ratio of output and input power. It is a dimensionless number and higher the number better is the performance.

$$COP_{REF} = Q_o/W\ [-] \tag{2.4}$$

$$COP_{HP} = Q_c/W\ [-] \tag{2.5}$$

$$COP_{COM} = Q_c + Q_o/W\ [-] \tag{2.6}$$

The reversed Carnot cycle is the ideal refrigeration process which operates between the high temperature and low temperature and the process is reversible, which makes it different from the real processes, which are irreversible. Efficiency of Carnot process is the ratio between the real COP and Carnot COP. The Carnot COP for the cooling and heating process can be expressed as:

$$COP_{Cac} = T_L/T_H - T_L\ [-] \tag{2.7}$$

$$COP_{Cah} = T_H/T_H - T_L\ [-] \tag{2.8}$$

$$\eta_{Ca} = COP/COP_{Ca}\ [-] \tag{2.9}$$

2.3 Refrigerants

Refrigerants are the fluids that transfer heat from low temperature side to the high temperature side of the refrigeration system. With the advent of the refrigeration systems by Jacob Perkins in 1834, ethyl ether (R-610) was used as first refrigerant. It's use restricted shortly due to safety concerns and new fluids ammonia (R-717), carbon dioxide (R-744), sulfur dioxide (R-764) and air (R-729) etc. came into operation. In 1930, a new class of refrigerants chlorofluorocarbons (CFCs) introduced, succeeded by hydrochlorofluorocarbons (HCFCs) in 1950, with a slogan of environmental concern, better operating and safety conditions. In fact, many accidents happened with their handling and adverse effect on the ozone layer soon realized (Dincer and Kanoglu, 2010).

In 1987, Montreal protocol initially signed by 26 countries to regulate the use and production of chemicals that contribute to the Ozone layer depletion. The treaty defined time frame to ban the use of these chemicals. In developed countries, CFCs phased out in 1996 and HCFCs are due until 2030. In comparison developing countries phased out CFCs in 2010 and are expecting to phase out HCFCs in 2040 (Britannica Academica, 2019). In the late 1980s after Montreal protocol, hydrofluorocarbons (HFCs) utilization increased due to no effect on Ozone layer but they do contribute to greenhouse effect. In 1997, Kyoto protocol signed to control global warming by reducing emissions of HCFCs. Latest regulations are the EU F-Gas 2015 and Kigali amendment 2016, the later came into effect by January 2019. Kigali amendment aim is to target 80% reduction in HFCs consumption by 2047 (UNIDO, 2016). Hydrofluoroolefins (HFOs) are the latest successor of HCFCs after the adoption of European Directive 2006. HFOs series come with a label of no effect on ozone depletion, less GWP and better safety, but issues are reported concerning flammability and formation of dangerous acid (Makhnatch, 2019).

R22 widely used in an early refrigeration systems of fishing vessels, but the refilling of R22 in the EU has been banned since 1 January 2015 because of it's ozone depletion potential of 0.055. Tokle et al. (1993) investigated the usage of different refrigerants in various sectors. The fishing fleet of 600 ships reported to use 91% HCFCs, utmost R22 and the remaining 9% CFCs, most likely R12. Haukås (2007) reported a change, 82% (351 vessels) used HCFCs (R22), 4% (19) HFCs and a new trend towards natural refrigerant ammonia 14% (60) (Hafner et al., 2019). In Norway, natural refrigerants like CO_2 and NH_3 are gaining more popularity. The scope of this project is also limited to natural refrigerants, mainly CO_2.

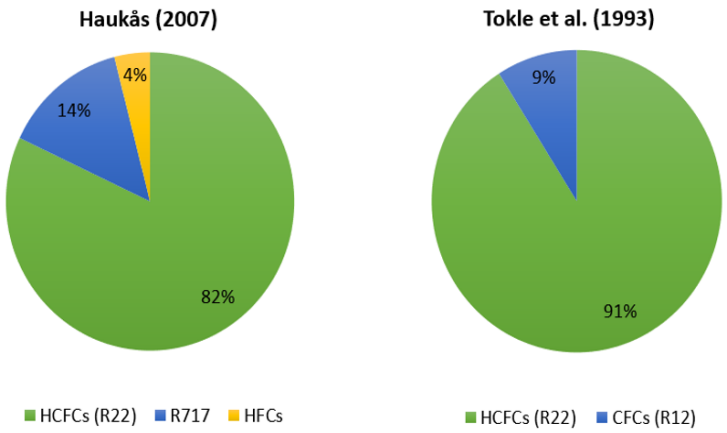

Figure 2.3: Fishing vessels refrigerants transitions (Hafner et al., 2019)

2.3.1 Ammonia

Ammonia is a natural refrigerant with good thermophysical properties. The critical temperature and pressure of ammonia is 132.4 °C and 112.8 bar, respectively. It has no GWP and ozone layer impact. It is a prominent working fluid in industrial applications. The amount of ammonia charge in the refrigeration systems vary from 300-1100 kg. Ammonia has a high specific enthalpy of condensation and evaporation, relatively high volumetric cooling capacity, average 20% higher COP than other working fluids. Ammonia systems having moisture content initiate the corrosion of Copper and its alloys. The fluid is poisoning, flammable in a volume concentration of 15-28% with air, irritating to skin and eyes. It has stinking odour which may creates panic but this gives an early warning of leakage (5-10 ppm) (Widell et al., 2016).

Additional safety measures are necessary for ammonia systems, which includes the low working fluid charge, gas-tight machinery room, leak detectors, independent ventilation system with scrubber systems and emergency exits with self closing doors. However, ammonia system with a required safety measures is a reasonable choice (Eikevik, 2019a).

2.3.2 Carbon dioxide

In 1988, Professor Gustav Lorentzen at NTNU reintroduced the CO_2 working fluid. The fluid has marvellous properties. It is non toxic, no flammability and is not harmful to atmosphere. CO_2 is not produced directly as a refrigerant, it is a byproduct of many industrial process. The critical temperature and pressure are 31.1 °C and 73.8 bar respectively. High energy density due to high pressure results in high volumetric heating capacity (VHC). High VHC reduce the compressor volumes, and size for CO_2 compressors are normally 5-6 times smaller than for ammonia. Pipes and valves etc. dimensions would also reduced

but need more strength and durability due to high pressure in the system (Eikevik, 2019a).

CO_2 has a low critical temperature. Condensing temperature near 28 °C reduce the COP to a greater extent. To be able to work in higher heat rejection temperatures, the system operates in a transcritical process. It is a process, which works at a pressure higher than critical pressure, heat absorption at constant temperature but heat rejection at gliding temperature. There is not any liquid formation above critical pressure due to presence of fluid in the supercritical region. So, the condenser is replaced by a gas cooler. Expansion loss would be high near the critical point and it is necessary to optimize the high pressure side for better COP factor. In real systems, there are many benefits of using CO_2. The compressor works at high isentropic efficiency and low pressure ratio. High heat transfer and low pressure drops results in higher COP of CO_2 systems (Eikevik, 2019a). CO_2 is a long term environment friendly refrigerant. A large number of CO_2 systems are working in EU. Due to latest modifications of parallel compression and ejector technology, it is possible to utilize these systems in high ambient temperatures with high COP. CO_2 is expecting to become a standard refrigerant in the EU supermarkets in future (Gullo et al., 2017).

Properties	**units**	**R717**	**R744**
Molecular weight	g/mol	17.03	44.01
Evaporation heat	kJ/kg	1261.7	232.0
Thermal conductivity, liquid	W/m.K	0.5455	0.1110
Thermal conductivity, gas	W/m.K	0.0260	0.0187
Specific volume, liquid	dm^3/kg	1.566	1.073
Specific volume, gas	dm^3/kg	289.39	10.20
Ignition temperature	°C	630	ND
Density(liquid) at 0°C	kg/m^3	639	928
Density(gas) at 0°C	kg/m^3	4	98
Boiling point at 1 bar	°C	-33.33	-78.03
Critical temperature	°C	132.3	31.1
Critical pressure	Bar	113.3	73.8
Flammability	-	No	No
Toxic	-	Yes	No
GWP	-	0	1

Table 2.1: Properties of R717 and R744 (Eikevik, 2019a)

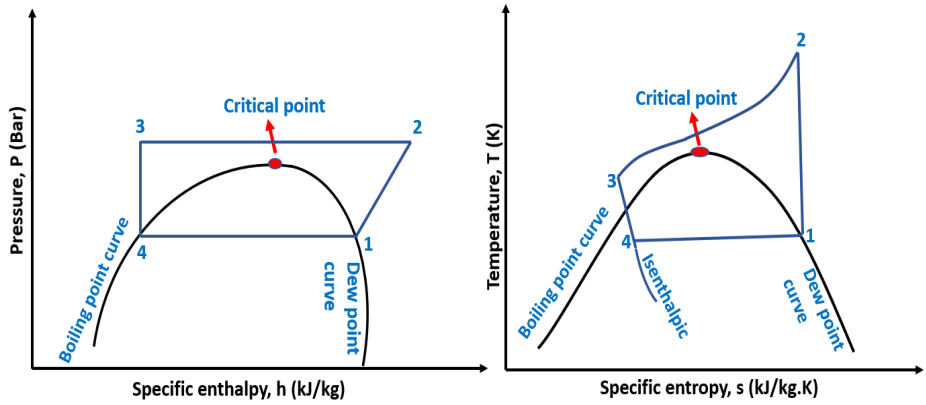

Figure 2.4: Trans-critical cycle of R744 on Ph and Ts diagram

2.4 Marine refrigeration

Ice was traditional source of storing fish on the fishing vessels in boxes. The development of fish industry within pelagic species such as herring, mackerel, capelin and blue whiting increased rapidly during 1960s. The increased size and catch of fishing vessels caused the ice storage to be labor intensive and insufficient to maintain desirable temperature. This was resulted in loss of profit and inadequate quality of fish for human consumption. Fish meal and oil were produced with this poor quality fish but it is a low value product. Product shelf life is highly dependent on storage temperature, micro biological activity increase at high temperatures. Shelf life of fish is twice at 0 °C as compared to shelf life at 5 °C or even higher at -1 °C. Refrigerated sea water (RSW) tanks were found to be suitable for preserving fish onboard after research and testing. The main requirements for the RSW tanks are insulated tanks, enough chilling capacity to maintain around -1 °C, uniform temperature distribution in tanks, cleaning and loading equipment and temperature monitoring system. Different voyage length, fishing method, species and vessels demands unique equipment requirements. The onboard RSW systems save almost all the pelagic loss and ensure the quality in the cold supply chain. This industry contributed 25% of Norway's fish export (Widell et al., 2016).

2.4.1 RSW system

Sea water freezes at -2 °C with a salt concentration of 3.5%. In the RSW tanks, the water chilled around -1.5 °C before the fish is caught. Uniform temperature distribution and proper circulation of water ensure high quality, until the fish is unloaded at harbor. The evaporation temperature in the refrigeration system of RSW is typically around -5 °C. Sea water is used to condense the refrigerant in the condenser. In the Norwegian sea, water temperature ranges between 5-12 °C. Mostly the fishing vessels have more than one chilling tank, and it can be used as a freezing storage. Two independent refrigeration

systems ensure the safety of catch in-case having problem with one system (Widell et al., 2016).

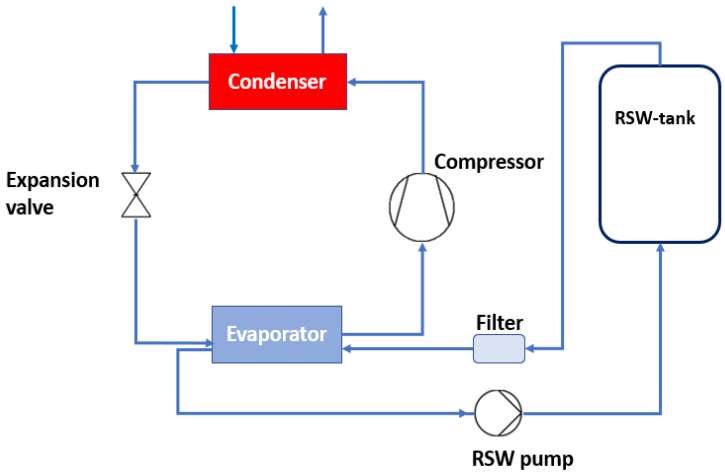

Figure 2.5: Flow diagram of RSW system

2.4.2 Ammonia RSW system

There is a clear transition towards natural refrigerants in the fishing industry and ammonia is one of the natural refrigerant with good properties (see section 2.3). There is a continuous growth of ammonia RSW systems. Havyard MMC, since 2013 has sold 25 systems and order of 13 more to be delivered in 2016 and 2017 for fishing vessels. A low charge 85 Kg ammonia system developed by Havyard MMC with a cooling capacity of 250 KW. The system was tested on land without fish in sea water tanks with a COP between 3 and 4.3. At that time, the condenser cooling with a water temperature of 27°C was insufficient. This system, which is called SX cooler, installed on the ship MS slettenberg in 2012 and working as expected from that time. The system is very efficient in terms of energy and space requirement (Widell et al., 2016).

In 2015, Teknotherm delivered an ammonia system to the Scottish trawler. It has two units with a capacity of 1000 KW (-5/30 °C). Shell and tube heat exchanger was used as evaporator, refrigerant spray outside and water inside the tube. Spray type reduce the refrigerant mass as compared to flooded evaporators. In most cases, refrigeration systems assemble as one unit in the manufacturing unit, and this reduce the installation time onboard (Widell et al., 2016).

2.4.3 CO_2 RSW system

CO_2 in RSW systems were not common in Norway nor elsewhere. SINTEF and NTNU played an important role in the development of safe and energy efficient CO_2 systems. The

first CO_2 RSW system launched in early 2012, and it was manufactured for MS Viking Midøy. The system works with 4 transcritical compressors (Dorin), shell and tube condenser with refrigerant on tube side and flooded evaporator. Titanium heat exchangers are used, which are suitable for sea water systems. Cooling capacity is 250 KW and evaporation temperature is -5 °C. Chilling temperature ranges between -1 °C and 0 °C. There are 6 RSW tanks and CO_2 system was meant to chill 3 tanks and rest with the old R22 system. CO_2 system is capable for all the tanks but R22 system is also in use to increase the chilling capacity for catch. The CO_2 system was working as expected under bad weather and different ambient conditions (Widell et al., 2016).

The second CO_2 system in Norway was built for fishing vessel, Trønderhav. NTNU and SINTEF was in cooperation with CADIO AS for the construction and system design. The system is equipped with 2 units, each with 150 kW refrigeration capacity. The RSW unit work with a water temperature of -1.3°C and reported to be more stable than the old R22 system. A new "dimple type design" plate heat exchanger is used as condenser and evaporator, which is easy to open, clean and compact in size. However, small challenges were encountered during startup of the system but they solved at dock and it has worked well. The system reported to has less noise and vibrations due to small compressor size of CO_2. The number of visits to engine room has reduced due to operation of RSW system from the bridge (Widell et al., 2016).

2.4.4 Combined RSW and freezing system

A combined system works for both chilling and freezing. Such system gives the freedom to do fishing of multiple types. For instance, cod and saithe filleted and frozen in vessels using plate freezers. Many ships are equipped with these systems for better resource utilization. A fishing vessel, Fugløyhav has an ammonia refrigeration system, which can work both as RSW and a freezing unit. Low COP and refrigerant distribution are the main issues associated with these installations (Widell et al., 2016).

Ammonia has an evaporation temperature of -33 °C at 1.08 bar, and it is not common to operate any refrigerant below 1 bar. CO_2 in comparison has better properties and can work as allow as -50 °C without any complex issues, but COP would effect with a large temperature lift. In such a case, Cascade system of NH_3 and CO_2 is a better solution (see section 2.4.5).

CO_2 booster and ejector systems are the latest developments in the the CO_2 refrigeration. Ejector system can increase the COP up to 17% (Hafner, 2019). CO_2 booster systems with chilling and freezing are common in supermarkets. This system works on one fishing vessel, M/S Roaldsnes with a fast freezing capacity and better product quality (Widell et al., 2016).

2.4.5 Cascade system (CO_2 and NH_3)

Cascade system is a closed multi loop refrigeration circuit connected in a single heat exchanger, which is called cascade heat exchanger. It works as an evaporator for high tem-

perature circuit (HTC) and condenser for low temperature circuit (LTC). Heat is able to transfer with a large temperature difference, reasonable pressure and better efficiency by cascade system. This allows the flexibility of two different or same refrigerants operating in different conditions in one system. It is suitable for both freezing and cooling. The design of a cascade system is shown in figure 2.6. The evaporation temperature of HTC must be lower than the condensing temperature of LTC, this is explained in the figure 2.7 by a middle temperature line (T_m). COP of such system depends on the temperature lift in the individual circuit. Both circuits should have optimum temperature lift to have high COP.

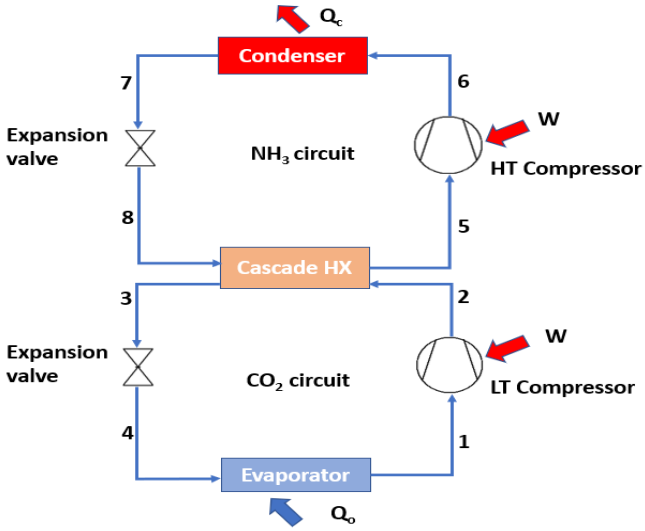

Figure 2.6: Principal sketch of cascade system

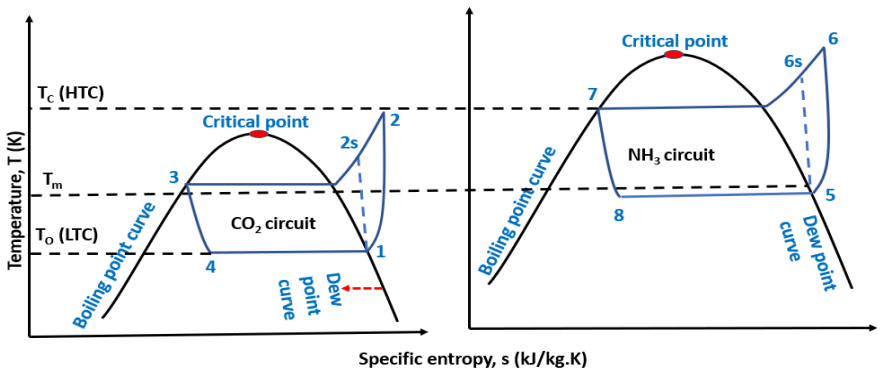

Figure 2.7: Ts diagram of cascade system

York Refrigeration developed the first cascade system with NH_3 and CO_2 in Århus Denmark and installed in 2002 on a Norwegian fishing trawler, MS Kvannøy. CO_2 was selected in low LT side with an evaporation temperature of -48 °C and NH_3 in the HT side. Freezing capacity of fish within 24 hours is 210 tons. An experiment of freezing fish from 2 °C to -25 °C showed that the whole fish could freeze within 1 h 45 min. The analysis of the results figured out that the new system is faster and has 25% more production capacity than the previous R22 system, which was operating at an evaporation temperature of -40°C. The unit includes RSW tanks, flake ice machine and a freezing storage. Sea water ($300m^3$) from 18 °C to 2 °C can be chilled within 5 hours. Ice can made from fresh water and sea water with the flake machine (Widell et al., 2016).

It is clear from the above example that cascade system with CO_2 in the LTC increase production capacity and decrease the operating time. Another big advantage is that in case of leakage, CO_2 would not harm the fish. Presence of less ammonia on the ship reduce the risk of contamination. Before, it was an issue with the availability of CO_2 system components due to its high pressure but its no longer an issue. Dimensions of the CO_2 components are small which makes it cost competitive with other systems. As the components are small, they are sensitive to water because of ice formation. The problem can be avoided by selecting highly purified CO_2 with no moisture content and vacuuming of the system before running (Widell et al., 2016).

2.5 Plate freezers

Plate freezers are a set of parallel plates in which coolant or refrigerant flow. The plates can be arranged either vertically or horizontally. During loading and unloading, hydraulic system is used to close and open the space between plates. To protect the food against excessive pressure or damage, stop limits or spacers and pressure control valves are used in the hydraulic system (Valentas et al., 1997).

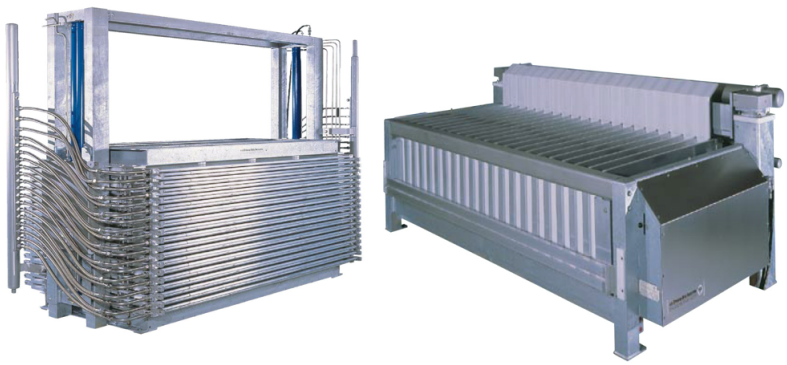

Figure 2.8: Horizontal and vertical plate freezer (Teknotherm)

Vertical plate freezers are good choice for freezing of unpacked deformable products such as meat and fish. Blocks of the product are formed by gravity feed between the

plates. Defrosting, block removal process and may be cleaning is essential at the end of freezing process. Horizontal plate freezers are used for rectangular packed products in cartoons or products to be formed in rectangular shape. Automation have been developed for continuous operation of loading and unloading of product rows from feed conveyors, but plate freezers operate manually most often (Valentas et al., 1997).

For effective operation, the uniform and high contact between product and plate surface is important. This can be attained by applying moderate pressure on the plates and with high product package density (low void space). For packed products, low void and free space is good for high heat transfer (Valentas et al., 1997).

Plate freezers have big advantage over other freezes due to high heat transfer rates. For good contact, heat transfer coefficient ranges between 200 to 500 W/m^2K and for poor contact the range is 50 to 100 W/m^2K. The products can be easily handled and bulk stacked after freezing. Infrequent defrosting and low energy use are other pros. On the other hand, high capital cost and limitations on the product types are the drawbacks (Valentas et al., 1997).

2.6 Product heat load and refrigeration capacity

Heat load is the amount of heat in the product at different temperatures which is needed to remove to chill or freeze the product. The heat removal rate depend on the thermal properties of the product and temperature difference between the cooling fluid and product. In freezing process due to transient conditions, the heat load from the product decrease as the temperature start decreasing. The Figure 2.9 shows the freezing load behaviour of beef in tunnel freezer.

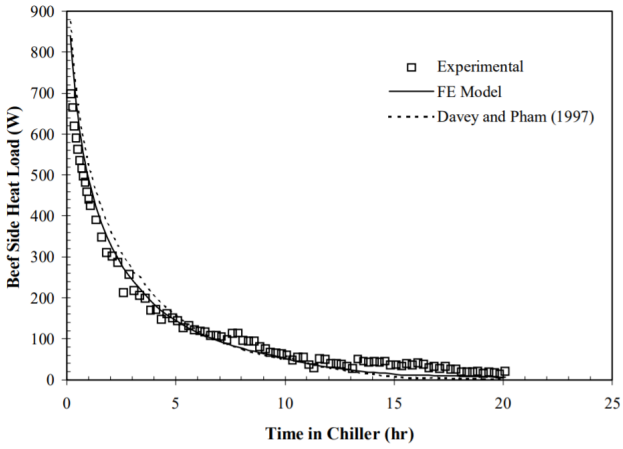

Figure 2.9: Heat load transition of food with time (Pham, 2002)

The peak heat load in batch freezing process is 2 to 4 times higher than the average load due to change in the product load. Refrigeration system must be able to deal with some peak loads higher than the predicted average load for better quality and higher production

rate (Valentas et al., 1997). If the refrigeration capacity is lower than the product load, then it will prolong the freezing time and this happens often during the start of the process. One practical reason for having high starting load in plate freezers is due to defrosting of surface after each cycle. On the other hand, if the heat load is less than refrigeration capacity, the refrigeration system will adjust to lower capacity by reducing flow of refrigerant and maintain equilibrium. For better resource utilization, this high refrigeration capacity can be used for thermal storage.

2.6.1 Fish heat load

To predict heat load precise, accurate thermal properties are requisite. Thermal properties are mostly predicted by simple equations using composition of food. Many foods are very different in composition and even the two items of same product can have different composition. For such reasons, prediction methods using compositional data are consider accurate and much better than poorer measured values (Valentas et al., 1997). Figure 2.10 shows the calculated properties of Mackerel.

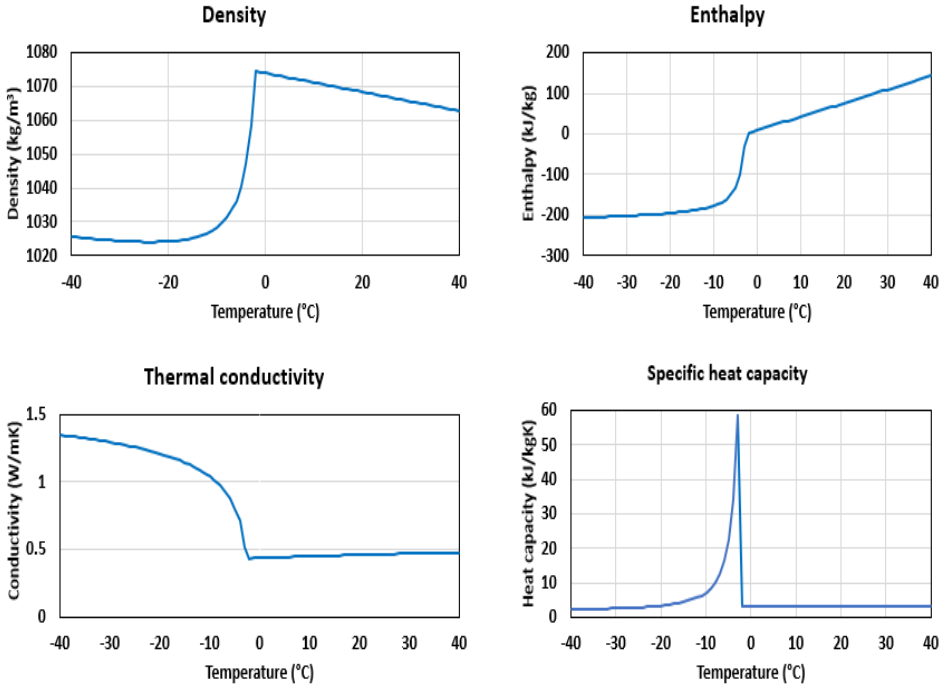

Figure 2.10: Calculated thermal properties of Mackerel

The composition of fish used in this thesis is Mackerel (Table 2.2). Mackerel composition is seasonal, it means the fish has different composition in different seasons. So, this

composition cannot consider accurate for all seasonal variations.

Fish type	Moisture content %	Protein %	Fat %	Ash %
Mackerel, Atlantic	63.55	18.60	13.89	1.35
Herring, Kippered	59.70	24.58	12.37	1.94
Cod	81.22	17.81	0.67	1.16
Salmon, Pink	76.35	19.94	3.45	1.22
Tuna, bluefin	68.09	23.33	4.90	1.18

Table 2.2: Composition of different fish (Eikevik, 2019b)

Mackerel and Herring is a good option for onboard production of fish oil due to it's high percentage of fats as compared to other species. However, the small size of Mackerel is a big question for onboard processing in terms of economic sustainability.

2.7 Rest raw material

The left over from the processing of fish main product (fillets) are head, bones, skin, trimmings and guts, these remaining are called rest raw material. The rest raw material (RRM) are not as valuable as fillets (Søvik, 2005). Few RRM parts have enough commercial value to be sold on land but most of them dump at sea. These discarded parts can account up to three quarters of the catch volume. So, this is an environmental and economical issue (Rustad et al., 2011). According to FAO (2014), globally 80 million tonnes of fish processed for filleting, canning or curing and freezing, of which rest raw material accounts for 50 to 70% that are not fully utilized (Olsen et al., 2014).

There is a difference between utilization of rest raw material on land and onboard. Most of the RRM from the onshore processing are already in consumption. The highest potential for technology advancement lies for onboard processing, which are facing challenges of facilities, inadequate space for RRM and economic sustainability.

RRM is a good source of nutritional ingredients for food industry, animal feed industry and pharmaceutical industry. It is also a raw material for fish oil (omega-3) production, which is highly valuable among other RRM products.

2.7.1 Fish oil production

There are two methods of fish oil production.

- Thermal treatment.
- Hydrolysis.

Thermal treatment

In thermal treatment, rest raw material is first crushed in mincer to make it easy for flow by pump. Then heated in heat exchanger up to 90 °C. The temperature of rest material can

set less than 90 °C (for example, 60, 70, 80 °C) but may have effect on the quality and production rate. After heating, RRM is treated in a tri-canter. It is a special component that separate the stick water (water phase), sludge (solid phase) and oil. Tri-canter is also called three phase separator. After tri-canter, the oil phase is further treat in polishing centrifuge to remove the impurities (Carvajal et al., 2015). Figure 2.11 shows the flow of rest raw material in thermal process.

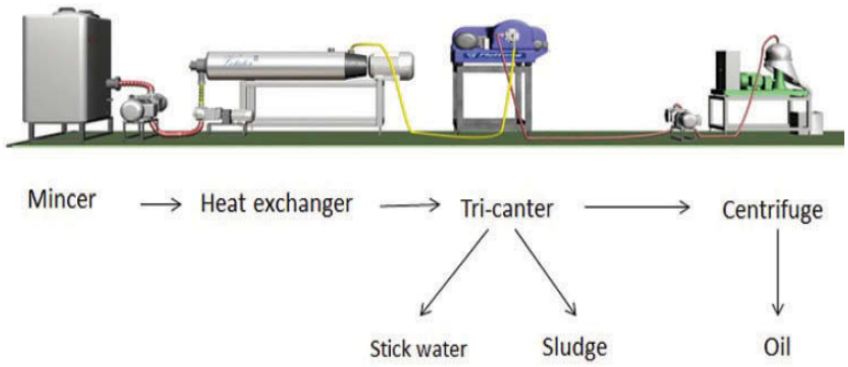

Figure 2.11: Fish oil production by thermal treatment (Carvajal et al., 2015)

Hydrolysis

In hydrolysis process, the rest raw material heated up to 50 to 60 °C after mincer. After heating, the RRM treat in hydrolysis tank. In hydrolysis tank, the RRM mixed with equal amount of water (1:1) and with addition of chemicals or enzymes. Common enzymes of treatment are Papain and Bromelain. Normal processing time of RRM treatment in enzymatic hydrolysis tank is 1 hour. Inactivation of enzyme is necessary at 90 °C for 10 minutes after hydrolysis process (Carvajal et al., 2015).

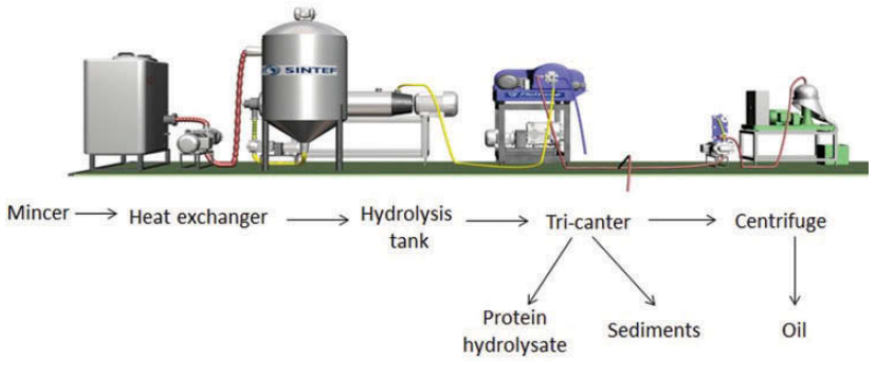

Figure 2.12: Fish oil production by enzymatic hydrolysis (Carvajal et al., 2015)

2.8 Liquefied natural gas (LNG)

LNG is a liquid mixture of Methane (85-95 mol %) and other hydrocarbons, often contains a nitrogen fraction (less than 1 mol %). LNG and natural gas volume ratios are 1:600 at standard conditions. The saturation temperature of LNG at 1 bar is -162 °C. The density of LNG is 450 kg/m^3, which is small in comparison to diesel density, i.e., 860 kg/m^3 (Jafarzadeh et al., 2017) but due to the high calorific value of LNG, the required mass flow rate of LNG is less than diesel engine for the same power, which is an advantage for LNG. The density difference between LNG at 1 bar and CNG at 200 bar is 275 kg/m^3, which means LNG fueled vessel can travel 2.5 times more as compared to CNG vessel for the same volume of a fuel tank. LNG is stored onboard in the cryogenic tanks at different pressures depending on the permissible value (Sihvonen, 2018).

LNG is odourless, colourless, non-corrosive and non toxic, but the evaporated LNG can cause human suffocation by displacing Oxygen. At temperatures below -110 °C, LNG vapours are heavier than air and they can spread above sea water or on the ground. It is lighter than air at higher temperatures and would diffuse. Methane flammability range is 5 to 15 vol % in air. Self ignition temperature is 540 °C (Pettersen, 2018).

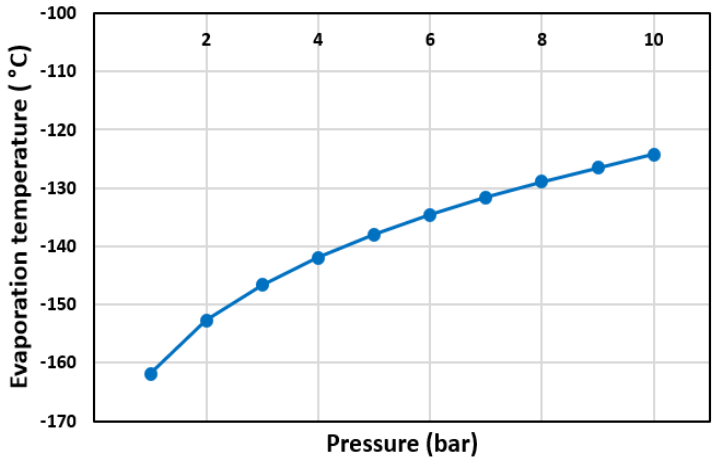

Figure 2.13: LNG (Methane) pressure versus evaporation temperature (Coolpack, 2020)

2.8.1 LNG fueled ships

LNG fueled ships use dual-fuel engines that operate both on diesel and natural gas. Natural gas used as primary and diesel as a backup fuel. Dual fuel engines can be classified as low, medium, and high-pressure engines. Low-pressure engines operate approximately 5-6 bar, medium pressure engines 17 bar and high-pressure engines 300 bar at the inlet fuel conditions to the engine (Jafarzadeh et al., 2017) and (Koo et al., 2019).

2.9 Thermal energy storage (TES)

Energy demand on the fishing vessels, industries and different sectors varies with the time and needs. The energy demands can be optimized with the thermal energy storage (TES). A complete TES process includes three steps, charging, storing and discharging. TES stores energy by heating, cooling, solidifying, melting, or vaporizing a material, by reversing the process energy can be made available. TES has been used for heating and cooling applications and gaining more attention in the recent years.

In the mid 19^{th} century, chemical storage batteries were common to supply power for signal lighting, telegraphs and other electrical devices. In 1896, an inventor from Toledo, Homer T. Yaryan established a thermal storage system to utilized the excess heat for hot water district heating plant in that city at the time of peak electric demand . Steam storage in other plants were not as successful as his plant. Other TES methods in the 1890s were compressed air and hot water flashing into steam to drive the engines of cars (Dincer and Kanoglu, 2010).

There are two methods of thermal energy storage, which are Sensible and Latent TES.

2.9.1 Sensible TES

Sensible TES is the storage of energy by either increasing or decreasing the temperature of the material without any phase change. The efficacious of energy storage depends on the specific heat capacity and density of the material. The heat stored in a material in a unit time can be expressed as:

$$Q_{sensible} = \frac{m.c_p.\triangle T}{3600\ s} = \frac{\rho.V.c_p.\triangle T}{3600\ s}\ [kWh] \tag{2.10}$$

There is a wide range of materials for storing energy but the selection of the medium is highly dependent on the application and temperature range. Each storage medium has its own pros and cons. Some materials for the sensible heat storage are oil, air, sand, soil and bricks. One important consideration during selection of storage medium is the heat transfer rate, the rate at which the energy can be be stored and extracted. The main components in TES are storage tank, medium and charging/discharging device. The storage tank must be able to hold the thermal storage material, avert the heat losses and maintain thermal gradient. High thermal losses means the tank can't hold the desired temperature for a longer period (Dincer and Kanoglu, 2010).

For sensible heat storage, water is a common choice. It is inexpensive, high specific heat capacity, easily available and no safety hazards. Water is a liquid, which makes it easy to transfer thermal energy at high rates by pumping. However, the applications range is limited due to freezing and boiling point of water.

2.9.2 Latent TES

Latent TES is the storage of energy with phase change material (PCM). PCM store energy during conversion (liquid to solid) and released in the reverse process (solid to liquid). For example, water conversion to ice at 0 °C stores a latent heat of 333 kJ/kg and the same amount of energy release in the reverse process (Dincer and Kanoglu, 2010). The latent TES equation can be expressed as:

$$Q_{latent} = m.\triangle h_L \; [kJ] \tag{2.11}$$

where, m is mass in kg and $\triangle h_L$ is the latent enthalpy change. It is an efficient method of storing energy. The amount of energy stored is very high as compared to the sensible storage. The variety of phase change materials are shown in Figure 2.14. The ideal PCM meet following criteria (Pielichowska and Pielichowska, 2014).

Thermal properties

- Temperature within desired range.
- High latent heat per unit volume.
- High specific heat.
- Good thermal conductivity in both phases.

Physical properties

- Small volume change in phase transformation.
- Low vapour pressure at the operating temperatures.
- Favourable phase equilibrium.
- high density.
- Consistent melting of PCM.

Kinetic properties

- No supercooling.
- High nucleation rate.
- Normal rate of crystallization.

Chemical properties

- Chemical stability.
- Reversible cycle.
- Suitability with storage material.

- No flammability, non explosive and toxic.

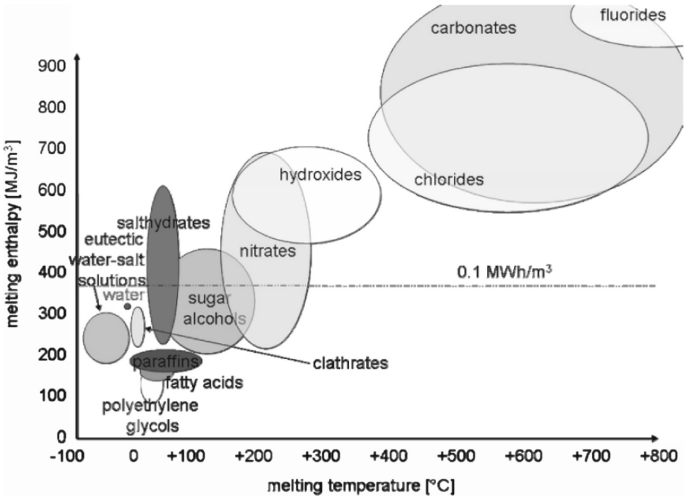

Figure 2.14: Various PCM with different temperature and enthalpy range (Mehling and Cabeza, 2008)

2.10 TES on fishing vessels

Chilling or freezing load on the fishing vessels varies a lot. It is different during fishing, return and moving towards the fishing ground and even in one freezing cycle. Thermal storage is a good option to balance the load, compatibility with less refrigeration capacity or extra capacity at peak load. TES can also boost the refrigeration capacity by chilling the catch in a short time, which would ensure high quality of product.

2.10.1 TES for chilling vessels

In chilling vessels, the required storage temperature for fish is -1 °C in RSW tanks. Water can utilize as PCM but it is only suitable to cover peak loads, when there is enough temperature different between water stream from RSW tank and ice storage to initiate heat transfer. For example, if the temperature difference in heat exchanger (thermal storage) is set to 5 K then water PCM can only useful to chill RSW stream up to 4 °C. However, Water is not suitable in case of re-condensing of super-heated refrigerant after evaporator.

For chilling of fish at -1 °C, a water based phase change material with a phase change temperature of -6 °C is an ideal choice. At -6 °C phase change temperature, there is always a high enough temperature difference between water stream and PCM for high heat transfer rate. This PCM can also used for re-condensing of super-heated vapours.

2.10.2 TES for freezing vessels

CO_2 as a PCM is suitable option for freezing storage due to it's storage temperature and negligible GWP. One benefit of storing dry ice above triple point pressure (5.18 bar) is that the phase change is from solid to liquid. On the other hand, if it is stored below 5.18 bar then the phase change is from solid to gas (sublimation). Sublimation will increase the pressure in the storage tank and elevate the storage temperature. After some instant at pressure above 5.18 bar , the phase will shift from sublimation to Solid-liquid. Phase change behaviour and other characteristics of CO_2 is shown in Figure 2.15.

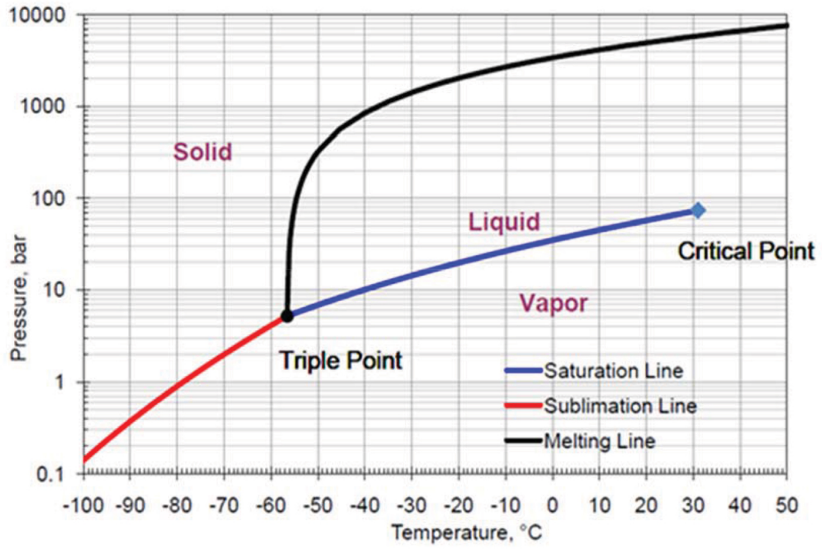

Figure 2.15: Temperature-Pressure diagram of CO_2 (Rycroft, 2019)

Chapter 3

System Design

This chapter will describe the study cases of chilling and freezing vessels. The goal is to designed different thermal systems and then optimise their performance Two independent cases are analysed for chilling and freezing vessel. A 760 kW engine, LNG powered vessel is a case study for chilling vessel. LNG fuel consumption, chilling load, heat recovery from refrigeration system and flue gases, and thermal storage system (water) are studied for chilling vessel in this chapter. For freezing vessel, the designed approach is narrow down as compared to chilling vessel. Freezing load, refrigeration system, heat recovery from refrigeration system, fish oil production from rest raw material and CO_2 thermal storage are investigated for freezing vessel in this chapter. The designed systems will be a base for the software simulation and result analysis.

3.1 System design for chilling vessel

A 760 kW engine capacity, coastal demersal trawler is a reference case for the chilling (RSW) vessel. Such trawlers are used for demersal fish like Cod, Saithe and Haddock. Herring and Mackerel are the pelagic fish. In chilling vessels, the catched fish is stored in RSW tanks and later processed on land facilities. The chilling load is designed from the properties of Mackerel, which is contradiction to demersal trawler, but the refrigeration loads are comparable to other species with some error. The selection is entirely made on the availability of the required data for this case. It is assumed that the trawler is equipped with CO_2 refrigeration system and ambient temperature is 15 °C, and it is analysed as a chilling facility. LNG is assumed as a fuel for trawler and the cold recovery from LNG and it's integration with the thermal system is studied.

3.1.1 Fuel consumption

The reference case 760 KW trawler use diesel as a fuel but the aim of this project is to study LNG fuelled fishing vessels. To make the study more realistic, diesel fuel consumption is converted to LNG consumption by using appropriate values and equation. The

characteristic values of the 760 kW trawler are derived from Norwegian Directorate of Fisheries (2014) presented in a research paper by (Jafarzadeh et al., 2017).

Characteristics	**Values**
Length overall (m)	33.18
Breadth (m)	7.20
Depth (m)	5.96
Gross tonnage	279
Main engine power (kW)	760
Days at sea in 2012	280
MGO consumption in 2012 (L)	407,030
Catch in 2012 (kg)	164,454

Table 3.1: Characteristics of a Norwegian Coastal demersal trawler (Jafarzadeh et al., 2017)

The round trip of one journey is assumed six days with a diesel consumption of 8.72 m^3. Specific fuel consumption (sfc) value of 845 kW gas engine is used for LNG estimation due to availability of this engine in the market. Sfc is considered constant through out the journey. The energy consumption of round trip is calculated by using values from the Table 3.2 and equation 3.1 (Jafarzadeh et al., 2017).

$$E = \frac{Fc * \rho}{sfc} \, [KWh] \tag{3.1}$$

Where, sfc, ρ, Fc and E are the specific fuel consumption, density, fuel consumption and energy of the engine, respectively. The estimated energy for the round trip is 35.17 MWh. If the vessel is using LNG as fuel then by using equation 3.1, the fuel consumption of LNG is 15.55 m^3. The usable volume of LNG tanks are approximately 80-85% depend on the maximum allowable pressure and relief valve adjustment. For this study case, the required volume for LNG tank for one trip is around 18.30 m^3 (Jafarzadeh et al., 2017).

Parameters	**Values**
Gas engine power (kW)	845
Average sfc gas engine (g/kWh)	198.99
LNG density (g/m^3)	45.10^4
Energy content of LNG (MWh/tonne)	13.8
Marine diesel engine (kW)	760
Average sfc of conventional engine (g/kWh)	213.30
Diesel density (g/m^3)	$86 * 10^4$
Energy content of MGO (MWh/ton)	11.90

Table 3.2: Characteristics of diesel and LNG fuels (Jafarzadeh et al., 2017)

Based on the above calculations and data, the average mass flow rate in a six days journey is 0.0135 kg/s or 0.0291 liter/s. As the fuel consumption is not constant through out the journey due to fluctuations in the power requirement. For trawling vessels, the highest fuel consumption is during trawling (Gulbrandsen, 2012). It is less during moving

towards fishing ground due to less wight on vessel and less refrigeration load. It is assumed that during trawling fuel consumption is 30% higher than average, 30% less than average when moving towards fishing and return fuel flow equal to average. This is shown in Table 3.3.

Vessel position	**Mass flow (kg/s)**	**Engine power (kW)**
Towards fishing ground	0.0095 (m_1)	372
Return from fishing ground	0.0135 (m_2)	532
During trawling	0.0176 (m_3)	760

Table 3.3: Engine power and fuel consumption pattern

3.1.2 Chilling load

The chilling load of fish and water is estimated by enthalpy change from initial temperature to the final temperature. The Properties of Mackerel is utilized for calculation purpose. The internal temperature of Mackerel in Norwegian sea is around 17 °C. The RSW tanks are always pre-cooled to -1 °C before the start of fishing. So, it is assumed that the actual heating load of fish is from 10 °C. The 7 °C chilling is with already chilled water. The required chilling temperature of fish is assumed -1 °C. Water ratio in the chilling tank is set to 20%.

Tank size, m^3	**water portion, m^3**	**Mass of water, kg**	**Refrigeration load, kJ**
50	10	998,0	409,180
100	20	199,60	818,360
150	30	299,40	122,7540
200	40	399,20	163,6720
250	50	499,00	204,5900
300	60	598,80	245,5080

Table 3.4: Refrigeration load of water in tank

The corresponding size of the chilling tank for a 760 kW trawler is assumed 300 m^3 and refrigeration capacity in the range of 170 kW to 250 kW, the estimation is by interpolation of data (Skipsteknisk, 2003) and (Nordtvedt and Widell, 2019). The Figure 3.1 shows interpolation from these references. Refrigeration capacity of vessel 3 is the interpolated value.

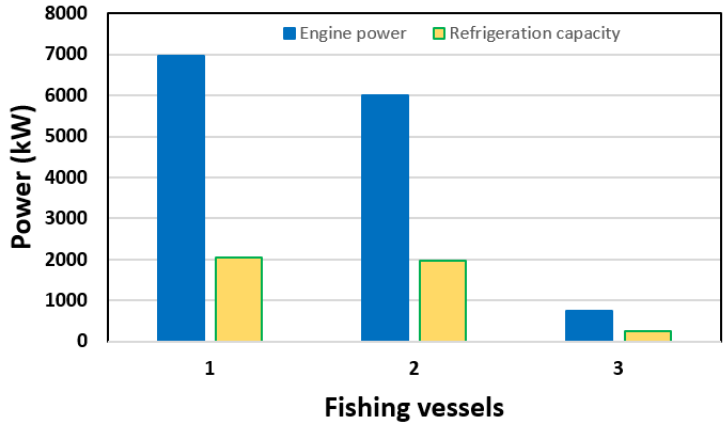

Figure 3.1: Engine power versus refrigeration capacity

The refrigeration load of water is high as compared to the same amount of fish. This effect is mainly due to the high specific heat capacity of water, which in result increase the heat load. The enthalpy change of sea water from 10 °C to -1 °C is approximately 41 kJ/kg. Sea water is the heat transfer fluid in the RSW system, so it can expect no phase change until -2 °C.

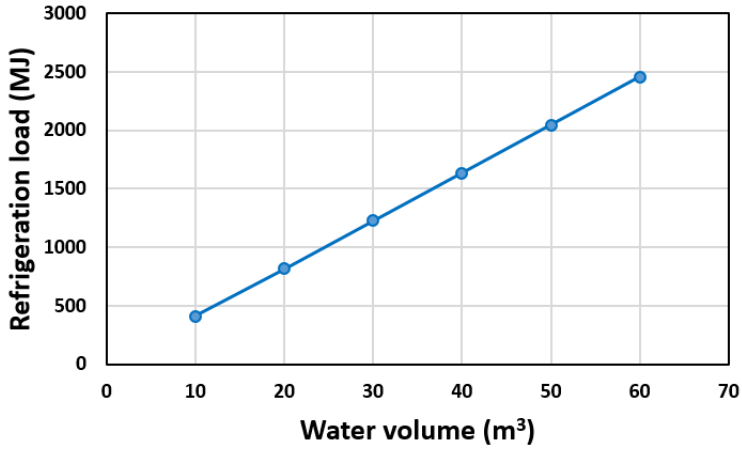

Figure 3.2: Chilling load of water (10 °C to -1 °C)

The refrigeration load of fish is shown in Table 3.5. Density is assumed constant (1072.8 kg/m^3) in the temperature range of 10 °C to -1 °C. Thermal conductivity of fish is less than water until initial freezing point, so it take more time to chill. The variation in properties of fish is small before initial freezing point. The calculation method of time tolerance (maximum allowed time to chill fish) for chilling of fish depends on the quality

standards.

Tank size, m^3	Fish portion, m^3	Mass of fish, kg	Refrigeration load, kJ
50	40	429,12.2	157,4534.4
100	80	858,24.4	314,9068.9
150	120	128,736.6	472,3603.3
200	160	171,648.8	629,8137.8
250	200	214,561	787,2672.2
300	240	257,473.2	944,7206.7

Table 3.5: Refrigeration load of fish in tank

The time tolerance for chilling of fish is set to 2 hours and the value is an approximation with respect to refrigeration capacity range 170-250 kW. For 40 m^3 of fish, the refrigeration load is 1574 MJ (Table 3.5). The required refrigeration capacity is approximately 215 kW with a chilling time tolerance of 2 hours. The fishing time is set to 48 hours (2 days). The linear distribution of catched fish is 40 m^3 in 8 hours and 240 m^3 in 48 hours. To generate a load profile, the catch is evenly distributed into six cycles, but for each cycle of 8 hours, the load divides in a non-uniform way. For each cycle of 8 hours (40 m^3 fish), there can be many cycles of catch. However, the total refrigeration load of fish in each cycle of 8 hours is not greater than 1574 MJ. An additional load of 10 kW is added after each fishing cycle due to internal heat generation by microbiological activity, recycling water and fish input losses.

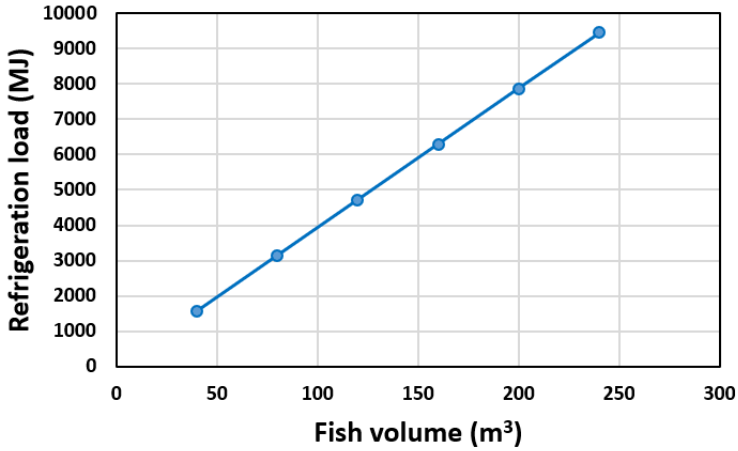

Figure 3.3: Chilling load of fish (10 °C to -1 °C)

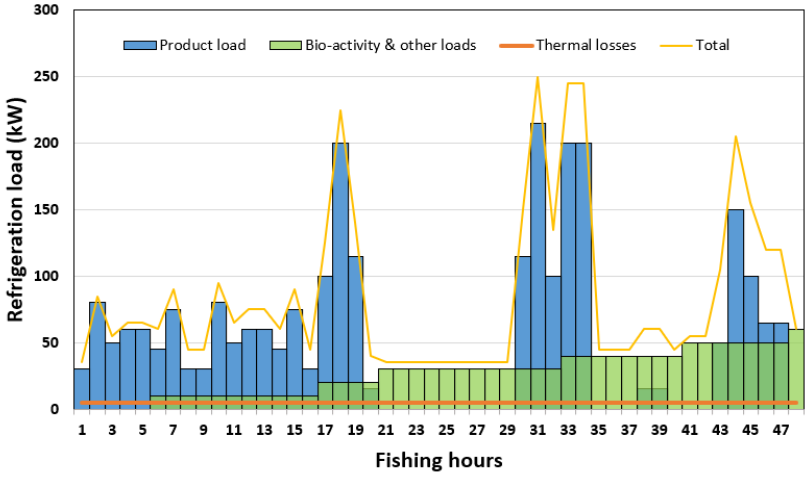

Figure 3.4: Chilling load of fish in 48 hours (10 °C to -1 °C)

Thermal losses from the surface of chilling tank is set to 5 kW with overall heat transfer coefficient of 0.25 $W/m^2.K$ and surface area of tank 1331 m^2 (assumed one big tank). A deviation from the real catch process can expect because of assumptions. A complete load profile is presented in Figure 3.4. In Figure 3.4, the product load and bio load are assumed constant for each hour and the total load is represented by linear line, which is also a case in dynamic systems.

3.1.3 Heat recovery

Heating on the fishing vessel (except onboard processing units) is for the use of crew members. The heating demand is entirely depend on the ambient conditions. In this project, heat recovery potential from the flue gases of the engine and refrigeration system is analysed. To estimate the heat recovery from the engine, it is assumed that the 760 kW trawler engine is an internal combustion four stroke piston engine. Air fuel ratio in such engines are 14.7:1 (Zahai et al., 2011). The flue (exhaust) gases leaves the engine at a normal range of 450 °C to 650 °C (Boukhanouf, 2011). For heat recovery estimation, specific heat capacity values of air (Engineering toolbox, a) is utilised for flue gases. It is supposed that the heat recovery from flue gases is used for water heating from 15 °C to 80 °C (Tap water heating) with flue gases temperature up to 100 °C from the exhaust temperature.

Fuel flow, kg/s	Air flow, kg/s	Total flow, kg/s	Exhaust gas temperature, °C	Heat capacity air, kJ/kg.K
0.0095 (m_1)	0.1397	0.1492	450	1.0805
0.0135 (m_2)	0.1985	0.2119	550	1.1039
0.0176 (m_3)	0.2587	0.2763	650	1.1257

Table 3.6: Characteristic values for heat recovery from flue gases

The energy flow of flue gases is fixed with three conditions of m_1, m_2 and m_3. The energy balance on the water side is by altering the water flow rate. Equation 3.2 is used for energy balance.

$$Q = m.C_p.\triangle T\ [kW] \tag{3.2}$$

where Q, m, C_p, $\triangle$T are the heat recovery, total flow of exhaust gases with three fuel flow conditions, heat capacity of air and temperature difference of flue gases, respectively.

The heat recovery from the refrigeration system is dependent on the refrigeration load and operational conditions. The CO_2 refrigeration system is working in the sub-critical state due to ambient temperature condition of 15 °C as described in the system description of this chapter. The recovery potential from this system is low temperature heat recovery. Water is use as heat recovery medium with inlet and final conditions of 30 °C and 35 °C in the desuperheater of the refrigeration system. The application of this heat recovery is low temperature water heating for crew members.

3.1.4 Thermal energy storage with water/ice (PCM)

A water thermal storage size of 1 m^3 is investigated on a simulation software. The function of this thermal storage is to discharge during peak loads and charge during less load condition. The thermal storage charging and discharging conditions are different from ideal scenario due to heat transfer area, heat transfer coefficient and temperature difference constraints between PCM and refrigerant. The properties of water PCM are phase change temperature 0 °C, density 999 kg/m^3 at 0 °C (liquid), specific heat capacity solid phase 2.1 kJ/kg.K and specific heat capacity of liquid phase 4.218 kJ/kg.K.

Charging

The thermal storage will charge, when the refrigeration load is less than refrigeration capacity. The temperature sensor that shows the inlet temperature of RSW stream to evaporator can use to operate charging. At less load conditions, the temperature of RSW stream will decrease and approach towards -1 °C and act as a indicator for charging.

Discharging

This PCM can not use to re-condense the super-heated vapours of refrigerant due to phase change temperature of 0 °C. However, the water stream from chilling tank will cool at peak loads. The temperature of water stream can be as high as 10 °C at high loads. The concept

of this case is that the PCM will cool down the water stream first in thermal storage and then in evaporator.

3.1.5 Thermal energy storage with E6 (PCM)

A eutectic (water solution) phase change material (PCM) E6 with a phase change temperature of -6 °C (liquid to solid) is adopted as an example for refrigerant side (PCM products LTD). This PCM is only investigated on ideal calculations of charging and discharging as it is not included in the scope of this work. A thermal storage size of 1 m^3 is investigated, whose function is to cover the peak loads and make the system adjustable with less refrigeration capacity. The PCM E6 properties are density 1110 kg/m^3, specific heat capacity 3.83 kJ/kg.K, and latent heat 300 kJ/kg (PCM products LTD). At first charging cycle in the fishing journey PCM is assumed at ambient temperature of 15 °C in the storage tank. During recharging cycles within fishing, the initial conditions are -6 °C (liquid phase). It is assumed that the storage system is fully charged in the time of moving towards fishing ground. It can also recharge during the fishing period but this depends on the load profile of Figure 3.4.

TES case (S1): 1 m^3

At the initial storage condition, moving towards fishing ground. The temperature difference between ambient temperature and storage temperature is 21 °C. This is one time temperature difference in a single fishing journey. The required refrigeration capacity for this storage is 117.3 kWh without thermal losses. If the time spam increase, the required refrigeration capacity for storage would decrease subsequently.

$$Q_{initial} = \frac{1m^3.\ 1110\frac{kg}{m^3}.\ 3.83\frac{kJ}{kg.k}.\ 21 + (1m^3.\ 1110\frac{kg}{m^3}.\ 300\frac{kJ}{kg})}{3600\ s} = 117.3\ kWh \tag{3.3}$$

In recharging during fishing, the required capacity for phase change of PCM is 92.5 kW with a precondition of no superheat of PCM during discharging process. $Q_{phasechange}$ is also the available cold energy which could use for chilling at peak loads. The discharging from cold storage is utilized in peak load times in an effort to reduce the maximum capacity of refrigeration system.

$$Q_{phasechange} = \frac{1m^3.\ 1110\frac{kg}{m^3}\ .300\frac{kJ}{kg}}{3600\ s} = 92.5\ kWh \tag{3.4}$$

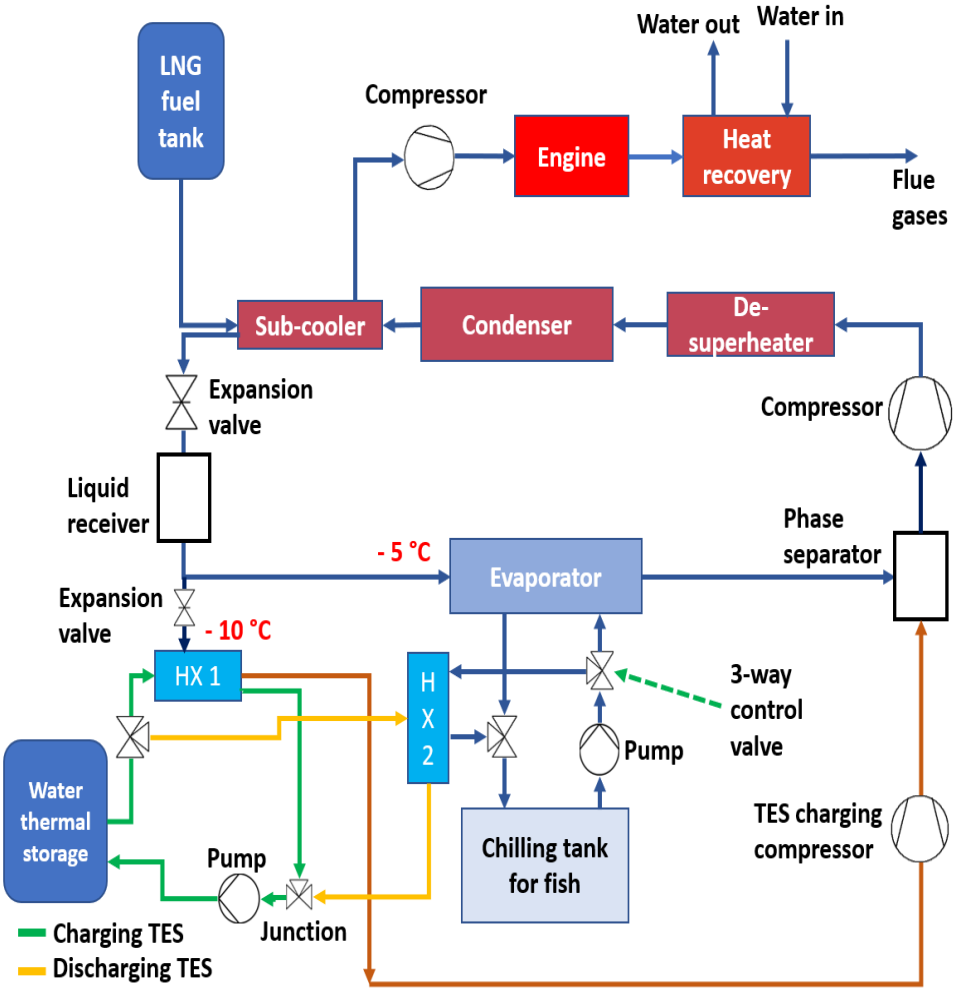

Figure 3.5: Simplified block diagram of energy system of RSW vessel

3.2 System design for freezing trawler

The main motivation of this section is to optimize the system performance by heat recovery and integration with thermal storage. The recovered heat is used for processing of rest raw material for onboard fish oil production. In this system design, the freezing refrigeration capacity and per day fish production is known from commercial system, which is described in Figure 3.9.

In freezing trawler factories, the processing of fish starts after catching and often by-passing the chilling process in RSW tanks, but if the catched fish is more then the handling capacity it would store in the holding tank or RSW tank. The initial processing of fish includes head and removal of guts. In some cases, only after gutting the whole fish is freeze onboard and process further on land facilities. Here, it is assumed that the filleting process is on the trawler and after filleting the fish is freezing onboard. The rest raw material from the fish processing of whole fish is assumed 50% (Section 2.7).

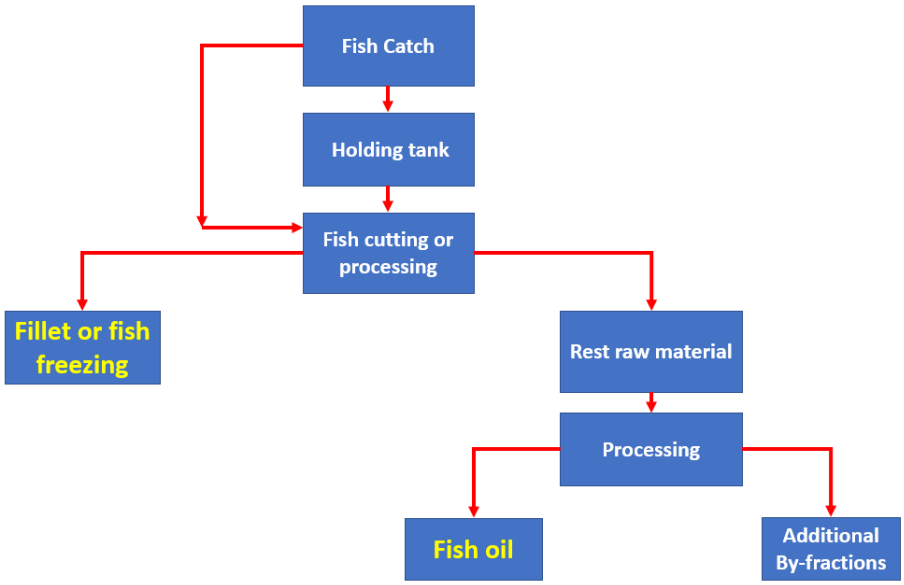

Figure 3.6: Fish flow in freezing trawler

The parameters used for thermal system design of freezing trawler are described in Table 3.7. The initial calculations are performed with respect to freezing load of one day and then reduced to 150 minutes freezing cycle.

parameters	Values
Refrigeration capacity (kW)	240
Fish handling capacity	40 tonne /day
Catched fish	40*2 tonne/day
Freezing time tolerance	2.5 hours
Rest raw material	50 % of catch
Refrigeration capacity for cargo storage	Neglected
Thermal losses	Neglected

Table 3.7: parameters for freezing trawler

3.2.1 Freezing load

Fish freezing process is similar to sea water, which contains salts in dissolved form and freezes below -1 °C. When ice forms, it does not contain salt molecules and the concentration of salts increase in the rest, which prevent the full crystallization of sea water at initial freezing point. The typical initial freezing point of food range between -0.5 °C and -2 °C (Eikevik, 2019b). Fish freezing is a transient process, Some amount of water freeze at initial freezing point that change the thermal properties of fish and concentration of salts in the remaining water of fish. This phenomenon of freezing point depression continues until final freezing temperature. The process up to required freezing point is a combination of sensible and latent heat. According to parameters discussed in Table 3.7, the catched fish in one day is 76.95 m^3 and 50% are the rest raw material. The fillets volume for freezing is 38.47 m^3. The freezing load for this volume of fish from 10 °C to -20 °C is presented in Figure 3.7.

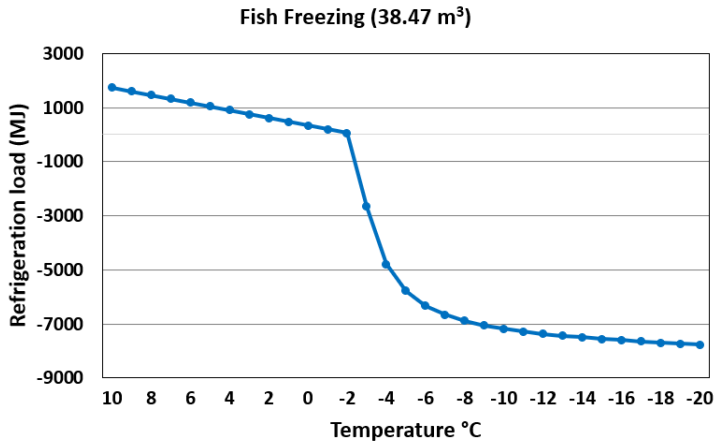

Figure 3.7: Freezing load of fish from 10 °C to -20 °C

The Figure 3.7 shows the heat load for one day. The division of volume of fish for each freezing cycle depends upon the designed strategy. For example, if the one day catch is divided into 5 cycles then the volume of fish for each cycle is 7.69 m^3 (8237 kg at 10 °C for Mackerel composition). Mean heat load for this volume of fish during each freezing cycle of 2.5 hours is 211 kW. Mean heat load indicates that the refrigeration system needs to run at constant capacity of 211 kW to finish process in 2.5 hours. In actual systems, the capacity adjusts according to heat load. It can say that the system run at full capacity (may need additional capacity) at the start of the process and even less than 211 kW at any instant close to initial freezing point. If thermal losses are added into mean load, then it will increase by few kilowatts. To have real freezing load profile, heat transfer area of the plate freezer, overall heat transfer coefficient, product handling capacity of each cycle and fish block size must known.

In real freezing systems with multiple plate freezers, each freezing cycle starts after 40-45 minutes. The reasons are to avoid high starting loads, defrosting of each freezer at different time and high production capacity. The Figure 3.8 shows a freezing load profile of a system with multiple plate freezers. It is adapted from a small commercial refrigeration system and interpolated for 240 kW system (reference system). The maximum time when the load is higher than capacity is 10 minutes.

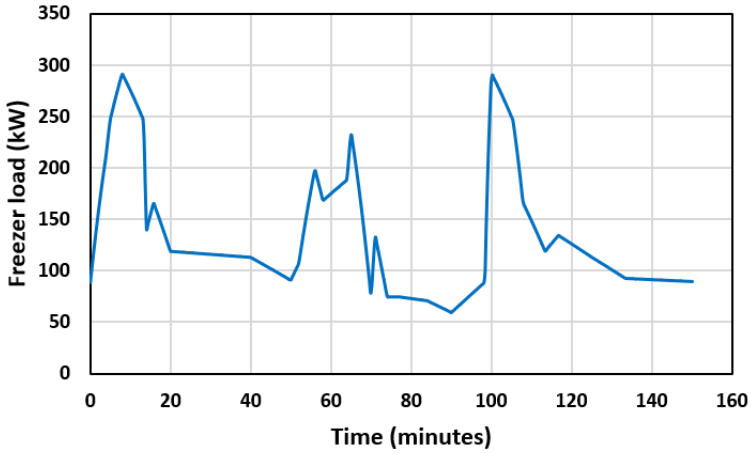

Figure 3.8: Freezing load profile of fish with multiple plate freezers

3.2.2 Refrigeration system for freezing

The advance refrigeration systems are integrated cooling and heating systems. The system described in Figure 3.9 is a CO_2 booster refrigeration system working in the trans-critical state. The operating conditions of the system are 6.8 bar (-50 °C) on the low pressure side and 90 bar on the high pressure side.

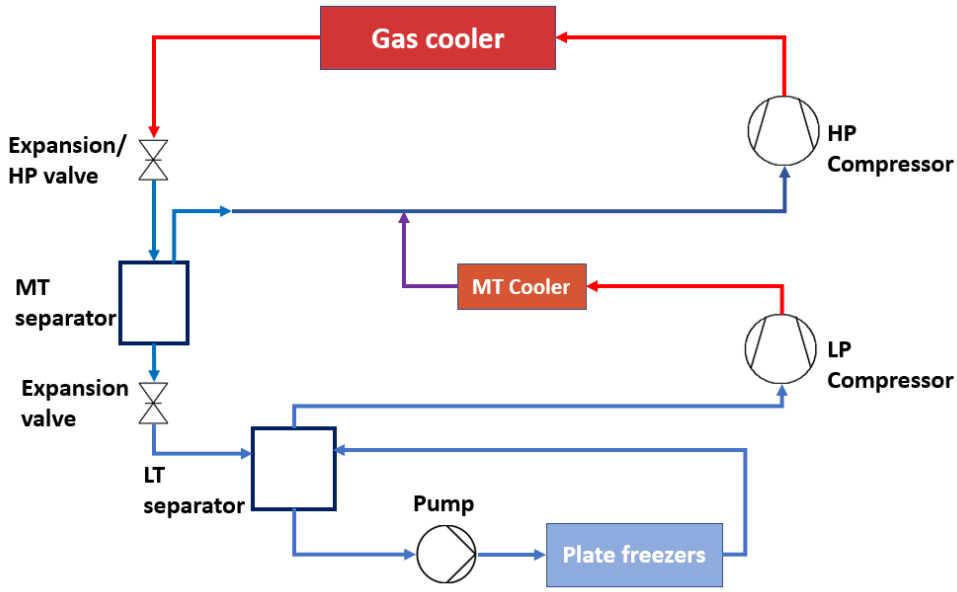

Figure 3.9: Freezing refrigeration system (commercial system)

In Figure 3.9, the refrigeration load is coming from the plate freezers. The vapour quality of the refrigerant in the return line to the low temperature (LT) separator is dependent on the load in plate freezers. If the refrigeration capacity is less than the load, super-heating of refrigerant at the end of plate freezer will happen and result in elevation of temperature in LT separator. In opposite scenario, vapour quality will be less than 1. LT separator ensure complete liquid flow (vapour quality 0) in plate freezer and make flooded evaporator condition with high heat transfer rate. Low pressure (LP) compressor lift the pressure from 6.8 bar to 26.4 bar. Medium temperature (MT) cooler reject heat to water and cool the refrigerant and then mix with the gas coming from MT separator. Temperature of the gas coming from MT separator is -10.1 °C (26.4 bar). High pressure (HP) compressor lift from 26.4 bar to 90 bar. The system can operate in sub-critical or trans-critical but this depend on the heating requirement or ambient condition. Gas cooler cool the gas and then gas expand in the expansion valve and reach the conditions of -10.1 °C (26.4 bar) in MT separator.

3.2.3 Heat recovery from freezing refrigeration system

Heat recovery from the refrigeration system is from two levels. One is from MT cooler and other from gas cooler. Heat recovery from MT cooler is low and from gas cooler is high temperature. Heat recovery potential from the refrigeration system depend on the load profile, higher the load then higher is the heat recovery. Heat can also recover from oil cooling of compressor but this is not included in this work. Heat recovery from the refrigeration can be used to heat rest raw material for onboard fish oil production, which

will further discuss in sub-section 3.2.4. Gas cooler and MT cooler are shown in Figure 3.9.

3.2.4 Fish oil production from rest raw material

For fish oil production, the system is designed in coherence with the freezing system. The rest raw material from processing of fish for each cycle of 150 minutes corresponds to 3000 kg. The process of fish oil production is described in sub-section 2.7.1. The amount of heat, which is needed to raise temperature from 10 °C to 90 °C is shown in Figure 3.10. The equations which were used to calculate thermal properties of Mackerel (sub-section 2.6.1) are valid in the range of -40 °C and 40 °C. As the heating behaviour of fish is linear, so interpolation is used to calculate properties up to 90 °C.

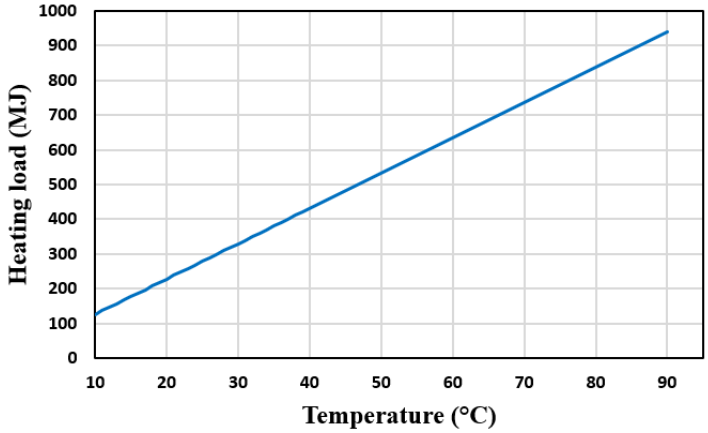

Figure 3.10: Heat load of rest raw material heating

3.2.5 Thermal storage for freezing

CO_2 as a PCM is investigated for integration with freezing system. The purpose of this PCM integration is to boost the refrigeration capacity at peak loads and reduce the freezing time of each cycle. Each m^3 of space on fishing vessel is very important. So, a size of 1 m^3 is initially analysed. The simulations for PCM were performed on a dynamic simulation software Dymola and complete control strategy will discuss in chapter 4. The storage conditions of PCM are -56.6 °C and 8 bar. The phase change (Solid-liquid) temperature of PCM at 8 bar is -56.6 °C (Figure 2.15).

Charging

Thermal storage will charge, when the refrigeration load is less than refrigeration capacity. When the refrigeration load decreases, the vapour fraction of refrigerant from the freezer start decreasing and liquid level in LT separator begin to increase. This sends signal to compressor/expansion valve and refrigerant pump to decrease flow. Vapour fraction sensor

and liquid/pressure level sensor in LT separator can use as a signal to open flow for thermal storage charging. The charging conditions of CO_2 refrigerant for thermal storage in main simulation case are 3 bar and -68.3 °C.

Discharging

Thermal storage energy is required, when the refrigeration load increase than the refrigeration capacity. When it happens, the refrigerant super-heat at the outlet of freezer and more and more gas enters into LT separator. This cause the pressure in the LT separator to increase, which in result elevate the temperature as well. This causes the freezing time to increase. To utilize the cold energy, temperature sensor will send signal of super-heat as an indication to open the valve towards thermal storage. The super-heated vapour will partially re-condense in thermal storage and help to maintain the pressure in LT separator. The discharging conditions of thermal storage are studied with constant 8 K super-heat after evaporator.

Chapter 4

Simulations

This chapter will describe the simulation tools and software models used for energy analysis of chilling and freezing vessel. The models are simulated with the load and system conditions designed in chapter 3.

4.1 Simulation software

Dymola software with components and refrigerant libraries from TLK-Thermo GmbH were utilized for dynamic simulations. Four libraries were used, TIL 3.5.0 for components like heat exchangers, compressor and valves, TIL Media 3.5.0 for refrigerants and secondary fluids, TIL file reader 3.5.2 to read and input refrigeration load files and TIL AddOn SLEHX for thermal storage. DaVE is another software from TLK which is used for plotting of Dymola results. TLK DaVE also make it possible to visualize results on Ph and Ts diagrams.The software read two input load formats, Matlab (.mat) and Excel (.csv). The software has built in components with a high degree of control on the input parameters and boundary conditions.

4.2 LNG cold recovery

In this section, LNG cold recovery is estimated on dynamic basis. Pure methane is used as an input for simplifications and some limitations in software. Inlet conditions of LNG are 3.5 bar pressure and at bubble point. A tube and tube HX is used as LNG HX and its properties are thermal resistance 1e-10 K/W and heat transfer area 3.1 m^2. Glycol is used as a secondary heat transfer fluid with an inlet conditions of - 8 °C, 1 bar and variable flow in the LNG HX. The heat rejection is in second heat exchanger to water flow. The simulation run for a time spam of six days with first order linear interpolation of three mass flows. The three LNG fuel flow conditions are already discussed in Table 3.3. A model for LNG cold recovery potential is shown in Figure 4.1.

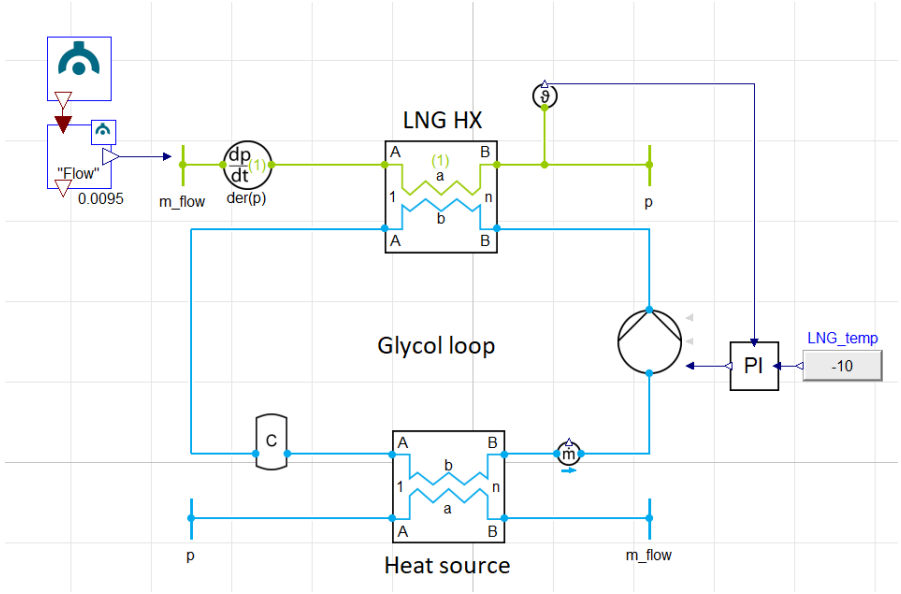

Figure 4.1: LNG cold recovery potential

4.3 Chilling system simulation model

The initial model was started with a simple CO_2 refrigeration system at different refrigeration capacities and complexity level increased by adding LNG sub-cooler and de-superheater according to system layout in Figure 3.5. Each model analysed completely before addition of complexity. The convective heat transfer coefficients of refrigerants and secondary fluids are according to their properties. Stainless steel plate heat exchangers (HX) are used for all simulation scenarios.

Evaporator super-heat is controlled by expansion valve opening with PI controller and the super-heat value is fixed to 5 K to ensure safe operation at low loads. Refrigeration load in the evaporator can control by RSW flow and temperature variations. The control of load in the simulation is with variable water flow , which is provided as an input .csv file to TIL file reader. Efficient Compressor (compressor type in Dymola) is controlled by two PI controllers, one control the relative displacement of compressor by using RSW temperature at outlet of evaporator as an input. Second controller control the suction pressure limits by adjusting frequency (Compressor can work with fixed frequency, no special need for this controller). Isentropic efficiency of compressor is fixed to 70%. Outlet temperature from the de-superheater is controlled by a mass flow of pump with PI controller, which take outlet temperature of refrigerant from desuperheater as an input. Inlet and outlet temperature of water in desuperheater is fixed to 30 °C and 35 °C, respectively. The outlet temperature of condenser is controlled by adjusting the water flow in condenser with PI controller. To remove the condenser heat, water with an inlet temperature of 15 °C (ambient temperature) is used. After the condenser, a phase separator is added to ensure the

liquid flow to the LNG HX. Controlling of LNG HX is challenging due to independent behaviour of refrigeration load and fuel supply. It is controlled in the simulation by adjusting the heat transfer area and heat transfer coefficient in such a way that gas temperature could not increase than -6 °C at minimum LNG flow. However, the precise way of controlling is by an indirect circuit as described in section 4.2. The complete simulation model is presented in Appendix B.

4.3.1 Chilling refrigeration system (C1)

In this scenario, a refrigeration system set up with an evaporation and condensation temperature of -5 °C and 20 °C, respectively. In all simulations, the inlet RSW temperature from fish tank to evaporator is fixed to 5 °C. The load variations in the evaporator is by altering the flow rate of water. The flow rate values are adjusted in comparison with the refrigeration load. The simulation time for all cases is 48 hours (2 days) and this time is in correlation with the system design for chilling system.

4.3.2 Chilling system with LNG sub-cooler (C2)

In this case, LNG sub-cooler is added to the simple refrigeration system (C1). The sub-cooler is added after the condenser. The aspiration is to transfer the vaporization energy of LNG to the refrigerant. A constant LNG flow of m_2 is used as an input to LNG heat exchanger. The inlet condition of the fuel is same as expressed in section 4.2.

4.3.3 Chilling system with desuperheater (C3)

The simulation conditions for this case is similar to simple refrigeration cycle (C1). The new addition is desuperheater. This heat exchanger is extracting heat at high temperature level as compared to the condenser. The heat extraction is with variable speed drive pump, which is already discussed in section 4.3.

4.3.4 Chilling system with desuperheater and LNG sub-cooler (C4)

This simulation study is the combination of above scenarios (C2 and C3). LNG sub-cooler and desuperheater adjust in the simple refrigeration system (C1). The system with this combination is shown in Figure 4.2. The refrigerant is coming from compressor and discharge heat first in desuperheater then condenser and finally in LNG HX.

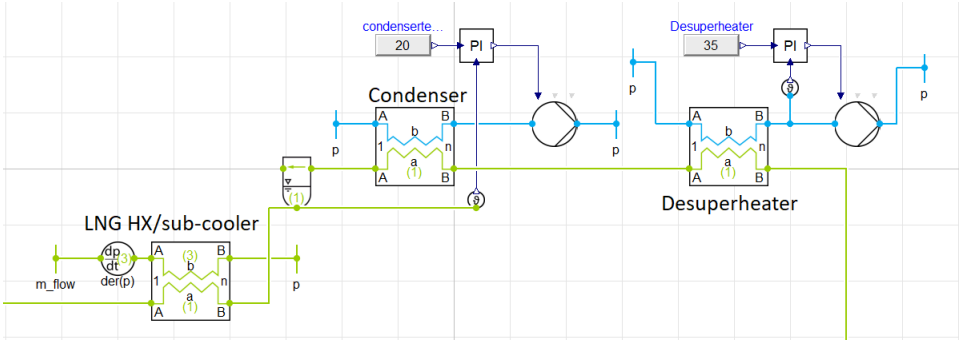

Figure 4.2: Ref system with sub-cooler and desuperheater

4.4 Thermal Storage water/ice for chilling vessel

In chilling vessels, water in the RSW tanks always chill before catch of fish. This instant is an option to completely charge the thermal storage before start of fishing. TES charging rate depend on the TES size, TES thermal properties and temperature difference between PCM and charging flow and the available charging power. According to the designed chilling load profile (Figure 3.4), there is always a potential for charging storage except 3 instants. So, the purpose is to reduce the installed refrigeration capacity by implementing water TES. The charging of water TES is with indirect circuit as described in Figure 3.5. At higher loads, the discharging will occur. Water stream from RSW tank will pass first from storage and then evaporator. The charging and discharging of TES is performed in two different simulations but the internal properties and their charging and discharging level were maintained. The properties of thermal storage is shown in Table 4.1.

Characteristics	**Values**
Length (m)	1
Width (m)	1
Height (m)	1
Material	Aluminium
Tube inner diameter (mm)	10
Tube wall thickness (mm)	0.5
Number of tubes	30*30
PCM phase change temperature (°C)	0
Total heat transfer area tube inner (m^2)	28.27
Total heat transfer area tube outer (m^2)	31.1

Table 4.1: Characteristics of thermal storage

4.4.1 Water/ice PCM charging

The charging simulation conditions in Figure 4.3 are set in resemblance with chilling system described in Figure 3.5. The secondary fluid for charging is glycol. The inlet tempera-

ture of glycol to TES is -5 °C during charging. The charging flow is fixed to two conditions 2 kg/s and 6 kg/s.The initial temperature of PCM is assumed 1 °C. The glycol is taking cold energy from refrigerant side, whose evaporation temperature is -10 °C, that side is not integrated in simulation for simplification. The outlet temperature of glycol after TES in the start of simulatuion was -2.7 °C. At fully charged condition, the temperature reduced to -5 °C (no charging).

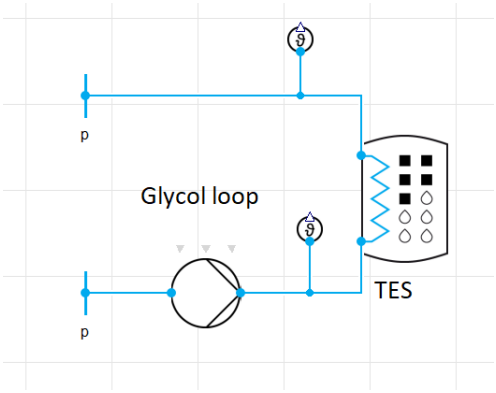

Figure 4.3: Thermal storage (water) charging

4.4.2 Water/ice PCM discharging with C1 system

In this PCM discharging method, thermal storage is installed before evaporator. At peak loads, water stream from RSW tank would first chill in thermal storage and then in evaporator. The discharging analysis is done by varying the inlet temperature of water stream from 10 °C to 8 °C at a constant flow of 6.8 kg/s. The simulation time is 1 hour, which is according to peak load conditions designed in Figure 3.4. The secondary fluid of TES side is glycol and the flow rate of glycol loop pump is also 6.8 kg/s.

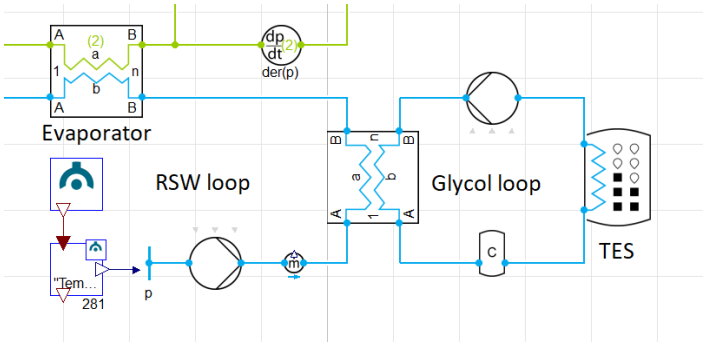

Figure 4.4: Thermal storage (water) discharging

4.5 Freezing system simulation model

The freezing refrigeration system model on Dymola was created with some simplifications. The initial freezing model was simple dynamic two stage system with flooded evaporator condition and later analysed with charging and discharging scenarios of thermal storage. The simulated model is similar to the system described in Figure 3.9. All Plate heat exchangers with same material i.e. stainless steel were used.

Evaporator outlet temperature is controlled by enthalpy/vapour fraction sensor that send signal to pump to increase or decrease flow rate. The enthalpy was fixed to 368 kJ/kg with vapour fraction of 0.80. The heat load to the evaporator is controlled by input load file. Freezing load profile of Figure 3.8 is used as an input to evaporator for the dynamic simulations. LP compressor is controlled by one PI controllers. The controller controls the relative displacement of the compressor. The compressor work with constant frequency of 60 Hz. After LT compressor, the refrigerant is cool down up to 15 °C (still gas) in MT cooler. The refrigerant then combines with flash gas coming from MT separator in junction (same pressure of both streams) and then both move towards HT compressor. HT compressor lift the gas from medium pressure (26.4 bar) to high pressure (90 bar). HT compressor is also controlled by one PI controller, which controls the relative displacement of the compressor. This compressor also works with constant frequency of 60 Hz. Efficiencies of both compressors are 70%. Two heat exchangers are used after HT compressor to reject heat. Refrigerant temperature at the exit of first heat exchanger is 45 °C and second 15 °C. Both temperatures are controlled by adjustment of water flow rates with PI controller. The refrigerant then expand in high pressure control/expansion valve from 90 bar to 26.4 bar. This valve is controlled by PI controller which takes high pressure as an input and maintain a pressure of 90 bar. In the MT separator, flash gas flow towards HT compressor and liquid towards LT expansion valve. LT valve reduce the pressure from 26.4 bar to 6.8 bar. The PI controller of this valve takes LT separator liquid level as an input and maintain the value of 0.5 in LT separator (Complete simulation model in Appendix B.

4.5.1 Freezing refrigeration system (S1)

The dynamic freezing refrigeration system is made on a software similar to a system describe in Figure 3.9. The input load file indicates the freezing load from 10 °C to -20 °C. In Figure 4.5, evaporator represent the plate freezers. The vapour fraction after evaporator is controlled with variable frequency drive pump at various load. The simulation run for a freezing cycle of 150 minutes (2.5 hours).

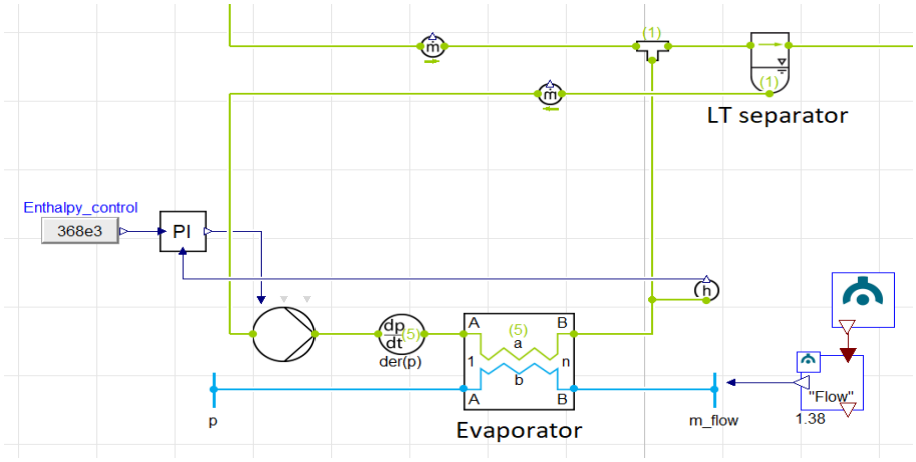

Figure 4.5: Freezing refrigeration system

4.5.2 Freezing system with LNG sub-cooler (S2)

In this case, LNG sub-cooler is introduced in S1 system after MT separator. The refrigerant from MT separator is sub-cooled before further expansion to 6.8 bar. In Figure 4.6, the glycol loop pump adjust flow rate in correlation with refrigerant flow in sub-cooler. The LNG flow rate in LNG HX is fixed to 0.0135 kg/s (m_2). The LNG inlet conditions are identical as discussed in section 3.3.

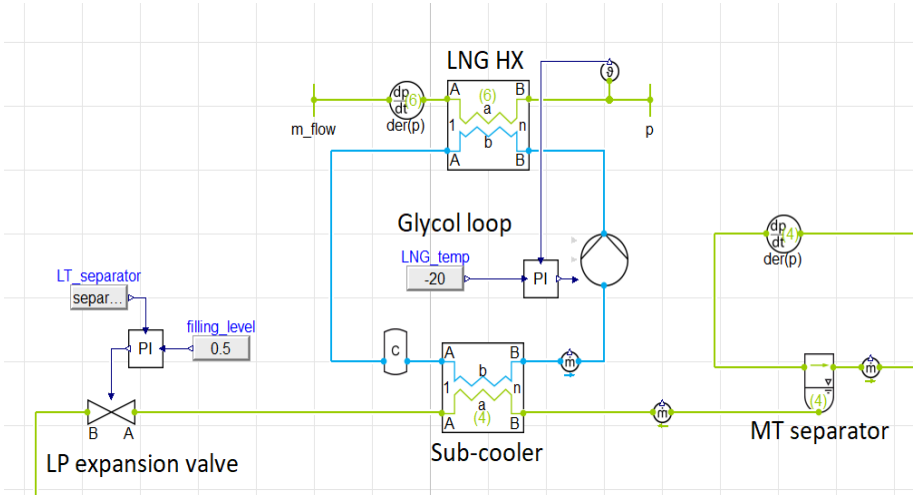

Figure 4.6: Freezing system with LNG sub-cooler

4.6 CO_2 thermal storage for freezing vessel

The freezing load profile of Figure 3.8 shows that during the first 10 minutes of each cycle, the product load is high enough to utilize thermal storage. After 10 minutes the product load is less than refrigeration capacity and this extra capacity is used to charge thermal storage. The charging time of thermal storage between peaks is 40 minutes. The initial temperature of PCM is assumed -55 °C. During charging, the flow rate of refrigerant is controlled by thermal storage compressor with PI controllers. The size of thermal storage is high enough to have super heated vapours after thermal storage. Pressure lift of refrigerant from thermal storage condition to LT separator is also studied with ejector, which would discuss in the sub section 4.6.2. The characteristics and parameters of CO_2 thermal storage are shown in Table 4.2.

Characteristics	**Values**
Length (m)	1
Width (m)	1
Height (m)	1
Material	Aluminium
Tube inner diameter (mm)	10
Tube wall thickness (mm)	0.5
Number of tubes	34*34
PCM phase change temperature (°C)	-56.6
Total heat transfer area tube inner (m^2)	36.3
Total heat transfer area tube outer (m^2)	40

Table 4.2: Characteristics of thermal storage

4.6.1 Freezing system with TES charging and compressor (S3)

In this case, CO_2 thermal storage is charged with S1 system. On the liquid line of LT separator, a junction is added to divide flow between evaporator and thermal storage. After thermal storage, compressor lift the pressure of refrigerant from 3 bar to 6.8 bar and the gas flow towards LP compressor. The charging time for this simulation is 40 minutes. The charging time is according to condition defined in Figure 3.8. The charging system is shown in Figure 4.7.

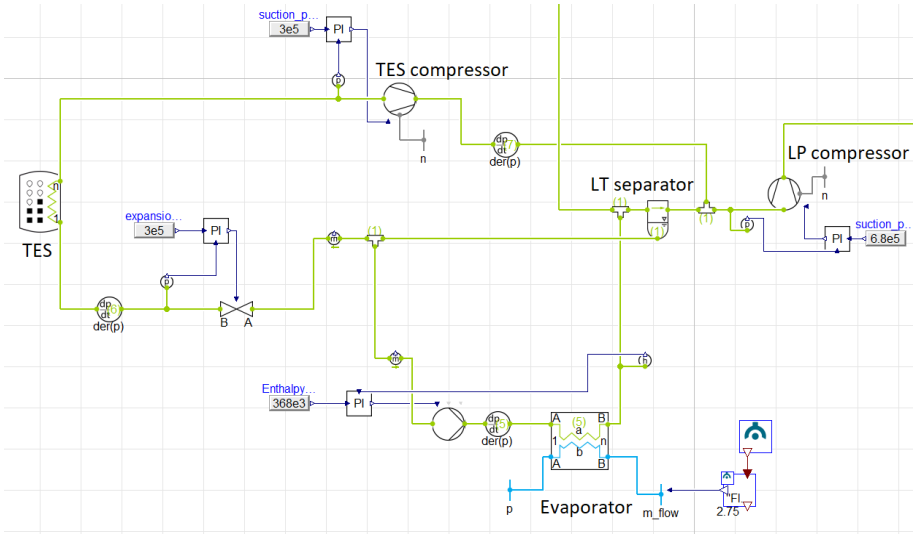

Figure 4.7: Freezing system with TES charging

4.6.2 Freezing system with TES charging and ejector (S4)

In this case, two phase ejector is installed instead of compressor to lift pressure to 6.8 bar. In Figure 4.8, the liquid refrigerant is coming from MT separator and gas suction from thermal storage side. Ejector convert the pressure of both streams (liquid line from MT separator and gas line from thermal storage) to LT separator pressure (6.8 bar). The ejector efficiency is 15% in simulations. The PI controller of ejector takes the liquid level of LT separator as an input to control and maintain the level of 0.5.

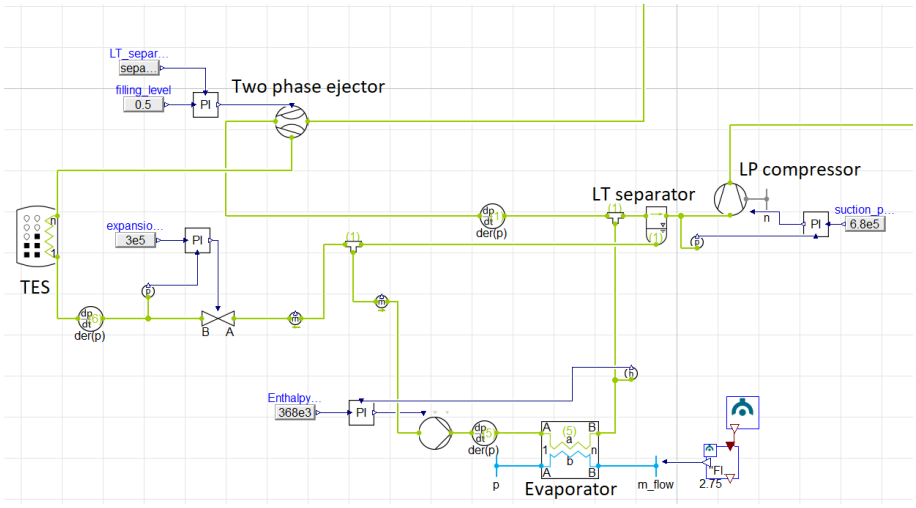

Figure 4.8: Freezing system with ejector and TES charging

4.6.3 Freezing system with TES discharging (S5)

In this case, the product load increased from 240 kW (maximum capacity of system). The discharging of thermal storage is with constant super-heat of 8 K. In simulation, the super-heat is controlled with the PI controller of the pump. The thermal storage properties were maintained in connection with charging conditions. The simulation time for this scenario is 10 minutes, the peak load condition of freezing is according to the description of Figure 3.8.

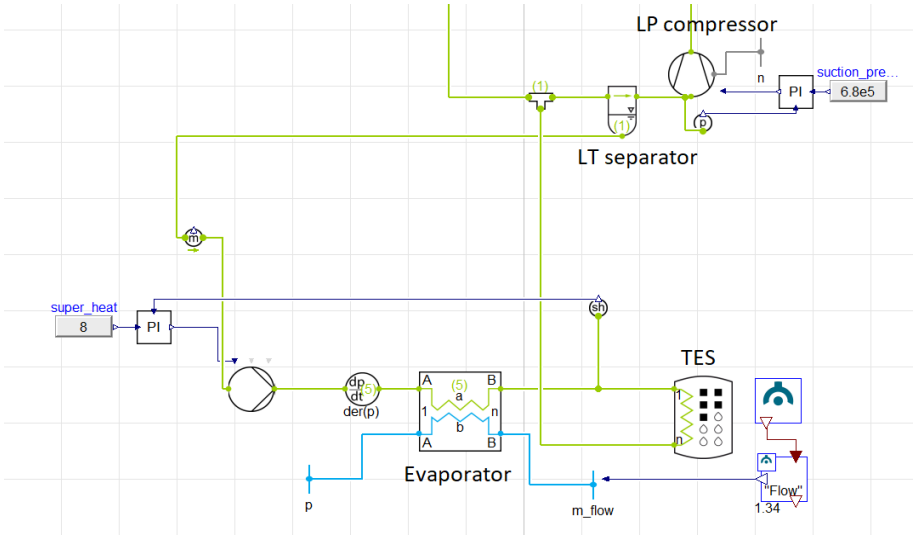

Figure 4.9: Freezing system with TES discharging

Chapter 5

Results

This chapter describe the results and discussions of the simulated and calculated results. A result comparison of different refrigeration scenarios for chilling system, heat recovery and thermal storage is presented. A similar analysis is also performed for freezing system.

The power calculation of COP chilling and COP freezing only account for compressor work and evaporator output. Combined COP calculation include output from evaporator and condenser/gas cooler. Input power to pumps are neglected due to its small value as compared to compressor work. Compressor efficiency is already included in system calculations.

5.1 LNG cold recovery

The maximum cold recovery is 13.7 kW and minimum recovery is 7.1 kW at LNG flow of m_3 (maximum) and m_1 (minimum), respectively. The methane (LNG) temperature after the LNG HX is in the range of -6 °C and -10 °C. The temperature after LNG HX is controlled by glycol flow rate and optimizing heat transfer area and thermal resistance of HX. The vaporization temperature after LNG HX depend on the engine requirements and the driving component of fuel i.e. pump or compressor. The choice of fuel outlet temperature is on the assumption that the reference system is equipped with low pressure engine (sub-section 2.8.1). LNG cold recovery from the simulation results is presented in Figure 5.1. The Cold recovery values are plotted with respect to designed case of six days (144 hours) journey. A simulation results with indirect circuit between LNG HX and the glycol loop shows good controlling of the system.

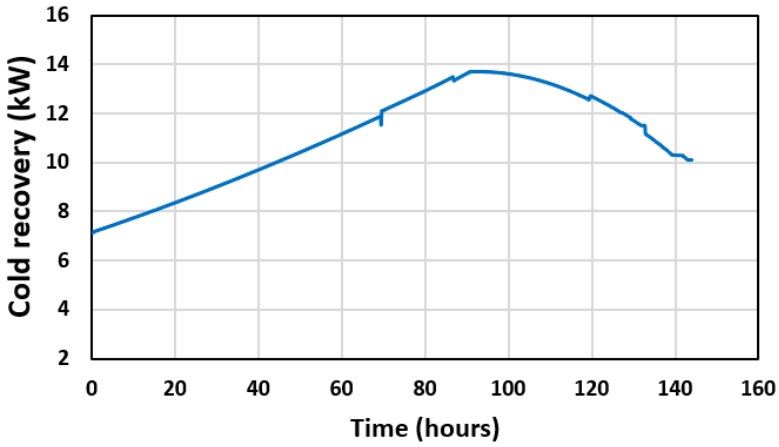

Figure 5.1: LNG cold recovery at LNG various fuel flow

In Figure 5.2, the plotted results are according to the fuel consumption values and is satisfactory to have an overview of LNG cold recovery for 760 kW vessel.

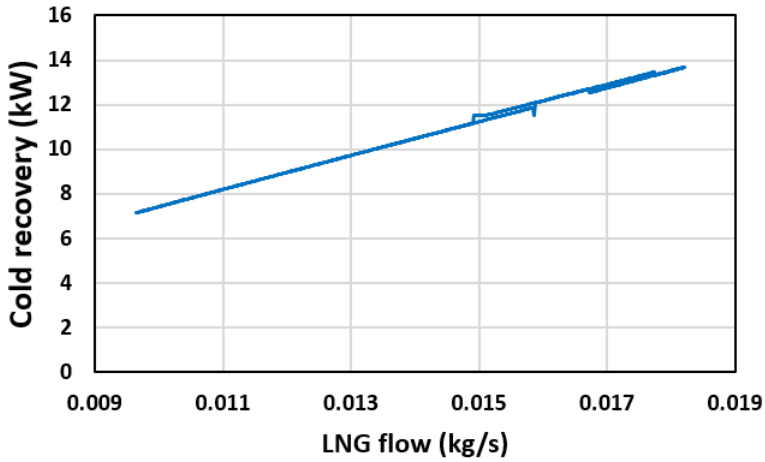

Figure 5.2: LNG cold recovery at LNG various fuel flow.

5.2 Simulation results of Chilling system

5.2.1 Chilling refrigeration system (C1)

As a first case, the simulation run with a simple refrigeration system without any desuperheater and sub-cooler. A load profile of Figure 3.4 is used. The results are presented in Figure 5.3. The maximum achieved COP in this case is 5.89 at a load of 35 kW and lowest

COP 4.03 at a load of 250 kW. The COP variations is mainly due to pressure fluctuations in the system. At lower load, the evaporation pressure increased because the evaporator is designed for high loads. The reduction of pressure lift in compressor reflects the high COP at low load and lower COP at high load.

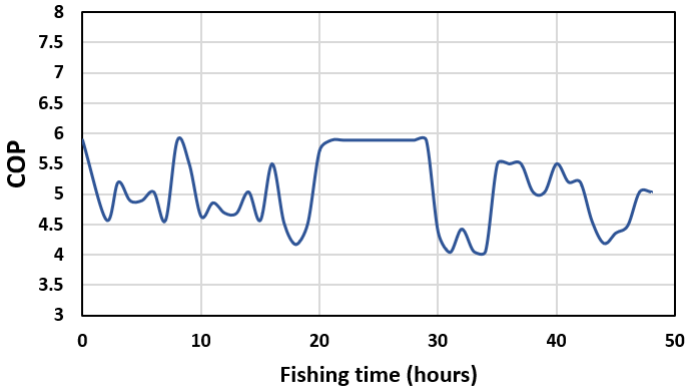

Figure 5.3: COP of the refrigeration system

5.2.2 Chilling system with LNG sub-cooler (C2)

In this scenario, LNG HX is installed after condenser in the C1 refrigeration system and used as a sub-cooler. The results are shown in Figure 5.4. The maximum COP is 7.15 at a load of 35 kW and minimum 4.4 at a load of 250 kW. The sub-cooling temperature difference with LNG cold is very high at low loads. At a load of 35 kW and refrigerant flow 0.142 kg/s, the refrigerant temperature and pressure after LNG HX is -2.8 °C and 57.29 bar, respectively. The simulation did not show any error but having such low temperature before expansion valve for CO_2 systems may cause issues.

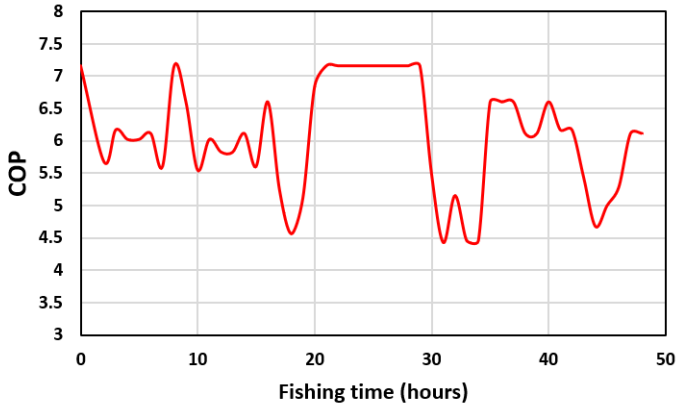

Figure 5.4: COP of the system with LNG sub-cooler

5.2.3 Chilling system with desuperheater (C3)

In this case, desuperheater is added to the C1 refrigeration system. A COP of this system is presented in Figure 5.5. The maximum and minimum temperature after compressor is 62 °C and 52 °C, respectively. Increase in temperature after compressor is a consequence of pressure increment from 57.29 bar to 62 bar (high pressure deviation from the preset value after compressor is only observed in this case) at high loads. Inlet and outlet water temperature from desuperheater was fixed by considering the temperatures after compressor. It is observed that the COP in this case is less than the C1 case, which is mainly due to the addition of desuperheater. In C1 case, all heat was removed in condenser with inlet water temperature of 15 °C. In desuperheater, the temperature difference between refrigerant and inlet water stream is less as compared to condenser, which caused the compressor to do more work to dissipate heat. If the heat recovery from the desuperheater is included in calculation, COP of this case will also increase. More details of heat recovery would discuss in section 5.2.6.

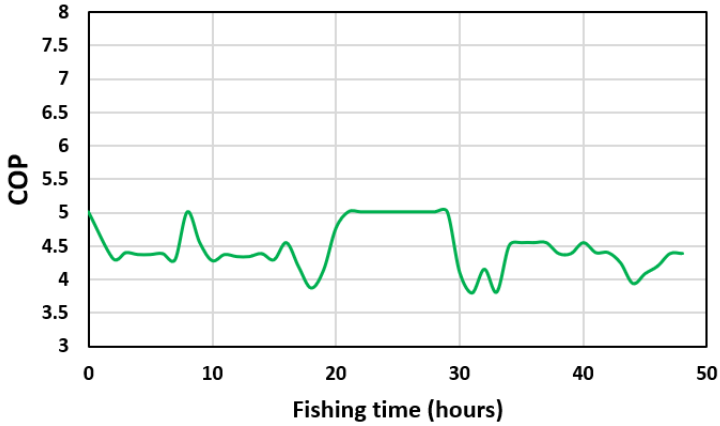

Figure 5.5: COP of the system with desuperheater

5.2.4 Chilling system with desuperheater and LNG sub-cooler (C4)

In this case, LNG sub-cooler and desuperheater is added to the C1 case, the results are improved COP as compared to C3 case. In this scenario, COP is also calculated by using only evaporation load. The results are shown in Figure 5.6. The maximum sub-cooling effect at a load of 35 kW and refrigerant flow 0.143 kg/s after LNG HX decrease to a value of -0.96 °C (compared to C2 case). This less value than C2 case can correlate with the mass flow of refrigerant, which is high in this case. Pressure after the compressor was also remained to preset value of 57.29 bar with minor fluctuations.

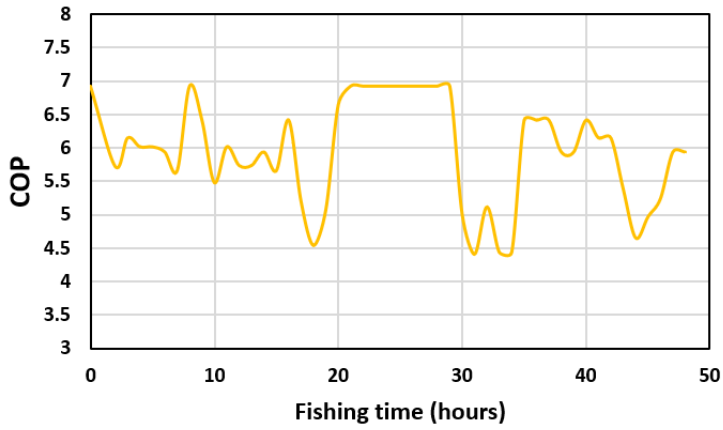

Figure 5.6: COP with sub-cooler and desuperheater with C1 system

5.2.5 Summarized results of different cases

The combined results of above four cases C1, C2, C3 and C4 are presented in Figure 5.7 and 5.8. The results show the highest COP in C2 case and the least in C3 case. The COP of these systems are according to the designed load profile of Figure 3.4. The real fishing pattern can be different from this case, the real pattern would alter the refrigerant load and subsequently effect the COP of these systems.

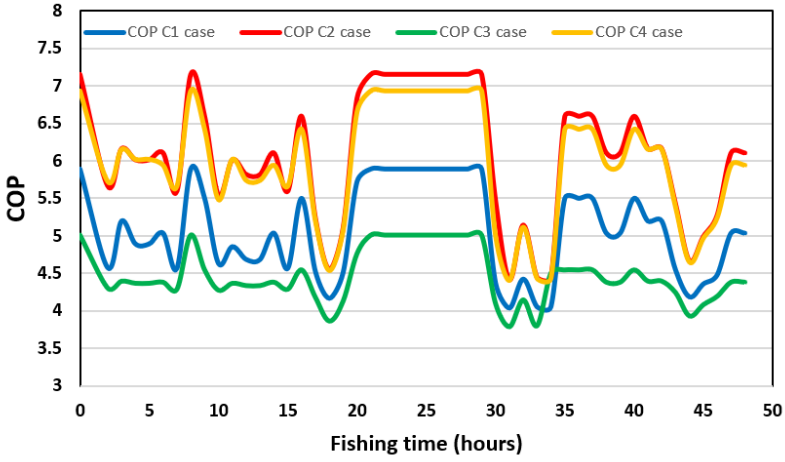

Figure 5.7: COP of above cases at load profile of Figure 3.4

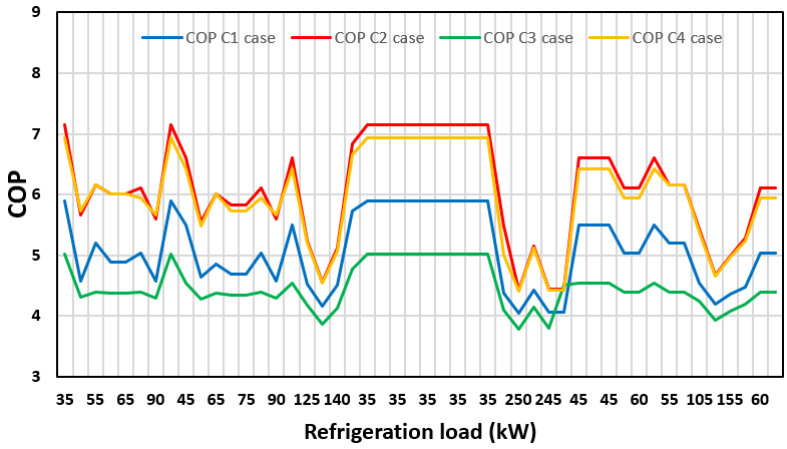

Figure 5.8: COP of above cases versus load profile of Figure 3.4

Figure 5.8 shows the refrigeration load during the fishing period of 48 hours and their corresponding COP. The results are similar to the Figure 5.7 but this figure show refrigeration load on x axis.

The performance difference between C3 and rest of the case at high loads is less, heat recovery looks a viable option and COP can be high by adding the useful heat recovery from desuperheater in COP calculations.

5.2.6 Heat recovery

Heat recovery from the flue gases with three fuel flow conditions are shown in Figure 5.9. The values are in the range of 56 kW to 172 kW. Mass flow of exhaust gases is a dynamic factor, speed fluctuations of engine would directly influence the heat recovery potential. Heat recovery from the flue gases under current conditions has potential to cover average hot water demand of 114 kWh. Heating demand and supply can be different at any time.

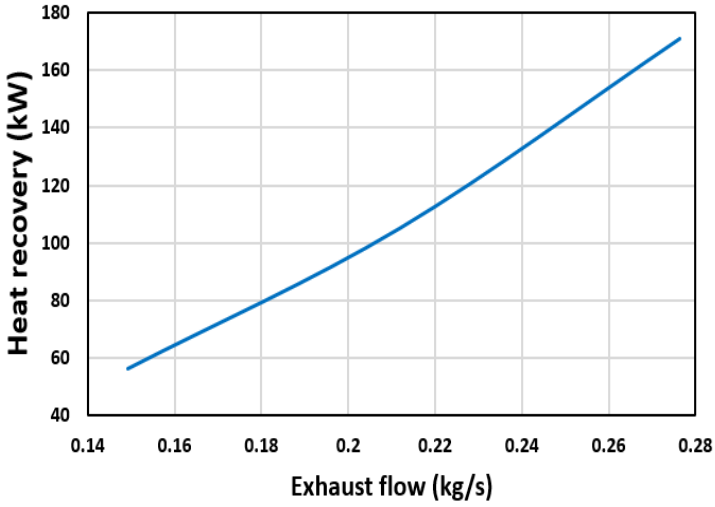

Figure 5.9: Engine exhaust flow versus heat recovery

Heat recovery potential from flue gases are dependent on air fuel ratio in the engine and temperature of flue gases. These two parameters are different for various engines. Alteration of these two factors would lead to different values of heat recovery.

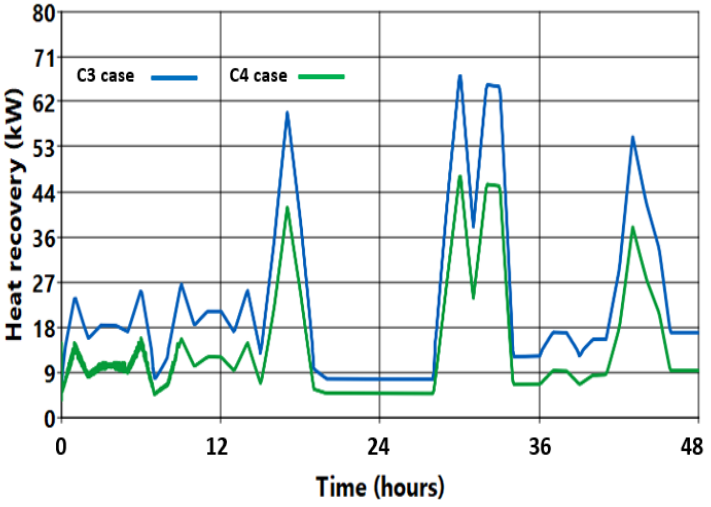

Figure 5.10: Heat recovery with desuperheater

Heat recovery potential from the refrigeration system is analysed with C3 and C4 case. The results are shown in Figure 5.15. The values are in the range of 8 kW to 68 kW. In C4 case, the heat recovery is less, there are two reasons for less recovery. One is that the heat

after compressor is dissipated by three heat exchangers and second the COP of C4 case is high, which means less work by compressor. Heat recovery from the refrigeration system under specified conditions has potential to cover average space heating demand of 38 kWh.

A small hot water storage system is a useful option on the fishing vessel. Heat recovery from both cases desuperheater and flue gases are not constant, a small storage system could ensure the constant supply of heat and maximum recovery.

5.2.7 Thermal energy storage for chilling vessel

The charging of thermal storage is performed with two flow conditions i.e 2 kg/s and 6 kg/s. It is shown in Figure 5.11. The complete charging of 1 m^3 TES with 2 kg/s (-5 °C inlet to TES) is in 318 minutes (5.3 hours). The time required for fully charged TES with 6 kg/s is 235 minutes (3.9 hours). In both cases, when the charging power decrease, the outlet temperature of glycol from TES is also decrease (towards -5 °C). At the end of charging, the inlet and outlet temperature of glycol in TES is same (no charging). A completely charged TES of size 1 m^3 corresponds to 838 kg ice including internal heat transfer area. The choice of charging condition completely depend on the size of thermal storage and chilling load profile. For the reference chilling vessel, charging with 6 kg/s is a better option as three peaks (31-34 hours, Figure 3.4) are very close to each other.

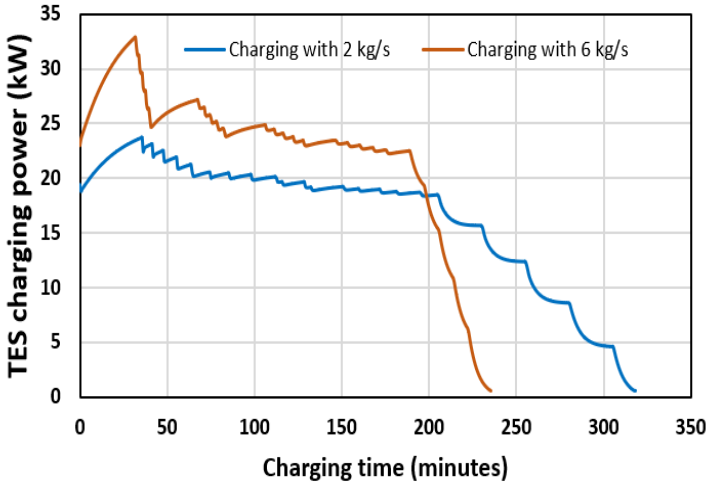

Figure 5.11: TES charging with glycol loop

The discharging of TES is analysed by varying the inlet RSW temperature from 10 °C to 8 °C in 1 hour. The RSW temperature range is according to the real systems. The simulation result of one hour discharging is shown in Figure 5.12. The maximum and minimum discharging power in the start and end is 57.4 kW and 19.6 kW, respectively. The average discharging capacity of this thermal storage is 30 kWh, the average is calculated by using all the data points of the simulation. In the start, the higher discharging value

is mainly due to high temperature difference between RSW stream and glycol stream. Afterwards, the lower discharging power is due to less temperature difference and more important the development of liquid layer in TES. As the liquid layer develop, it act as an additional thermal resistance between glycol side and ice.

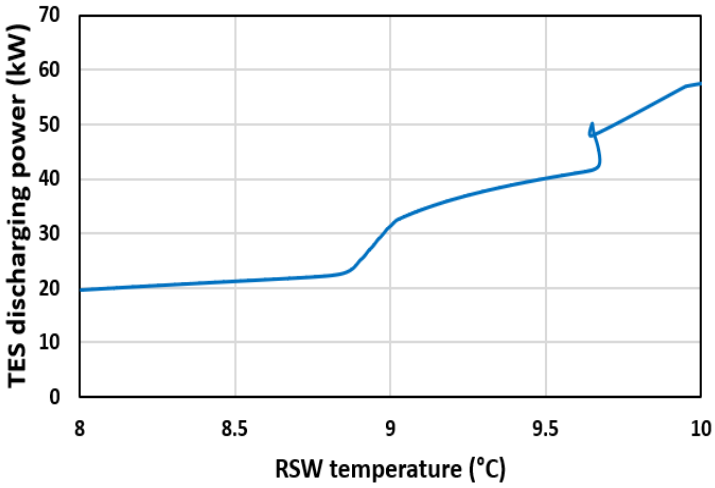

Figure 5.12: TES discharging with glycol loop HX

The melting of ice in 1 hour is 297 kg and formation of ice with 6 kg/s in 1 hour is 286 kg. To deal with three peaks of Figure 3.4 with a gap of one hour charging time, 605 kg ice is required. The new parameters by iterative process for storage to meet the criteria is 0.76 m^3 size and heat transfer area 36.4 m^2 (34*34 tubes).

An E6 PCM (sub-section 3.1.5) is another solution of TES integration in chilling system. Adopting low temperature PCM will eliminate the need of indirect circuit. This PCM can be adjusted on the refrigerant side to control the super heat during peak loads or to maintain system with less refrigeration capacity. On ideal basis, it shows that the storage has capacity to provide 92.5 kWh cold energy. The simulation work is not performed for this case as it is not included in the scope of this work.

5.3 Simulation results of freezing system

5.3.1 COP analysis of S1 and S2 system

The simulation analysis of S1 (freezing system) and S2 (freezing system with LNG subcooler) are performed with freezing load profile of Figure 3.8. The results of the simulation are presented in Figure 5.13. COP investigation is without taking into account the power consumption of pumps due to it's smaller values as compared to compressor work. The maximum and minimum COP of S1 system is 1.53 and 0.97, respectively. For S2 system,

the maximal and minimal COP is 1.62 and 1.12, respectively. COP is improved in S2 system, which is due to less work of both compressors as compared to S1 system. LNG sub-cooler reduced the flash gas in LT separator, which result in increased COP. The size of LT and MT separator is vital. When the load oscillates, the liquid level in a separator damps the the fluctuations for some instants until the compressor power change. The COP is low at lower loads, and high at higher loads. The reason of this COP trend is due to sizing of LT and MT separator, and maintaining constant 90 bar pressure in the gas cooler at low refrigeration loads.

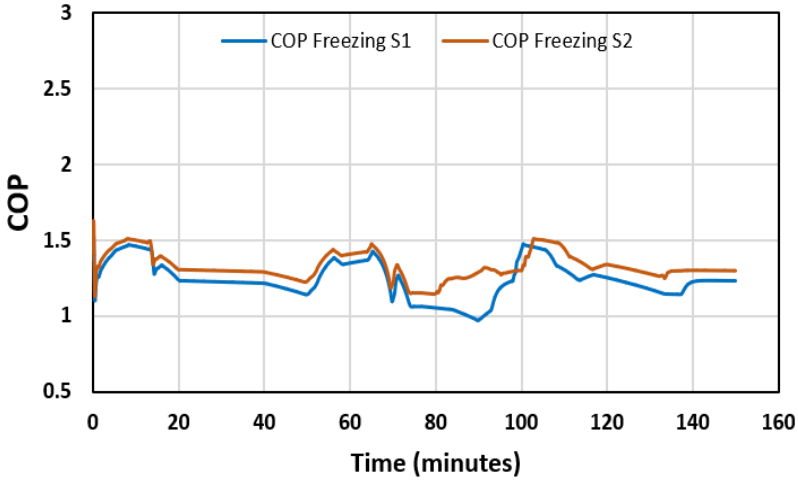

Figure 5.13: COP of S1 and S2 system

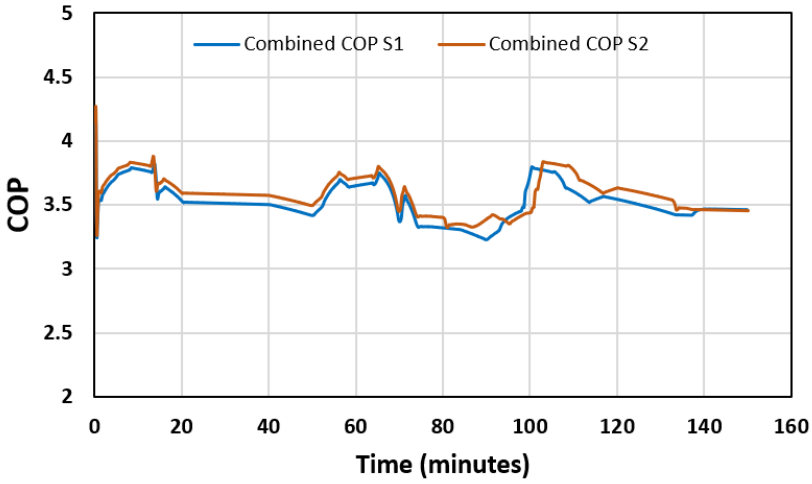

Figure 5.14: Combined COP of S1 and S2 system

The combined (freezing and heating) COP of both systems are high by an average factor of 2.8 compared with only freezing system. The heat recovery show that the system has high capability for energy efficiency. The combined COP of S1 and S2 system is shown in Figure 5.14.

5.3.2 Heat recovery and fish oil production

The heat recovery values presented in Figure 5.15 is the sum of both MT and gas cooler. The average heating demand for the fish oil production is 261 kWh, and average heat recovery is 298 kWh. If 10% thermal losses are included, then the recovered energy is still enough for the processing of RRM. For integration of process with RRM, refrigeration system heat exchangers can act as direct heating source or with a secondary glycol/water circuit. The choice depends on the free space on vessel and any possibility of hot water thermal storage. According to the composition of Mackerel (Table 2.2, the amount of fats in fish is 13.89%. At 100% production efficiency, the amount of fish oil that can be produced in relation with one freezing cycle is 450 liters.

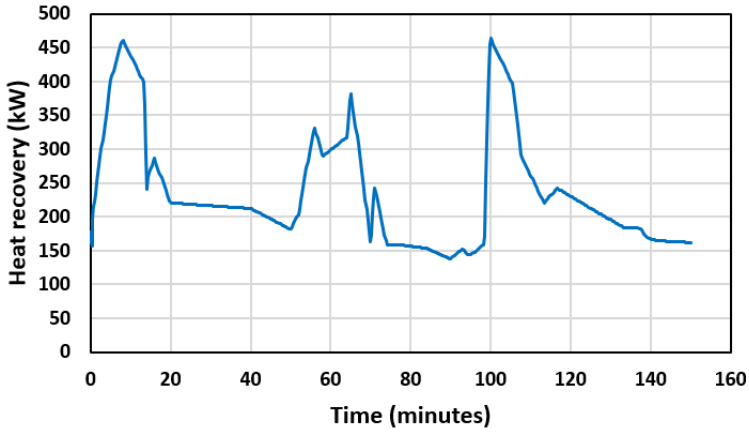

Figure 5.15: Total heat recovery of S1 system

5.3.3 TES charging with compressor (S3)

The charging of thermal storage with compressor is in the range between 16.8 kW and 25.6 kW. The average charging power is 20.2 kWh. The charging temperature (-68.3 °C), pressure (3 bar), flow rate (0.07 kg/s) showed minor fluctuation during simulation.The super heat of refrigerant after TES is 11 K. The high super heat is due to high heat transfer area and good thermal conductivity of aluminium. The super heat can control with TES expansion valve but high charging power is not desirable for the current case. The average compressor power and COP of TES system is 3.05 kW and 6.6, respectively. The amount of solid CO_2 formed after 40 minutes of charging is 171 kg. For fully charged storage, the required time of charging is 3.8 hours.

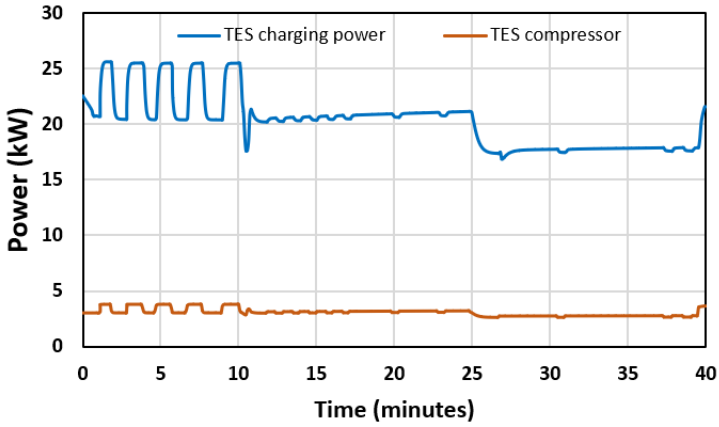

Figure 5.16: TES charging with compressor

5.3.4 TES charging with ejector (S4)

The charging power of TES with ejector is in the range of 11.9 kW to 15.9 kW. The average charging power is 13.75 kWh. The fluctuations were high for this TES system. Pressure varied from (3.4 bar to 3.61 bar), flow (0.0416 kg/s to 0.0406 kg/s) and temperature of refrigerant after TES was closed to pinch temperature (-56.6 °C). High oscillations were due to variation of refrigerant flow rate from MT separator. The mass of dry ice after 40 minutes is 116 kg, the less amount of dry ice compared to S3 system is due to low charging flow and lower temperature difference. The time for completely charged storage with ejector is 5.6 hours.

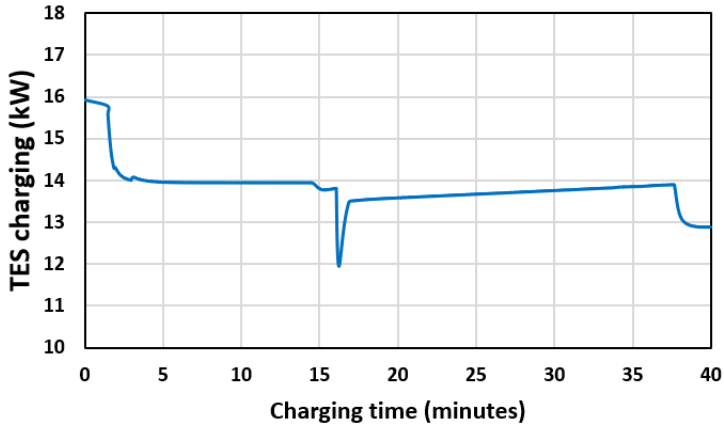

Figure 5.17: TES charging with ejector

The plot of Figure 5.17 illustrate clearly the charging behaviour of TES with ejector.

Figure 5.18 shows the charging of TES in comparison with refrigeration load. A correlation depict that TES charging decrease with decrease in refrigeration load but the trend is not very sensitive. A longer simulations can give more precise view.

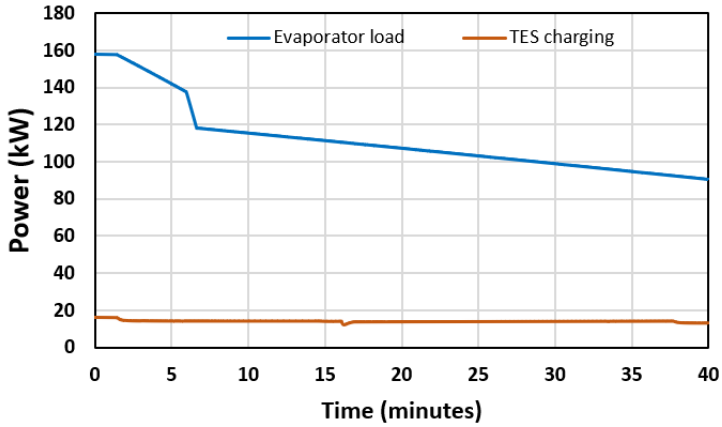

Figure 5.18: TES charging and evaporator load

5.3.5 Thermal storage discharging (S5)

The maximum and minimum discharging value is 51.4 kW and 48.5 kW, respectively. The discharging rate is high in the start and decrease linearly. The discharging power is a combination of three factors, i.e., refrigerant flow, super-heat, and TES heat transfer area. Above all, as the dry ice melt, the liquid layer act as thermal barrier, which also reduce discharging potential. The total melting of dry ice in 10 minutes is 112 kg.

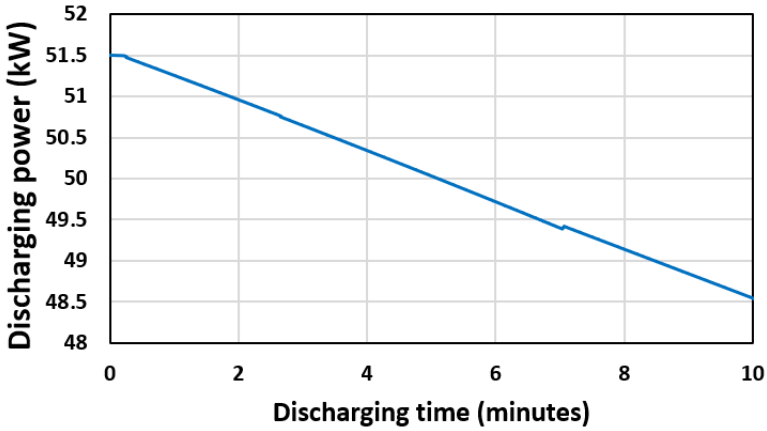

Figure 5.19: TES discharging

In the view of discharging results and iterative process, a thermal storage size of 0.3 m^3 (75 liters or 112 kg dry ice), including internal heat transfer area of 67 m^2 (54*54 tubes), is an ideal choice for the reference freezing system. The optimization for the heat transfer area can be performed by increasing the size of storage. Then the melting of dry ice in 10 minutes will be less than the total storing potential. This will help to amend the heat transfer area and number of tubes.

By implementing 50 kWh CO_2 thermal storage, the peak load time of Figure 3.8 is reduced from 10 to 8 minutes. Each day has almost 28 peaks of freezing. The saved time in 24 hours is 56 minutes, which means an additional production capacity of equivalent 56 minutes in one day.

Chapter 6

Discussions

Some of the results are thoroughly discussed in chapter 5 but this chapter will discuss the findings and technicalities in a broad perspective.

6.1 LNG cold recovery

The LNG cold recovery was investigated with assumed inlet and outlet conditions of vaporizer in coherence with vessel engine. The results are well enough to have a clear overview of the system. In comparison of cold recovery results with commercial technology, it has found that the maximum LNG cold potential can reach 19 to 20 kW for the reference chilling vessel of this work. There are two reasons for the difference, either the inlet/outlet conditions are different or the fuel consumption is underestimated.

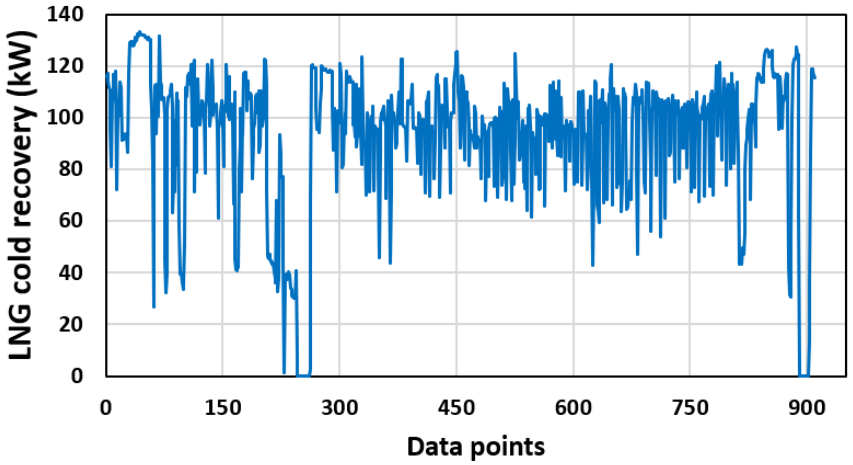

Figure 6.1: LNG cold recovery of 4.5 MW vessel

The cold recovery potential is a dynamic factor, and the fluctuations are very high. It is not feasible to have direct constant cold recovery. LNG cold recovery is also estimated for 4.5 MW fishing vessel with onboard data for validations. Diesel consumption is converted to LNG and the data is used as input to calculate LNG vaporization energy. The data is hourly and for a period of one month. The fuel consumption unit of the data is unknown but best prediction has made. The recovery potential is presented in Figure 6.1. The zero recovery values show that the vessel is stationary or the engine is not in operation. The estimation is with the identical inlet/outlet conditions of reference chilling vessel. The results show precision compared to commercial technology.

6.2 Chilling vessel

The chilling load profile was designed from the properties of Mackerel. A hypothesis formed for fishing sequence, which may deviate from the actual process. The COP pattern fits well with actual chilling systems. The pressure or temperature oscillations at various thermal loads in evaporator is reasonable. A frequency controlled pump was used to alter the thermal loads but this can also be done by constant flow and variable input temperature. LNG sub-cooler combination with chilling system shows favourable improvements. At lower thermal loads, the refrigerant temperature after LNG HX at one instant decreased to -2.8 °C. This low temperature can be a problem for CO_2 system and may cause pressure loss before expansion. The onboard heat recovery from desuperheater for space heating is a valuable option but it is only suitable for low temperature heating. Increasing temperature of water side of desuperheater will reduce the chilling COP. Heat recovery from flue gases is a viable source for onboard hot tap water demand.

The size of thermal storage is case specific and sensitive to load profile. The duration of peaks and their frequency will effect dimensions of storage. In the chilling load profile (Figure 3.4), the three peaks are close to each other, which determines the size of TES. The material of TES has direct influence on the internal heat transfer area. For example, thermal conductivity of aluminium is 236 W/m K and steel 36 W/m K (Engineering toolbox, b). This huge difference shows that how compact is the storage with aluminium. However, economic analysis is necessary.

The charging of big water/ice thermal storage is feasible during initial chilling of RSW tanks before actual fishing. After all, a huge thermal storage is impractical due to discharging limitations. The Figure 5.12 shows that the discharging power decrease with time. For fast discharging, it is an efficient way to have multiple small thermal storage in parallel.

To set up indirect charging and discharging loop for water/ice thermal storage, two additional heat exchangers are required including one seawater/RSW heat exchanger. A plus argument is that water is sustainable as compared to other Phase change materials. Another choice is a suitable and environment friendly PCM on the refrigerant side. This will eliminate the need of an extra heat exchangers and additional thermal losses.

6.3 Freezing vessel

The freezing load profile was adopted from a smaller freezing system. By using COP and compressor data, freezing profile calculated and interpolated for 240 kW system. The freezing load and norms are precise enough to address the practical challenges and find solutions for energy efficiency. In freezing system, the pressure levels were maintained constant. At part load operations, the COP reduced, which can correlate with the need of gas cooler pressure optimization. The size of LT and MT separator is another factor of COP trend. Implementing LNG sub-cooler after MT separator improved the COP. With sub-cooler, the power consumption of both compressors reduced. The combined (freezing and heating) COP shows a great opportunity for improving energy efficiency. Rest raw material heating demand onboard for fish oil production shows a favourable potential for integration with refrigeration system for the study case. An economic assessment is necessary to compare the capital investment and financial gain from fish oil.

The freezing load profile (Figure 3.8) clearly emphasize the necessity of energy efficiency and better resource utilization. CO_2 thermal storage is a promising solution in terms of sustainability and in perfect match for the required temperature levels. The charging of thermal storage with compressor mode is fast but it has one constraint, the temperature after the thermal storage compressor is around 10 °C at simulated conditions. The mixing of 10 °C and -50 °C stream in LT separator or LP compressor inlet might affect the performance of LP compressor or plate freezers. Ejector is a better option to have free pressure lift and without any additional compressor work. The charging level of thermal storage with ejector in 40 minutes and discharging level in 10 minutes at peak load is close to each other. The extra mass of stored dry ice is only 4 kg. For the reference freezing vessel, 0.3 m^3 TES best match the peak load scenario. A full melting of PCM in one cycle requires high heat transfer area and should analyse to find a point where the total heat transfer area and size of the storage is optimal for implementation.

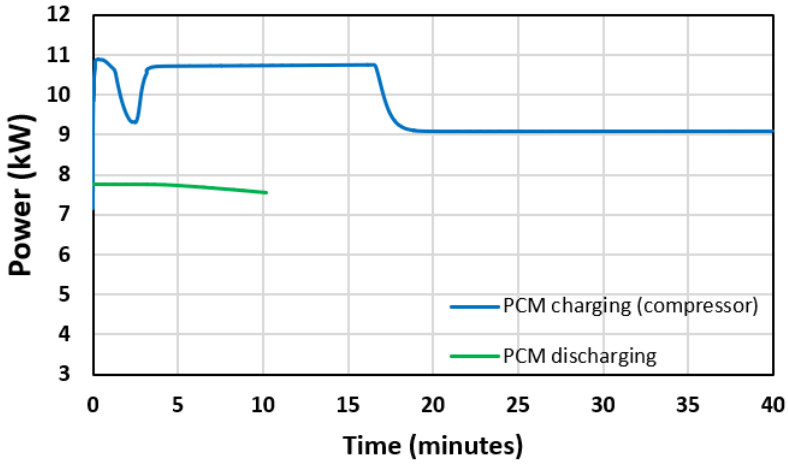

Figure 6.2: Stainless steel CO_2 thermal storage charging and discharging

The Figure 6.2 is a simulation results of stainless steel CO_2 thermal storage. The internal heat transfer area is identical to the aluminium thermal storage (1 m^3). By comparing these results with Figure 5.16 and Figure 5.19, it is perceived that the material choice (thermal conductivity) of thermal storage is vital for compactness.

Chapter 7

Conclusion

An energy efficiency analysis of the chilling (RSW) and freezing vessel was performed on a CFD simulation software Dymola/Modelica. A reference case of chilling vessel was 760 kW coastal demersal trawler. Simulations were performed with the designed loads to have a complete energy performance overview of LNG cold recovery, RSW system, heat recovery from flue gases of engine, recovery from desuperheater of refrigeration system and integration of water/ice thermal storage. A separate case was investigated for freezing vessel. An optimization was made for 240 kW freezing system with LNG sub-cooler, utilizing heat recovery of refrigeration system for fish oil production from rest raw material and integrated low temperature CO_2 thermal storage.

LNG cold recovery from the vaporization was estimated 13.7 KW and 7.1 KW at maximum and minimum fuel flow, respectively. The LNG temperature after vaporization is in the range of -6 °C to -10 °C and controlled by indirect glycol loop. LNG cold recovery can be utilized for many applications. For example, sub-cooling in refrigeration system and charging thermal storage.

For chilling system, LNG cold was used as sub-cooling of refrigerant. Sub-cooling effect was in the range of 8 to 10 kW with average fuel flow. Results show an increment of COP by an average 15.2% as compared to simple chilling system. By deploying LNG sub-cooler, evaporation pressure increased, which resulted in high COP. At lower load, the trend is more visible as related to higher loads. Other reason is less vapor fraction after expansion valve by using LNG sub-cooler. Heat recovery from the flue gases of engine are in the range of 56 kW to 172 kW. The heat recovery has potential to cover an onboard average 114 kWh hot tap water demand. Heat recovery from the desuperheater is in the range of 8 kW to 68 kW. It has capacity to cover an average 38 kWh space heating demand, but this is a low temperature heating (30 °C to 35 °C). It is observed that by installing desuperheater, chilling COP of the system decreased by 6.3 % at maximal load and 17.4 % at minimal load (correlated to simple refrigeration unit), the reduction is due to increased pressure after compressor. However, combined (chilling and heating) COP

raised by 24 %. A water/ice aluminium thermal storage of size 0.76 m^3 including internal heat transfer area of 36.4 m^2 has ability to provide an average 30 kWh discharging power. By implementing this thermal storage, the reference chilling system can operate with 220 kW evaporation capacity. This thermal storage can be seen in two perspective, either to reduce the refrigeration capacity of new installations or to boost the capacity of existing units.

In freezing system, the LNG sub-cooler was introduced after medium temperature separator. Sub-cooling effect was constant 9.8 kW due to controlling of LNG cold with indirect glycol loop. Results show that an average COP increased by 6.4 % with LNG sub-cooler. The effect of sub-cooler is reduced flash gas in low temperature separator, which resulted in less compression work of both compressors and hence high COP. The combined (freezing and heating) COP increased by a factor of 2.8 compared with only freezing COP. The mean heat recovery from the freezing system is 298 kWh, which is in good match with the mean heating demand of 261 kWh for rest raw material processing. At 100 % efficiency of fish oil production, the amount of oil that can be produced in relation with designed freezing cycle of 150 minutes is 450 liters. A CO_2 thermal storage exhibits promising results. An aluminium thermal storage of size 0.3 m^3 (75 liters or 112 kg dry ice) including an internal heat transfer area of 67 m^2 is an option for the reference freezing system to cover peak loads. An average 50 kWh discharging of stored energy reduced the peak from 10 to 8 minutes. Each day corresponds to almost 28 freezing peaks. The saved time in one day is 56 minutes, which means an extra production capacity of equivalent 56 minutes in 24 hours.

Chapter 8

Further work

In this chapter a suggestions for further work is presented. Some of them are related to improvement in the existing work and rest are the extension of work.

- Further investigations are required to identify and implementation possibilities of LNG cold recovery applications. Other potential applications could be thermal storage integration with LNG cold, direct RSW chilling and onboard air-conditioning or freezing etc.
- Thermal storage integration with chilling system could optimized by implementing ejector for charging. It has to be examined.
- Other suitable low temperature PCMs for chilling vessels on refrigerant side should evaluate to avoid indirect circuits.
- The rest raw material integration was thoroughly discussed. This should analyse further and determine the need of direct/indirect circuit and hot water thermal storage.
- An investigation of CO_2 thermal storage with variable super-heat should perform to visualise the effect on discharging.
- TES simulations should carried out with load profiles of various species to find the more accurate dimensions of thermal storage to deal with multiple species.
- CO_2 thermal storage charging with ejector must perform by varying the gas cooler pressure, MT separator size and more diverse freezing load to verify the stability.
- Due to slow TES discharging constraint for longer periods, multiple small thermal storage in parallel should analyse for high discharging efficiency.

Bibliography

Boukhanouf, R., 2011. Small and micro combined heat and power(CHP) systems. Woodhead publishing series in energy.

Britannica Academica, 2019. Montreal protocol. URL: https://www.britannica.com/event/Montreal-Protocol.

Carvajal, A., Slizyte, R., Storrø, I., Aursand, M., 2015. Production of high quality fish oil by thermal treatment and enzymatic protein hydrolysis from norwegian spring spawning herring by-products. Journal of Aquatic and Food product Technology 24, 807–823.

Coolpack, 2020. Software.

Dincer, I., Kanoglu, M., 2010. Refrigeration systems and applications. John Wiley and sons, Ltd, Chichester, UK.

Eikevik, T.M., 2019a. Compendium master course, Heat pumping processes and systems,TEP 4255, NTNU.

Eikevik, T.M., 2019b. Compendium master course, Thermal and process engineering of food, TEP 4265 NTNU.

Engineering toolbox, a. Dry air properties. URL: https://www.engineeringtoolbox.com/dry-air-properties-d_973.html.

Engineering toolbox, b. Thermal conductivity. URL: https://www.engineeringtoolbox.com/thermal-conductivity-metals-d_858.html.

Gulbrandsen, O., 2012. Fuel saving for small fishing vessels, A manual. URL: http://www.fao.org/3/i2461e/i2461e.pdf.

Gullo, P., Tsamos, K., Ge, Y., Tassou, A., 2017. State-of-the-art technologies for transcritical r744 refrigeration systems-a theoretical assessment of energy advantages for european food retail industry. Energy procedia 123, 46–53.

Hafner, A., 2019. Compendium master course, Heat pumping processes and systems,TEP 4255, NTNU.

Hafner, A., Gabrielii, C.A., Widell, K., 2019. Refrigeration units in marine vessels. Alternatives to HCFCs and high GWP HFCs, Nordic council of ministers, Team nord .

Jafarzadeh, S., Paltrinieri, N., Utne, I., Ellingsen, H., 2017. Lng fueled fishing vessels, a systems engineering approach. Transportation research part D 50, 202–222.

Koo, J., Oh, S.R., Choi, Y., Jung, J.H., Park, K., 2019. Optimization of an organic rankine cycle system for an lng powered ship. Energies 10.

LR, 2015. Your options for emissions compliance guidance for shipowners and operators on the Annex VI SO_x and NO_x regulations. Lloyd's register (LR), London, UK.

Makhnatch, P., 2019. Low GWP refrigerants. Department of energy technology, KTH. URL: https://www.kth.se/en/itm/inst/energiteknik/forskning/ett/projekt/koldmedier-med-lag-gwp/low-gwp-news/nagot-om-hfo-koldmedier-1.602602.

Mehling, H., Cabeza, L.F., 2008. Heat and cold storage with PCM. Springer, Berlin.

Nordtvedt, T.S., Widell, K.N., 2019. Chilling of pelagic fish onboard norwegian fishing vessels, in: The 25^{th} IIR international congress of refrigeration, Montreal, Canada.

Norwegian ministry of climate and environment, 2018. Norway's seventh national communication under the framework convention on climate change URL: https://www.regjeringen.no/contentassets/52d65a62e2474bafa21f4476380cffda/t-1563e.pdf.

Olsen, R.L., Toppe, J., Karunasagar, I., 2014. Challenges and realistic opportunities in the use of by-products from processing of fish and shellfish. Trends in Food science and Technology 36, 144–151.

PCM products LTD, . plusice range- phase change materials. URL: http://www.pcmproducts.net/files/E%20range-2018.pdf.

Pettersen, J., 2018. Compendium master course, Natural gas technology, TEP 4185, NTNU.

Pham, Q.T., 2002. Calculation of processing time and heat load during food refrigeration, in: AIRAH Conference, Sydney, Australia.

Pielichowska, K., Pielichowska, K., 2014. Phase change materials for thermal energy storage. Progress in materials science 65, 67–123.

Rustad, T., Storrø, I., Slizyte, R., 2011. Possibilities for the utilization of marine by-products. International Journal of Food and Science and Technology 46, 2001–2014.

Rycroft, M., 2019. Cryogenic carbon capture for clean coal power generation URL: https://www.ee.co.za/section/articles-eepublishers.

Sihvonen, J., 2018. CNG and LNG for vehicles and ships- the facts, a study by transport and environment. URL: https://www.transportenvironment.org/sites/te/files/publications/2018_10_TE_CNG_and_LNG_for_vehicles_and_ships_the_facts_EN.pdf.

Skipsteknisk, 2003. Pelagic trawler, Charisma. URL: https://www.skipsteknisk.no/product_sheet.aspx?type=4&menu=29&id=229.

Søvik, S.L., 2005. Characterisation of enzymatic activities in by-products from cod species. effect of species, season and fishing ground, Doctoral thesis, NTNU.

Teknotherm, . Horizontal and vertical plate freezers. URL: https://www.teknotherm.no/product/vertical-plate-freezer/.

UNIDO, 2016. Kigali amendment and hfc-phase down, the montreal protocol evolves to fight climate change URL: https://www.unido.org.

Valentas, K.J., Rotstein, E., Singh, R.P., 1997. Handbook of Food Engineering Practice. Taylor and Francis group.

Valentina, R., 2012. Analysis of existing refrigeration plants onboard fishing vessels and improvement possibilities, in: Second international symposium on fishing vessels efficiency e-fishing, Vigo, spain.

Widell, K.N., Nordtvedt, T.S., Eikevik, T.M., 2016. Natural refrigerants in refrigerated sea water systems on fishing vessels, in: Gustav Lorentzen natural working fluids, Edinburgh.

Zahai, Y.J., Yu, D.L., Tafreshi, R., Al-Hamidi, Y., 2011. Fast predictive control for air-fuel ratio of si engines using a nonlinear internal model. International journal of engineering science and technology 3, 1–17.

Appendix A: Log P-h diagrams

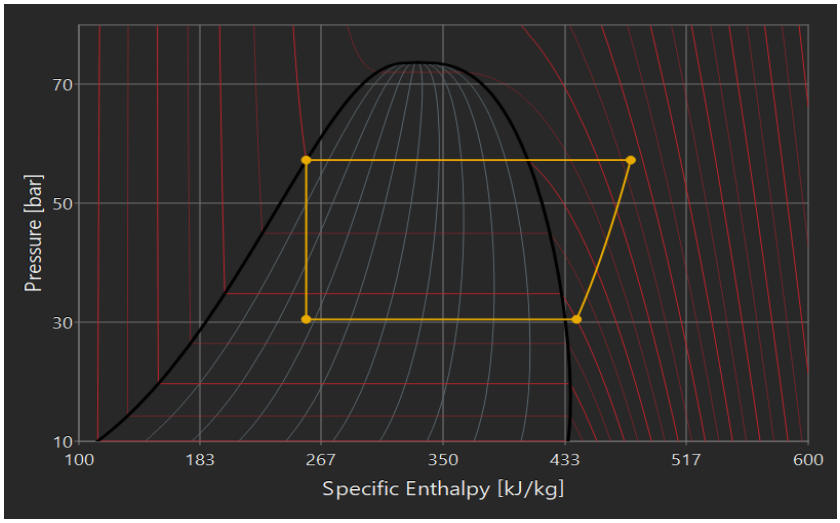

Figure A1: Chilling refrigeration system (C1)

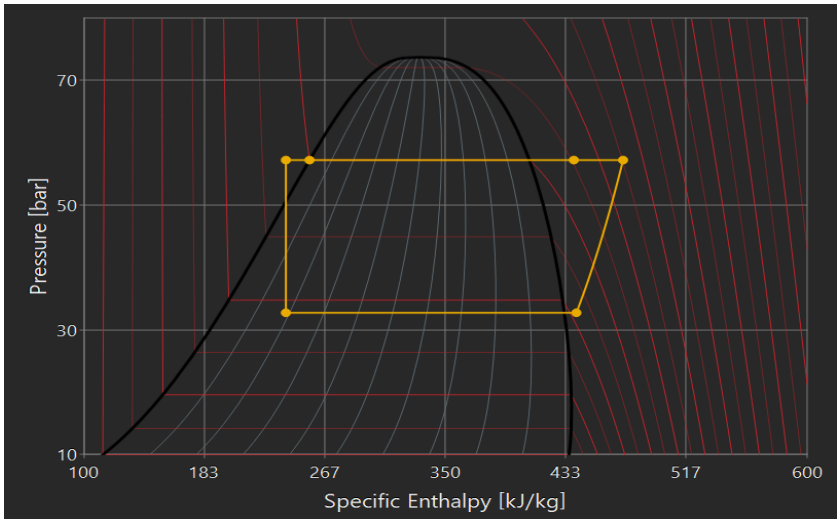

Figure A2: Chilling system with desuperheater and LNG sub-cooler (C4)

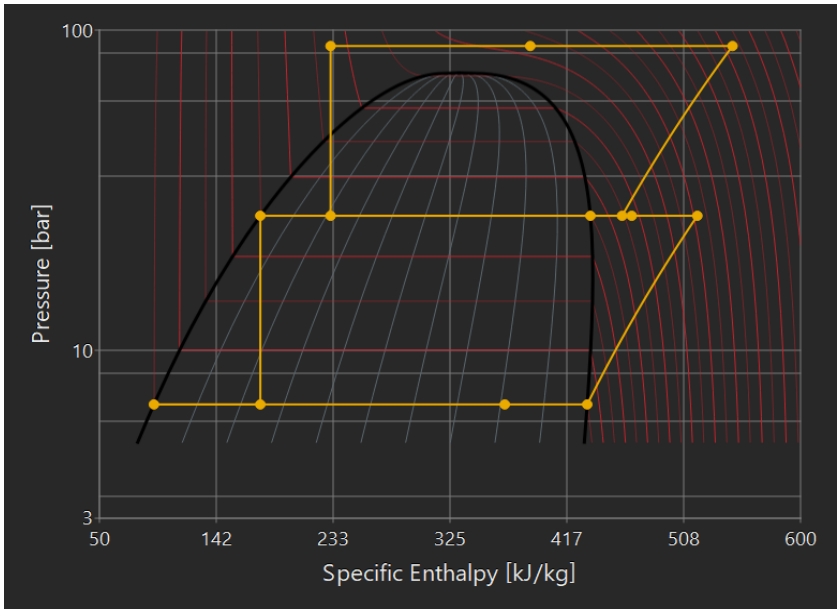

Figure A3: Freezing refrigeration system (S1)

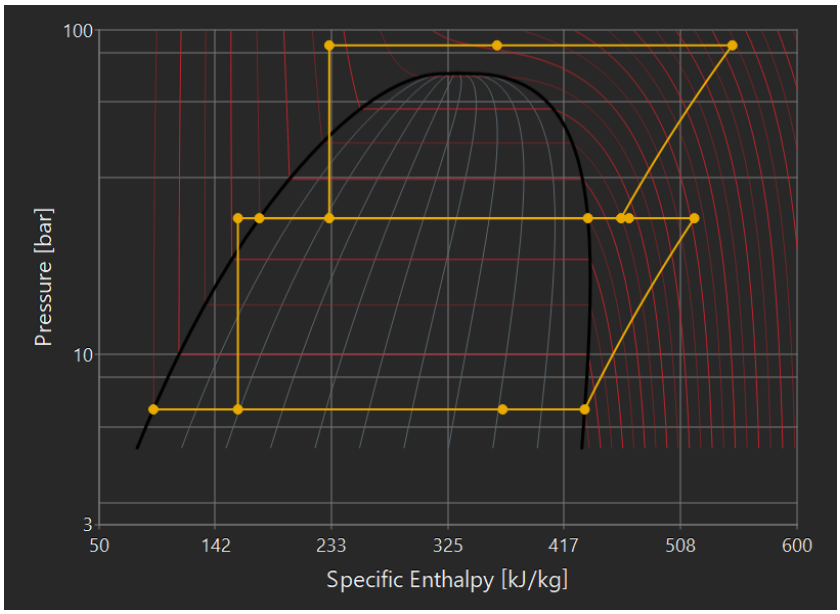

Figure A4: Freezing system with LNG sub-cooler (S2)

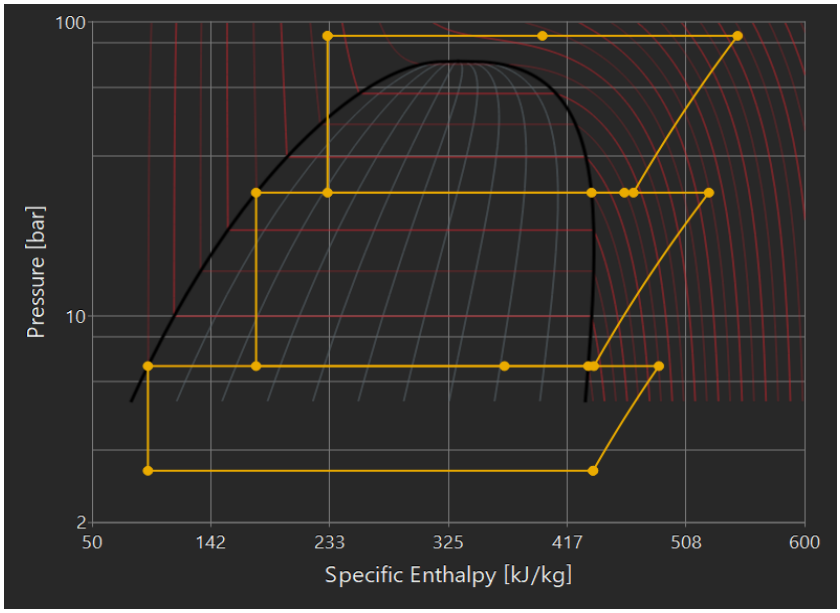

Figure A5: Freezing system with TES charging and compressor (S3)

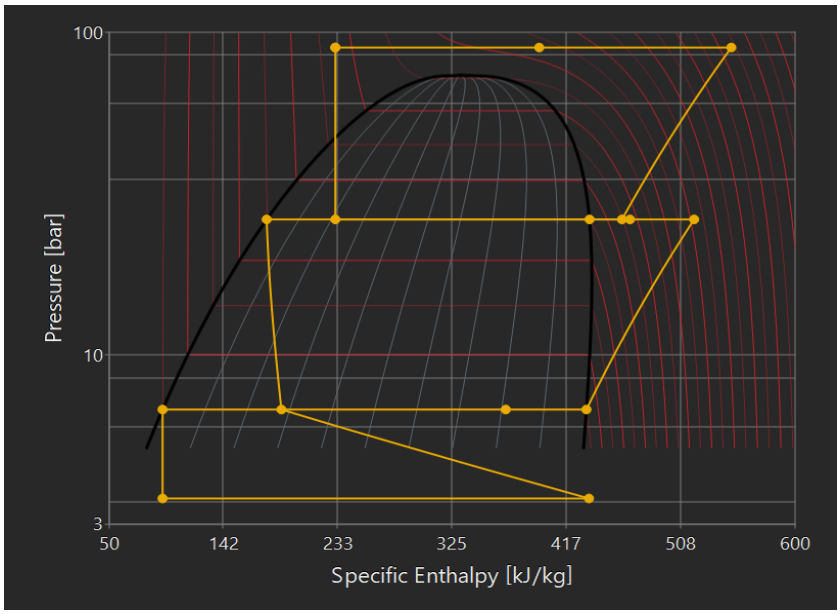

Figure A6: Freezing system with TES charging and ejector (S4)

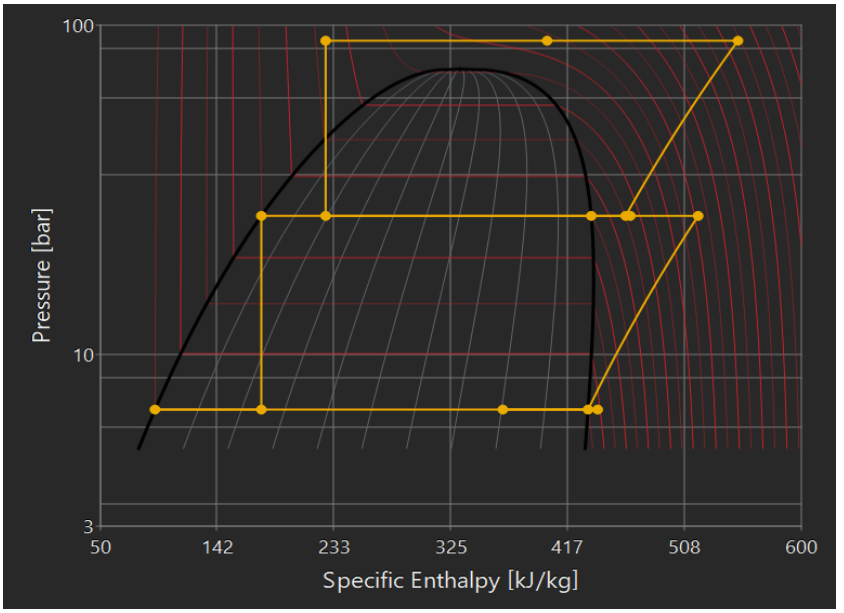

Figure A7: Freezing system with TES discharging (S5)

Appendix B: Simulation models

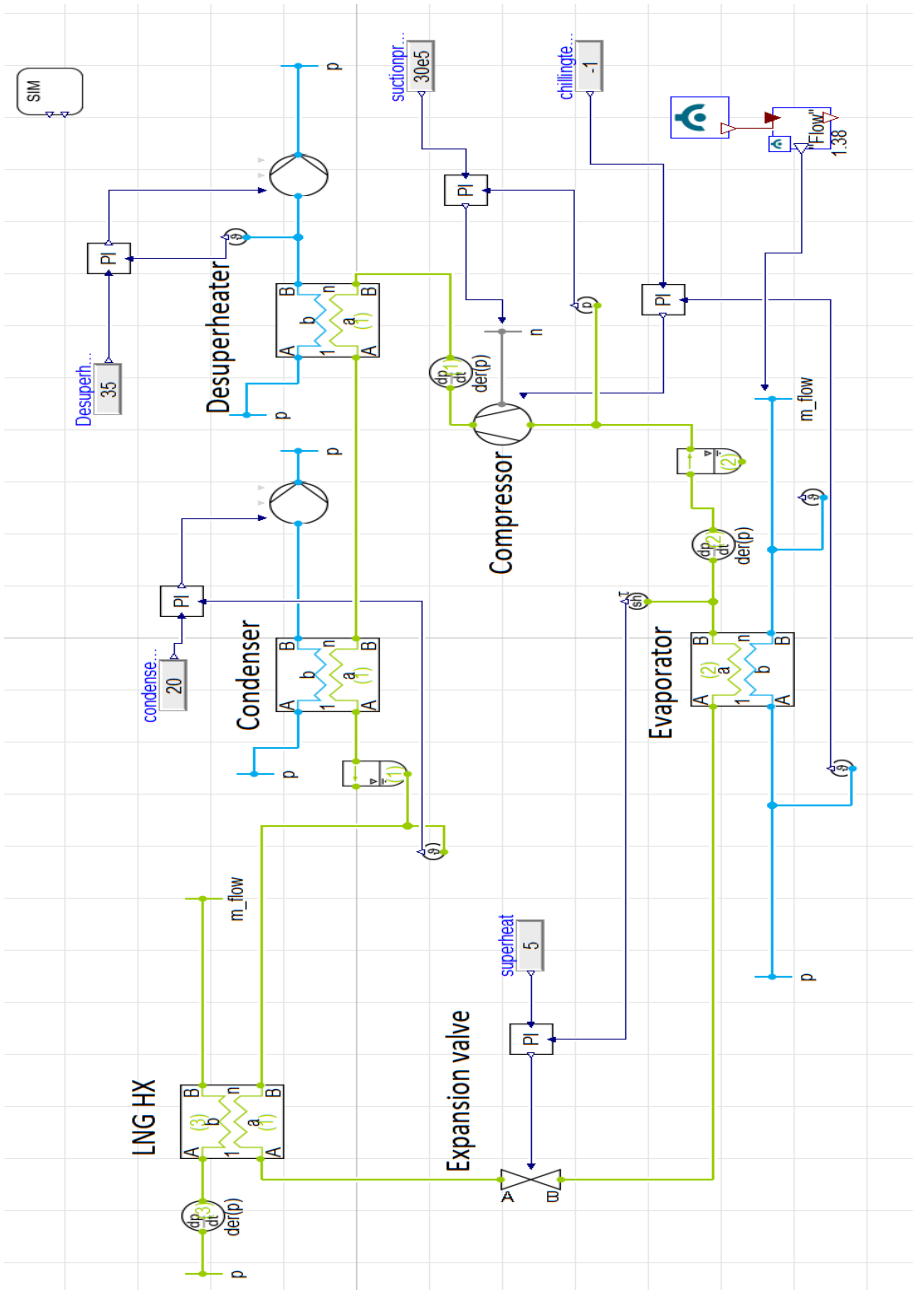

Figure B1: Chilling simulation model

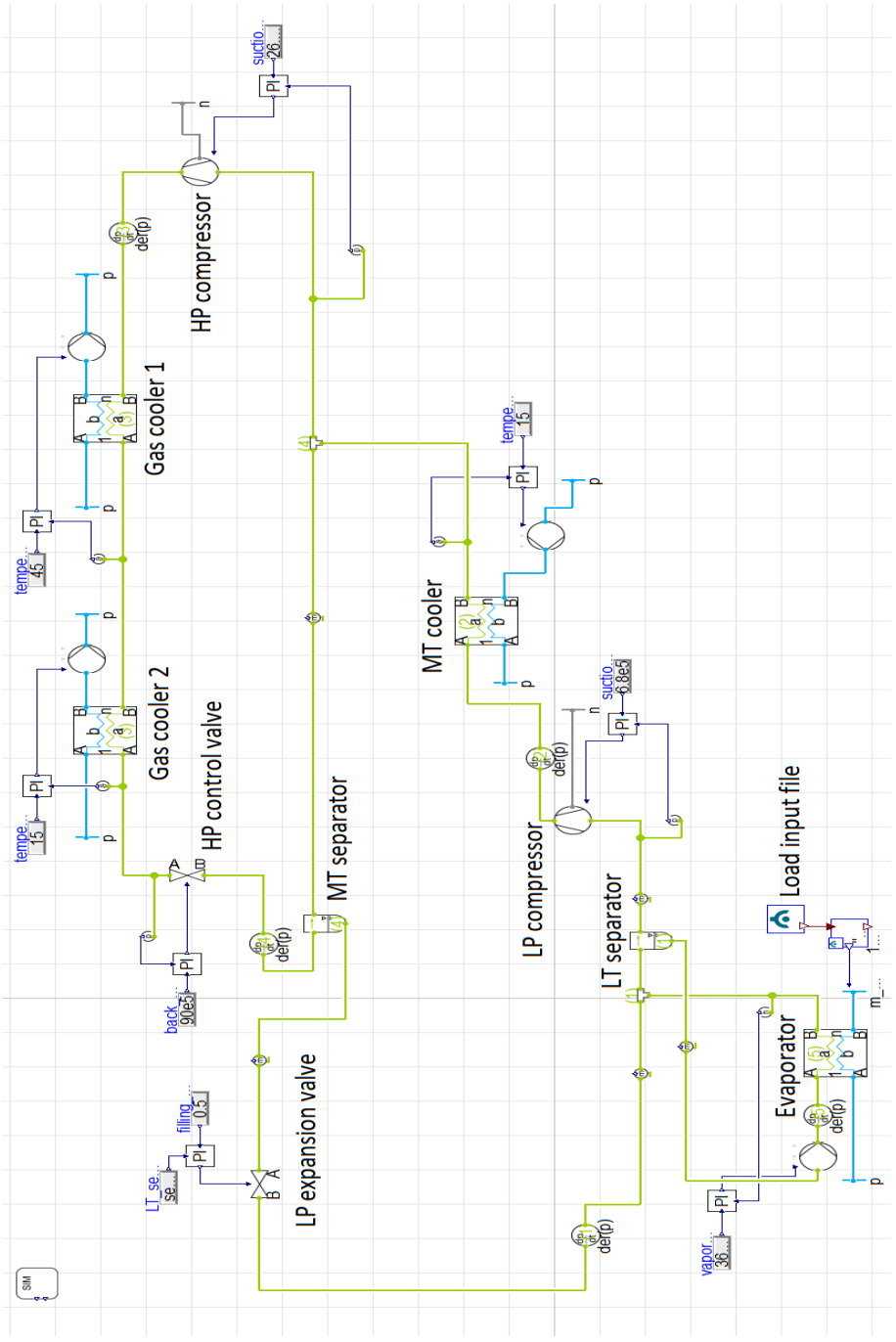

Figure B2: Freezing simulation model

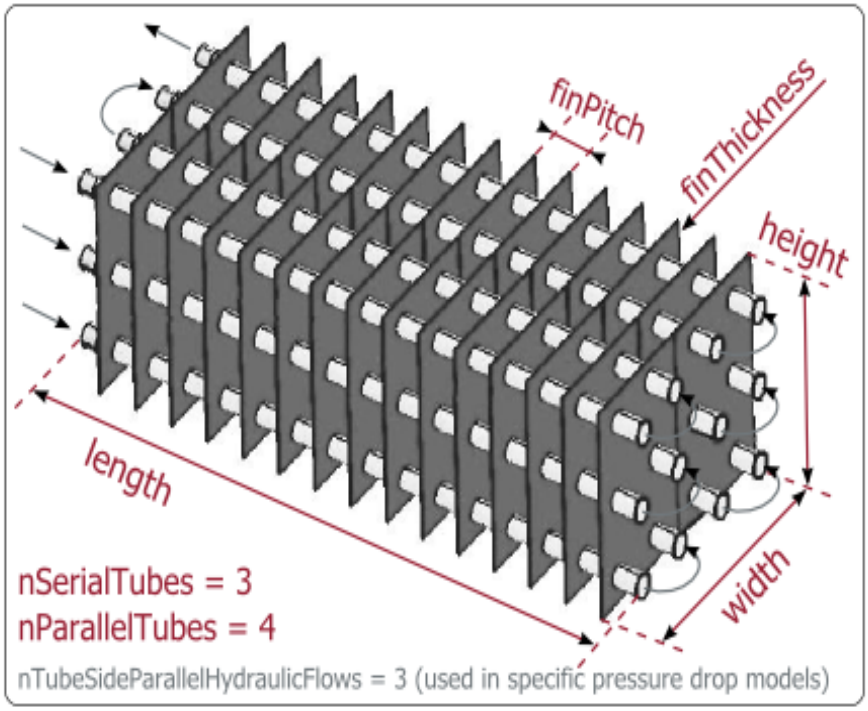

Figure B3: Thermal storage internal orientation (Dymola)

Appendix C: Scientific papers

PAPER ID: 1116
DOI: 10.18462/iir.gl.2020.1116

Integrated thermal storage and heat recovery of the CO_2 refrigeration system for fishing vessels

Muhammad Zahid SAEED[(a)], Kristina N. WIDELL[(b)], Armin HAFNER[(a)], Tom Ståle NORDTVEDT[(b)], Eirik Starheim SVENDSEN[(b)]

[(a)] Norwegian University of Science and Technology
Trondheim, 7491, Norway, muhammzs@stud.ntnu.no
[(b)] SINTEF Ocean
Trondheim, 7465, Norway, Kristina.Widell@sintef.no

ABSTRACT

The natural refrigerant CO_2 is gaining an attraction for fishing vessels due to its compact units, negligible global warming potential (GWP), and non-toxic behaviour. Chilling and freezing onboard are energy-consuming processes but are necessary to ensure high-quality products. Cold thermal storage is a smart feature that assists the refrigeration system at peak loads, and such setups are working efficiently on the onshore facilities. CO_2 thermal storage is suitable for fish freezing with which you can store cold energy as low as -57 °C. Heating is also necessary onboard, for warm water, snow melting, and processing of fish rest raw material. Currently, the onboard refrigeration system challenges are low coefficient of performance (COP) at part load operations and insufficient capacity at peak loads. This paper investigates the integrated CO_2 thermal storage and heat recovery from the gas-cooler of the CO_2 refrigeration system to improve the total system performance.

Keywords: Refrigeration, Thermal Storage, Carbon Dioxide, Fishing Vessels, Integration, Heat Recovery, Energy Efficiency.

1. INTRODUCTION

Modern refrigeration systems are integrated heating and cooling systems. Natural refrigerant CO_2 is a fair choice, with excellent thermophysical properties, non-flammability, and compact systems due to high volumetric capacity (Hafner et al., 2019). Thermal energy storage is a method to store energy in times when refrigeration load is less and utilize during peak load to reduce the chilling or freezing time. Thermal energy storage in the form of dry ice is the right choice for freezing systems operating at an evaporation temperature of -50 °C. The phase change temperature of CO_2 from liquid to solid is -56.6 °C at 5.18 bar. Storing cold energy in solid form is possible by charging the thermal storage system with CO_2 refrigerant pressure less than 5.18 bar (Niu et al., 2011), (Hafner et al., 2011).

The short journey fishing vessels store fish in refrigerated seawater (RSW) systems. The long journey vessels who spend weeks in the sea, freeze the fish to have a long shelf life. These vessels often have onboard processing units in which they produce fillets from the whole fish. The fish is processed and frozen after the catch and then stored in low-temperature cargo storage. In this way, the vessels can remain at sea until the cargo storage is full. The leftover from the processing of main fish product (fillets) are head, bones, skin, trimmings, and guts; typically called rest raw materials (RRM) in Norway. The RRM is not as valuable as fillets but can be processed further to value added ingredients. According to FAO (2014), globally, 80 million tonnes of fish are processed for filleting, canning, or curing, of which rest raw materials account for 50 to 70 % that are not fully utilized (Ølsen et al., 2014). RRM is a source of fish oil (omega-3) production, which is the highest profitable product among other additional by-fractions.

Refrigeration systems are designed to cover an average load, but they must also be able to cover some peak loads (Valentas et al., 1997). If the refrigeration capacity is lower than the product load, it will prolong the freezing time, and this problem happens during the start of the freezing cycle. In plate freezers, one reason for having a high starting refrigeration load is due to defrosting of the plates after each period.

This study aims to investigate the implementation of CO_2 thermal storage as dry ice to cover the peak loads. The charging and discharging potential of CO_2 thermal storage are evaluated for integration with the existing refrigeration system for fish freezing. The unused refrigeration capacity at part load operations is an option to

utilize and store cold thermal energy for later use. The heat recovery from the refrigeration system is also analyzed for fish oil production to improve the energy performance of the total system.

2. SYSTEM DESIGN AND SIMULATIONS

2.1. Dynamic modelling software

To simulate the dynamic energy model, Dymola software (Dymola, 2020) with components and refrigerant libraries from TLK- Thermo GmbH (TLK, thermo 2020) were used. TIL media is a model library for refrigerants and secondary fluids, while TIL for components like heat exchangers, compressors, and valves. The software has built-in components with a high degree of control on the input parameters and boundary conditions. It also has an add-on library for thermal storage, which combines with the designed refrigeration systems in TIL and Dymola.

2.2. Refrigeration system and freezing load

The reference refrigeration system for this paper is a two-stage CO_2 booster system working in the trans-critical state with a freezing capacity of 240 kW. The operating conditions of the unit are -50 °C evaporation (6.8 bar in low temperature (LT) separator) and 90 bar in the gas cooler. The medium temperature (MT) separator temperature and pressure are -10 °C and 26.4 bar, respectively. The temperature after the gas cooler and MT cooler is 15 °C. Both coolers are assumed water-cooled heat exchangers with an inlet seawater temperature of 10 °C. The source of refrigeration load is plate freezers in which fish is freezing from 10 °C to -20 °C (center temperature). The simplified sketch of the refrigeration system is shown in Fig. 1a. The fish freezing load is shown in Fig. 1b and it is adapted from the operational plate freezers for fish. Fish freezing is a transient process. At a temperature close to the initial freezing point, thermal properties change to a great extent, mainly the specific heat capacity, which prolongs the freezing time. In Fig. 1b, the peaks depict the new cycle of freezing after 40-45 minutes. Each peak corresponds to the addition of an average 357 MJ heat load from the fish.

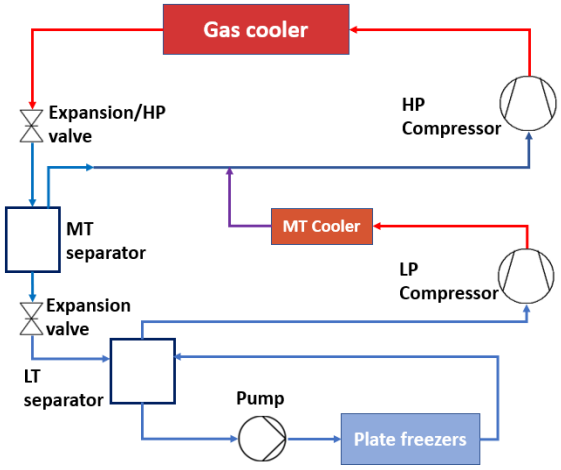

Figure 1a: Simplified two-stage system

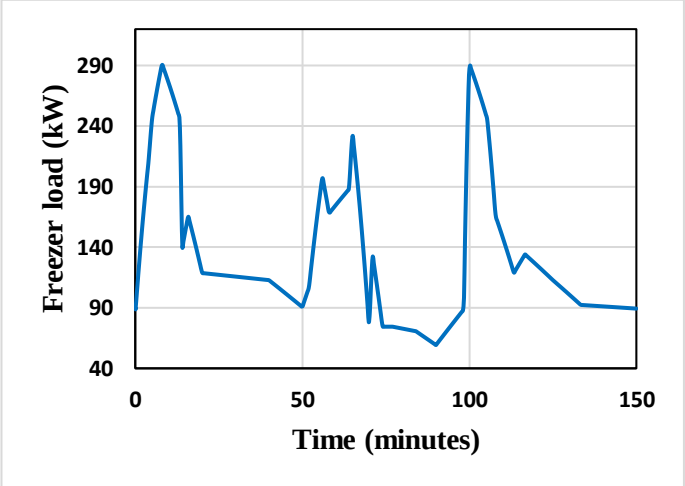

Figure 1b: Freezing load profile

2.3. Rest raw material processing

The thermal demand for onboard fish oil production is analyzed for RRM processing. This system is designed in coherence with the freezing volume of fish. The equivalent amount of RRM produced in 150 minutes freezing cycle is 3000 kg. The two methods of fish oil production are thermal treatment and hydrolysis. In the thermal treatment, the RRM is crushed in a mincer and then heated up to 90 °C. The heating temperature can be less than 90 °C but may have an effect on the oil quality and production rate. It is then further processed in the tri-canter. It is a unique component that separates the stick water (water phase), sludge (solid phase), and oil. It is also called a three-phase separator. After the tri-canter, the oil phase is further treated in a polishing centrifuge to remove the impurities. In the hydrolysis process, after crushing, RRM is mixed with an equal amount of water. It is then heated up to 60 °C before further treatment, as described in the thermal treatment process. The reasonable heating time for the hydrolysis process is 70 minutes (Carvajal et al., 2015). In this

paper, heat recovery from the refrigeration system is compared with the thermal treatment process. The heating load of RRM for this process is shown in Fig. 2.

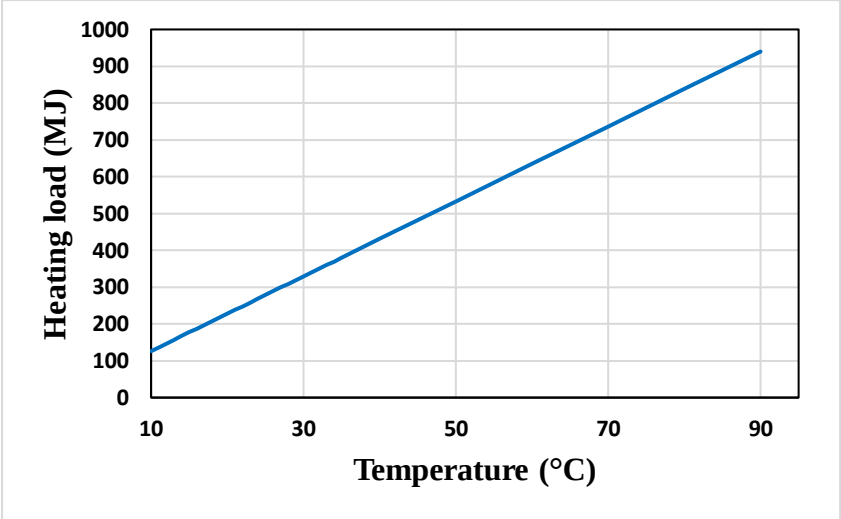

Figure 2: Heating demand for RRM thermal treatment

2.4. Thermal storage

CO_2 as phase change material (PCM) is investigated for integration with the freezing system. The purpose of this thermal storage is to boost the refrigeration capacity at peak loads and reduce the processing time of each cycle. Each m^3 of space on a fishing vessel is very important. So, a size of 1 m^3 (including internal pipes) is analyzed. The characteristics of aluminium thermal storage are shown in Table 1.

Table 1: Characteristics of thermal storage

Characteristics	Values
Volume of thermal storage (m^3)	1
Number of tubes	34*34
Total heat transfer area tube inner (m^2)	36.3
Total heat transfer area tube outer (m^2)	40
Tube inner diameter (mm)	10
Tube wall thickness (mm)	0.5

The storage conditions of PCM are 8 bar and -56.6 °C. The dry ice accumulation is on the shell side, and charging and discharging of the storage is with the refrigerant in the tubes. The storage is integrated with the refrigeration system described in Figure1a. The charging condition of thermal storage is 3 bar (-68.3 °C). The charging is done by deploying an additional expansion valve and compressor after LT separator. Thermal storage charging was also performed with an ejector to have free pressure lift from 3 bar to 6.8 bar. Both designs are shown in Fig. 3a and 3b. The available time for TES charging is an average 40 minutes between two peaks. Liquid level in LT separator or temperature after plate freezer is an indication for charging. According to the freezing load profile in Fig. 1b, the load is higher than the refrigeration capacity for a maximum of 10 minutes. The discharging of thermal storage is investigated with a constant super-heat of 8 K (-42 °C) after the evaporator or freezer. However, the super-heat is not a constant value and varies a lot during peaks. For the current case, the super-heat range is 0 to 8 K in LT separator. The discharging concept is to re-condense the vapors after plate freezers with stored cold energy without any effect on LT separator.

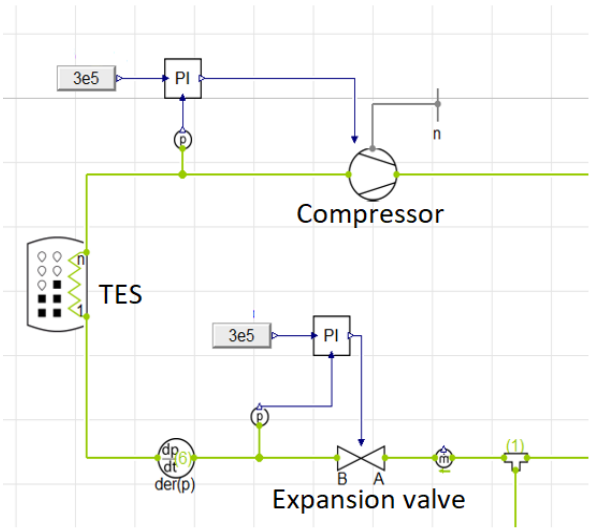

Figure 3a: Thermal storage charging using compressor

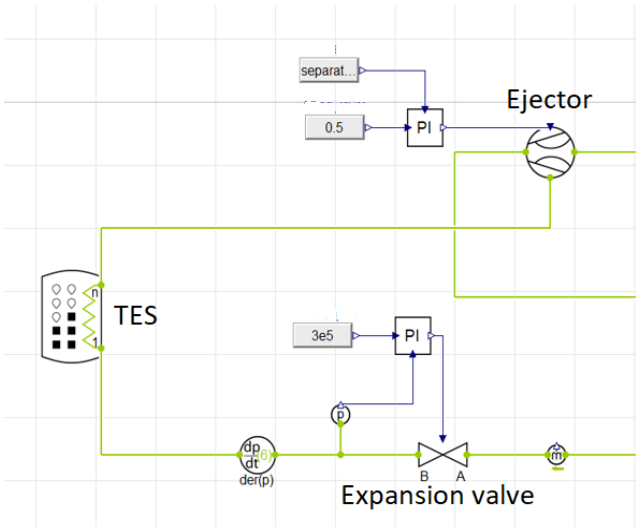

Figure 3b: Thermal storage charging using ejector

3. RESULTS AND DISCUSSION

3.1. Dynamic system performance

The simulation runs with the dynamic freezing load profile (Fig. 1b). The results for the coefficient of performance (COP) of the refrigeration system is shown in Fig. 4. COP analysis is without taking into account the power consumption of pumps because it is very low as compared to compressor work. The pressure levels in the simulation remained constant, irrespective of the load. The compressors isentropic and volumetric efficiency was 0.7. The maximum and minimum COP of freezing is 1.53 and 0.97, respectively. For a dynamic system, the size of LT and MT separator is vital. When the load changes, the compressor takes some time to change the power consumption. In the meantime, the liquid level in a separator damps the fluctuations. A high COP can be expected at a high load due to such consequences. The combined freezing and heating COP shows maximum and minimum values of 4.1 and 3.2, respectively.

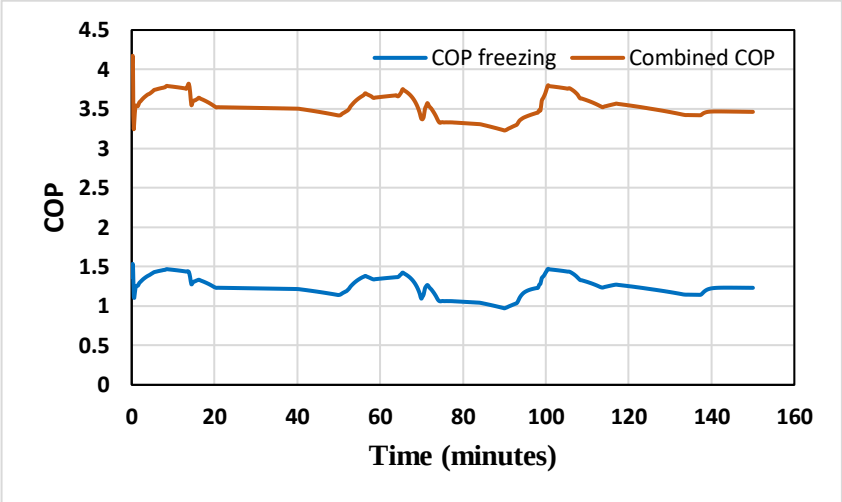

Figure 4: COP freezing and combined COP

3.2. Heat recovery

Heat recovery from the refrigeration system is shown in Fig. 5. The heat recovery values are the sum of both MT and gas cooler. The average heating demand for fish oil production is 261 kWh, and average heat recovery is 298 kWh. If thermal losses of 10 % are included, then the recovered energy is still enough for RRM processing. Integrated freezing and heating is a viable option for sustainable fishing. For RRM processing, MT, and gas cooler heat exchangers can act as a direct heating source or with a secondary glycol/water circuit However, the choice depends on the amount of RRM and hot water thermal storage.

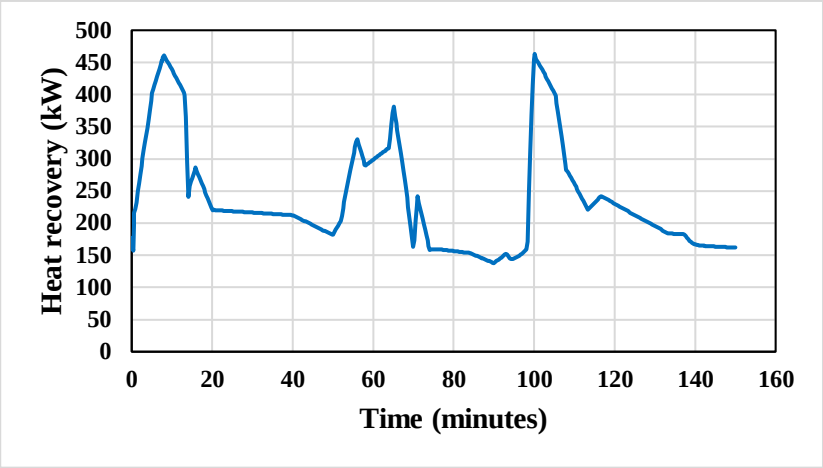

Figure 5: Total heat recovery of the refrigeration system

3.3. Thermal storage charging and discharging analysis

The pressure and temperature (3 bar and -68.3 °C) were maintained constant during the charging of thermal storage with a compressor. After 40 minutes of charging with a flow rate of 0.07 kg/s, the amount of solid CO_2 is 171 kg. For fully charged storage, the required time is 3.8 hours. The thermal storage charging with ejector shows a stable condition at 3.55 bar and -64.8 °C. The mass of dry ice at the end of the simulation is 116 kg, with a charging flow of 0.041 kg/s. The amount of dry ice is less in this case, which is mainly due to low-temperature difference (3.5 K) and lower charging flow.

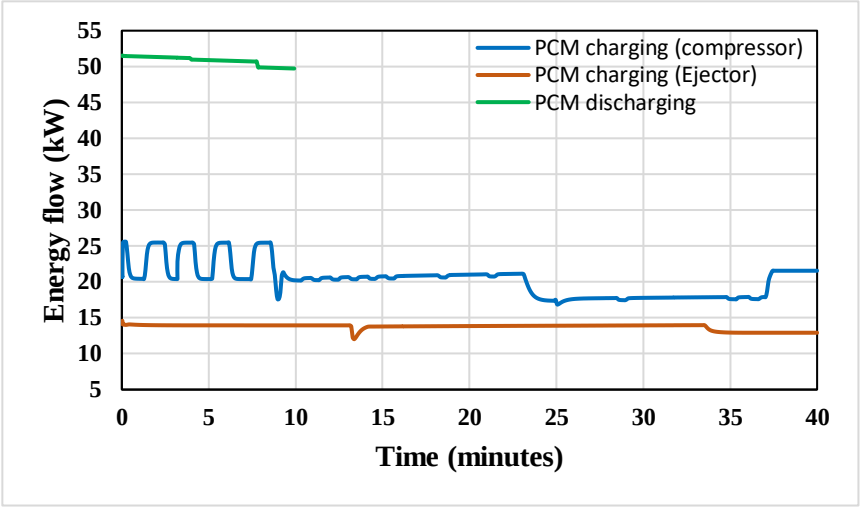

Figure 6: Thermal storage charging and discharging

The time required for fully charged storage with ejector is 5.6 hours under current conditions. In a simulation, the average power consumption of the compressor for charging is 2.9 kW to lift pressure from 3 bar to 6.8 bar. By using an ejector, this additional compressor power can be saved. Two-phase ejector implementation for such low-temperature conditions demands further investigation. However, simulation work shows good results.

The discharging of thermal storage was simulated with a constant super-heat of 8 K for 10 minutes according to the freezing load profile. The maximum discharging value is 51.4 kW. The total melting of dry ice in 10 minutes is 112 kg. The discharging rate of thermal storage is a combination of three factors, i.e., refrigerant flow, super-heat, and TES heat transfer area.

In the view of discharging results and iterative process, a thermal storage size of 0.3 m^3 (75 liters or 112 kg dry ice), including internal heat trasnfer area of 67 m^2 (54*54 tubes), is an ideal option for the reference system. By increasing the size of this small thermal storage, complete melting of dry ice can avoid, which will optimise the heat transfer area and number of tubes.

4. CONCLUSION

In this paper, an integrated freezing and heating refrigeration system was analyzed with low temperature CO_2 thermal storage. The simulations were performed with the dynamic simulation software Dymola with libraries from TIL. Results show an average COP increased by a factor of 2.8 for combined freezing and heating system, compared with only freezing. The average heat recovery from the refrigeration system is 298 kWh, which is in perfect match with the heating demand of 261 kWh for fish oil production by the thermal treatment process. CO_2 thermal storage exhibits promising results. An aluminium thermal storage of size 0.3 m^3 (75 liters), including an internal heat transfer area of 67 m^2 is an ideal option for the reference refrigeration system to cover peak loads. A 50 kWh stored energy reduces the peak time from 10 to 8 minutes. Each day corresponds to almost 28 peaks. The saved time in 24 hours is 56 minutes, which means an additional production capacity of equivalent 56 minutes in one day.

ACKNOWLEDGEMENTS

The authors gratefully acknowledge the Research Council of Norway for the financial support for carrying out the present research [NFR project No. 294662, CoolFish, and NFR project No. 257632, HighEFF].

REFERENCES

Carvajal, A., Slizyte, R., Storrø, I., Aursand, M., 2015. Production of high quality fish oil by thermal treatment and enzymatic protein hydrolysis from Norwegian spring spawning herring by-products. Journal of Aquatic and Food product Technology, 24, 807-823.

Dassault Systems, DYMOLA Systems Engineering, 2020. URL, https://www.3ds.com/products-services/catia/products/dymola/.

Hafner, A., Gabrielii, C. A., Widell, K. N., 2019. Refrigeration units in marine vessels. Alternatives to HCFCs and high GWP HFCs, Nordic council of ministers, Team nord.

Hafner, A., Nordtvedt, T. S., 2011. Energy saving potential in freezing applications by applying cold thermal energy storage with solid carbon dioxide. Procedia Food Science, 1, 448-454.

Niu, X. D., Yamaguchi, H., Iwamoto, Y., Nekså, P., 2011. Experimental study on a CO2 solid-gas-flow based ultra-low temperature cascade refrigeration system. International Journal of Low-Carbon Technologies, 6, 93-99.

TLK-Thermo GmbH, TIL suite Thermal Systems, 2020. URL, https://www.tlk-thermo.com/index.php/en/software/til-suite.

Valentas, K. J., Rotstein, E., Singh, R. P., 1997. Handbook of Food Engineering Practice. Taylor and Francis group. Boca Raton, New York, 106 p.

Ølsen, R.L., Toppe, J., Karunasagar, I., 2014. Challenges and realistic opportunities in the use of by-products from processing of fish and shellfish. Trends in Food science and Technology, 36, 144-151

PAPER ID: 292842
DOI: 10.18462/iir.iccc.2020.292842

Cryogenic cold utilization and system integration possibilities for LNG-driven fishing vessels

Muhammad Zahid SAEED[(a)], Kristina N. WIDELL[(b)], Armin HAFNER[(a)], Tom Ståle NORDTVEDT[(b)], Eirik Starheim SVENDSEN[(b)]

[(a)] Norwegian University of Science and Technology
Trondheim, 7491, Norway, muhammzs@stud.ntnu.no
[(b)] SINTEF Ocean
Trondheim, 7465, Norway, Kristina.Widell@sintef.no

ABSTRACT

Liquified natural gas (LNG) fuelled vessels are increasing in the fishing industry due to its reduced environmental footprint as compared to vessels using heavy hydrocarbon fuels. Cryogenic tanks are used to store LNG on ships, and the LNG vaporization can be done with different technology before used for engine fuel. The refrigeration system is essential to maintain the quality of fish. The operational power for the cooling system is produced by the engine. The challenge is to utilize the evaporation cold of the LNG efficiently, to reduce the overall energy consumption and to boost the cooling capacity. An objective of this paper is to describe different options for integration with the refrigeration system of the fishing vessel and to analyse their actual cold recovery potential from vaporizing LNG. Results show that for a 760 KW engine capacity coastal demersal trawler, 10.45 kW cold recovery is estimated under specified conditions.
Keywords: LNG Cold, Fishing Vessels, Cold Recovery, Chilling System, Refrigeration, Cryogenics, Thermal Storage.

1. INTRODUCTION

Fishing vessels are the most significant energy consumer, which holds them responsible for high emissions among the seafood product value chain (Jafarzadeh et al., 2017). In 2015, the fishing sector was responsible for 1.9 % of total Norway's emissions. Efforts are ongoing to reduce emissions and improve the overall energy efficiency to make the business more sustainable. Norway's ambition is to become a low emission society by 2050. Several steps are considered to achieve this. One effort is increased CO_2 tax (currently 508 NOK/tonnes) to incentivize businesses towards more sustainable solutions (Norwegian ministry of climate and environment, 2018). The European commission transport white paper (2011) set a target of 60 % lower carbon emissions by 2050 compared to 1990 and 70% compared to 2008 with the aim towards zero energy emissions (Sihvonen, 2018).

Transportation industry will require a change from mineral oil to electric batteries, hydrogen, or gas. Liquid natural gas (LNG) or gas use in the EU is encouraged by regulations, tax breaks, and subsidies (Sihvonen, 2018). LNG is gaining more attraction in the marine industry due to its high energy density, availability, and fewer emissions. LNG has a higher hydrogen-to-carbon ratio than diesel. LNG-fuelled ships emit 90 % less NO_x, 25 % less CO_2, and almost no SO_x as compared to heavy hydrocarbon fuels (Jafarzadeh et al., 2017).

LNG fuel is stored onboard in cryogenic tanks, and the storage pressure of LNG in the tank depends on the design of the system. The saturation temperature of LNG at 1 bar is -162 °C. The density of LNG is 450 kg/m^3 which is small in comparison to diesel density, which is 860 kg/m^3 (Jafarzadeh, 2017). Due to the high calorific value of LNG, the required mass flow rate of LNG is less than the diesel engine for the same power, which is an advantage for LNG. The density difference between LNG at 1 bar and compressed natural gas (CNG) at 200 bar is 275 kg/m^3, which means LNG fuelled vessel can travel 2.5 times more as compared to CNG vessel for the same volume of a fuel tank (Arteconi et al., 2019).

There is extensive research on different methods of vaporization at LNG regasification terminals, but a few data on onboard LNG regasification. Astolfi et al., (2017) studied the organic Rankine cycle (ORC) with various working fluids to enhance the effectiveness of LNG regasification terminals. Seawater used as a heat source and different condensing temperatures analysed for gasification. The expansion energy recovered from the ORC was converted to electricity. They summarized that this technology could be suitable for onshore

regasification terminals because specific energy consumption was less than other methods. Tan et al., (2010) examined the cold recovery from LNG refrigerated vehicles. Thermal storage investigated as an option to recover cold in the internally finned tube heat exchanger with LNG inside the tube and water as a phase change material outside the tube. Better results were found for internally finned tubes for thermal storage in comparison to a plain tube heat exchanger. Koo et al., (2019) studied the evaporation of LNG using ORC and its integration with the engine cooling system on ships. LNG gasification was done with heat energy from the condenser and cold energy from the evaporator utilized for the engine cooling circuit. High exergy efficiency and net power output were reported. Other literature on the cold recovery of LNG fishing vessels and its application for refrigeration system integration has not been found.

2. SYSTEM DESIGN

2.1. LNG on fishing vessels

LNG fuelled ships use dual-fuel engines that operate both on diesel and natural gas. Natural gas used as primary and diesel as a backup fuel. Dual fuel engines can be classified as low, medium, and high-pressure engines. Low-pressure engines operate at approximately 5-6 bar, medium pressure engines at 17 bar and high-pressure engines at 300 bar at the inlet fuel conditions to the engine (Jafarzadeh et al., 2017), (Koo et al., 2019).
A Norwegian coastal demersal trawler equipped with a 760 kW engine capacity is a study case. The inlet fuel conditions to the engine were set at 6 bar and 40 °C. LNG cold energy is dependent on the fuel consumption of the engine. The fuel consumption of the fishing vessel is not constant throughout the journey. It is different during fishing, towards the fishing ground and returns and the fuel consumption pattern is highly dependent on the fishing method and the type of vessel. Due to the variable fuel supply, cryogenic cold energy will also fluctuate. There can be many applications for the LNG cold, but for this paper, it is utilized for three separate options, sub-cooling of refrigerant in a refrigeration system, direct chilling of a fish tank and thermal energy storage. The 760 kW trawler was designed to use diesel as a fuel and the diesel consumption converted into LNG consumption by using characteristic values and equation. Yearly diesel consumption of this engine is 407,030 litres in 280 operational days. The round trip of one fishing journey was assumed six days. Two days each for moving towards the fishing ground, during fishing and return, with a total diesel consumption of 8.72 m^3 and estimated energy of 35.17 MWh by using Eq. (1). Specific fuel consumption of an 845 kW gas engine was used for LNG estimation due to its availability in the market. By using Eq. (1), LNG fuel consumption for 760 kW trawler in one trip is 15.55 m^3 (Jafarzadeh et al., 2017)

$$E = \frac{F * \rho}{Sfc} \text{ [kWh]} \qquad \text{Eq. (1)}$$

Where E, F, ρ, Sfc are energy, fuel consumption, density, and specific fuel consumption, respectively. The values used for calculation purpose are shown in Table 1.

Table 1. Characteristics values for calculation (Jafarzadeh et al., 2017)

Parameters	**Values**
Diesel engine power (kW)	760
Sfc diesel engine (g/kWh)	213.30
Diesel density (kg/m^3)	860
Gas engine power (kW)	845
Sfc gas engine (g/kWh)	198.99
LNG density (kg/m^3)	450

Based on the above calculations and data, the average mass flow rate in six days journey is 0.0135 kg/s or 0.0291 litres/s. For trawling vessels, the highest fuel consumption is during trawling (Gulbrandsen, 2012). It was assumed that during trawling fuel consumption is 30% higher than average (0.0176 kg/s and corresponding engine power 760 kW), 30% less than average when moving towards fishing (0.0095 kg/s and engine power 372 kW) and return fuel flow equal to average (0.0135 kg/s and engine power 532 kW). LNG fuel flow from

the cryogenic tank to the LNG vaporizer (cold box), and then to the engine can be done by using a pump before the cold box or by compressor after the cold box. Both cases are studied in the simulation software.

2.2. Refrigeration system

The natural refrigerant CO_2 was used as a working fluid in the refrigeration system. Refrigeration capacity is in the range of 170 kW to 250 kW with a total chilling tank volume of 300 m^3, the estimation was adapted from the interpolation of available data from Skipsteknisk (2003) and Nordtvedt et al. (2019). The performance of the refrigeration system is measured by the coefficient of performance (COP). COP is a ratio of evaporator output and compressor input and it is a unitless number.

2.3. Simulation model

A steady-state thermodynamic analysis of the LNG cold recovery was performed on Aspen HYSYS V10. Peng Robinson equations were used as a fluid package. For simplification, LNG was assumed as 100 % Methane at 3.5 bar and bubble point (-144.1 °C) in the LNG fuel tank. In the simulation, the fixed parameters were evaporation and condensation temperature -6 °C and 20 °C, respectively, compressor adiabatic efficiency 0.75 for both compressors, pump adiabatic efficiency 0.75, the temperature difference in the heat exchangers 5 K and the outlet temperature of methane from sub-cooler -6 °C. When a pump used to drive fuel, then the vaporization pressure of the methane in the sub-cooler was fixed to 6 bar, and 3.5 bar in the compressor case. The compressor increases both pressure and temperature. If the system is using a pump, then heating of fuel is necessary after the sub-cooler to meet the inlet fuel conditions of the engine. The flow diagram of the complete system is shown in Fig. 1.

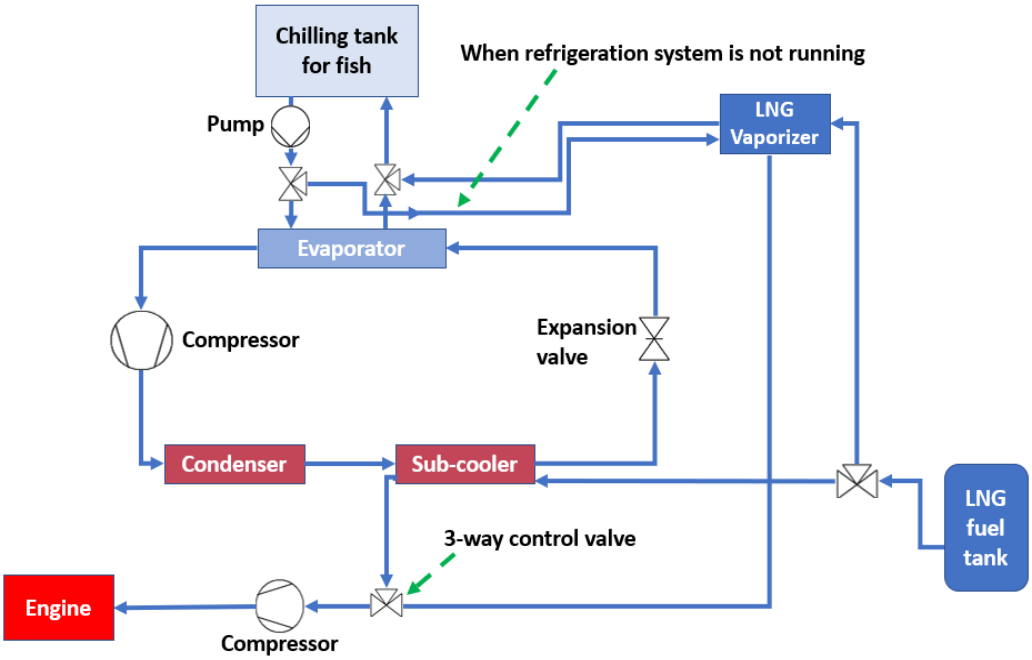

Figure 1: System layout

3. DIFFERENT OPERATING MODES/SCENARIOS

3.1. Sub-cooling of refrigerant

In the refrigeration system, sub-cooling of the refrigerant after condenser increases the volumetric refrigeration capacity. High refrigeration capacity with the same amount of work by compressor results in high COP. A shell and tube heat exchanger (HX) was used as a sub-cooler in the refrigeration system with methane inside

the tube and refrigerant on the shell side. The inlet temperature of the refrigerant to the LNG HX was fixed to 20 °C and liquid phase. Sub-cooling of refrigerant in LNG HX after condenser is analysed in this scenario.

3.2. Direct chilling of fish tank

Direct chilling of the fish tank with LNG cold is an option when the fish tank has a minimal load (only thermal losses). The simulation for direct chilling was also performed in the shell and tube heat HX with methane inside the tube and water on the shell side. It was assumed that inlet water temperature in the HX is 2 °C, with no freezing of water at -1 °C due to the utilization of seawater in the fish tank. The flow rate of the seawater circuit was estimated with constant C_p and constant temperature difference of 3 °C in the heat exchanger.

3.3. Thermal storage

Cooling demand in the fishing vessels varies with time and need. Thermal storage with LNG cold is a suitable option when the refrigeration system is not running, or the chilling tank has no load. A water-based (eutectic) phase change material (PCM) with a phase change temperature of -6 °C was used for analysis. The PCM properties were density 1110 kg/m^3, specific heat capacity 3.83 kJ/kg.K, and latent heat 300 kJ/kg (PCM products, 2018). The initial temperature of the water was assumed at an ambient temperature of 15 °C. Thermal storage of three sizes 0.5 m^3 (58.65 kWh), 1 m^3 (117.30 kWh), and 1.5 m^3 (175.95 kWh) were analysed with LNG cold potential without thermal losses of a storage tank.

3.4. Cold recovery potential at different fuel tank pressures

The storage pressure of fuel in the LNG tank is important for cold recovery potential. High pressure in the tank elevates the bubble point. Cold recovery potential at different LNG pressure is also studied and the corresponding results are presented in section 4.

4. RESULTS AND DISCUSSION

Cold recovery potential from the simulation results both with compressor and pump is presented in Table 2. The required power for fuel flow by a pump is less as compared to the compressor but it should be noted that compressor is mature technology than a cryogenic pump. An additional heat exchanger is also required after sub-cooler in case of a pump to meet the inlet fuel temperature of the engine.

Table 2: Cold recovery potential from simulation results

Trawler mode	Fuel flow (kg/s)	Engine power (kW)	Cold Recovery with pump flow (kW)	Cold recovery with compressor flow (kW)	Pump power (kW)	Compressor power (kW)
Towards fishing	0.0095 (m_1)	372	7.3	7.4	0.008	0.99
Return	0.0135 (m_2)	532	10.4	10.45	0.011	1.42
During fishing	0.0176 (m_3)	760	13.55	13.63	0.015	1.85

The simulation results show an increment in COP of the refrigeration system, with LNG cold recovery in the sub-cooler at a refrigeration load of 173 kW. The highest COP is observed at the maximum LNG cold recovery, which is 5.22 at full capacity (760 kW) of the engine. Fig. 2a shows this relation.
The sub-cooling effect with LNG cold is very high at low loads. At small refrigerant loads, the refrigerant mass flow is low, which leads to a significant temperature difference in the sub-cooler at maximum LNG cold recovery. At the maximum refrigeration load, the sub-cooling effect is minor but still contributes to increased COP as compared to a system without sub-cooler. Fig. 2b shows the temperature difference between in and out of the sub-cooler with the three LNG fuel flow conditions.

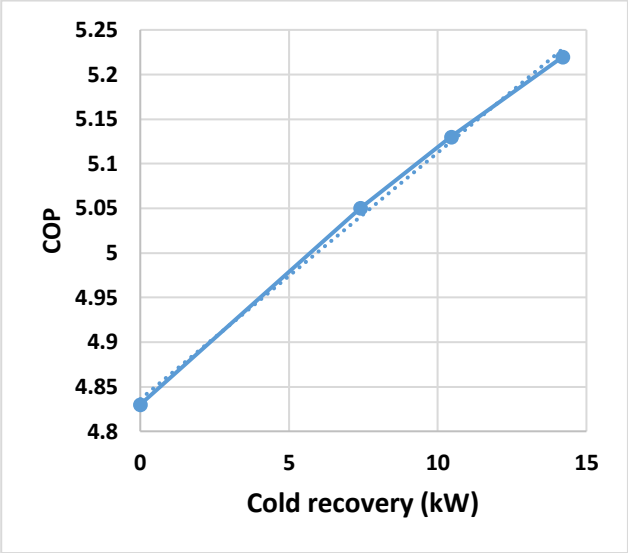

Figure 2a: LNG cold recovery versus COP

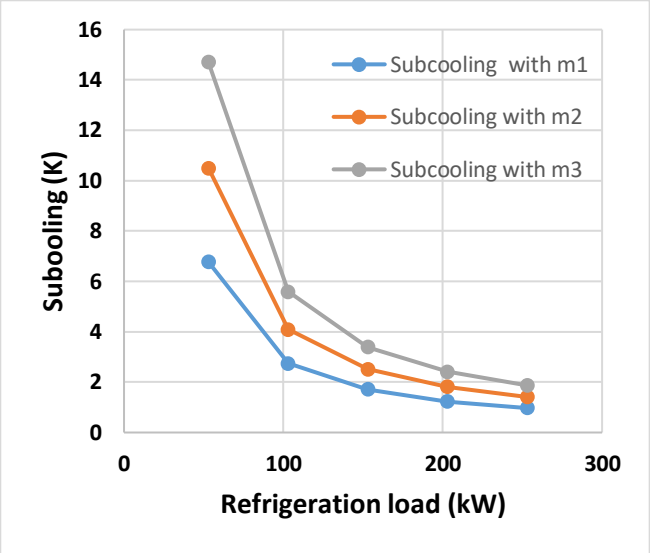

Figure 2b: Refrigeration load versus sub-cooling

Direct chilling of fish tank with LNG cold shows a small temperature gradient in the HX. The temperature difference in the LNG HX for fish tank water is dependent on the flow rate of water (load dependence), which is high in the case of water due to the involvement of only sensible heat. However, the temperature difference of refrigerant in the LNG sub-cooler is high due to small refrigerant flow in the refrigeration system.

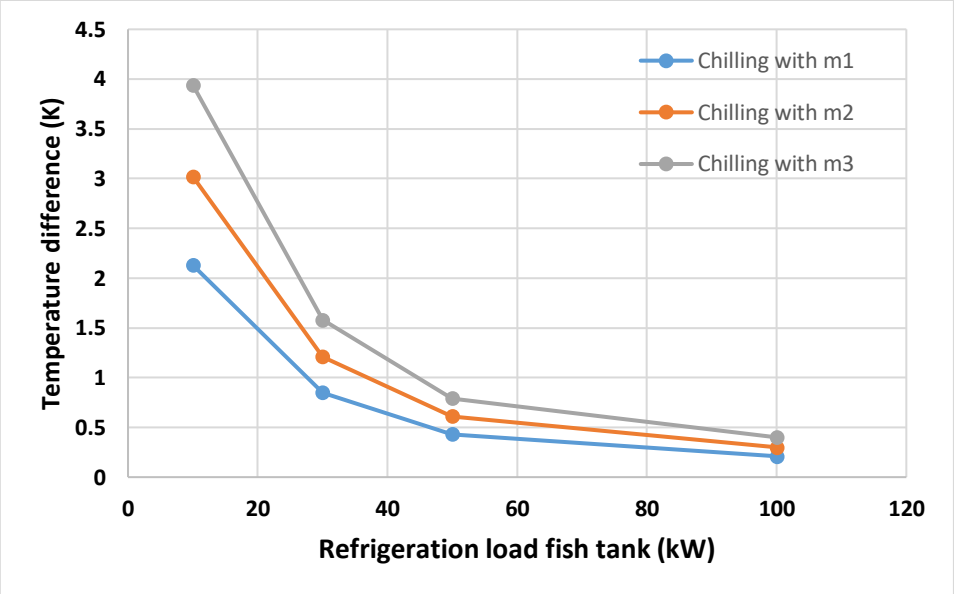

Figure 3: Water chilling at different loads in LNG heat exchanger

Direct chilling with LNG cold was studied at different refrigeration loads. At higher loads, it is not possible to attain a water temperature of -1 °C after LNG HX but the option looks suitable for low loads. The chilling water temperature difference between in and out of the heat exchanger with their corresponding LNG cold recovery is visualized in Fig. 3.

Thermal energy storage is an interesting feature that can increase system performance by assisting the refrigeration system at peak demands. The available storage energy is an offset between refrigeration demand and available LNG cold. The size of the thermal storage tank is a balance between the available cold energy, free space, and refrigeration load profile of the vessel. The shortest time to store energy is observed with 13.63 kW at m_3 (fuel flow) and the highest time with 7.4 kW. If thermal losses are considered, the required cooling time will increase. The results are shown in Fig. 4.

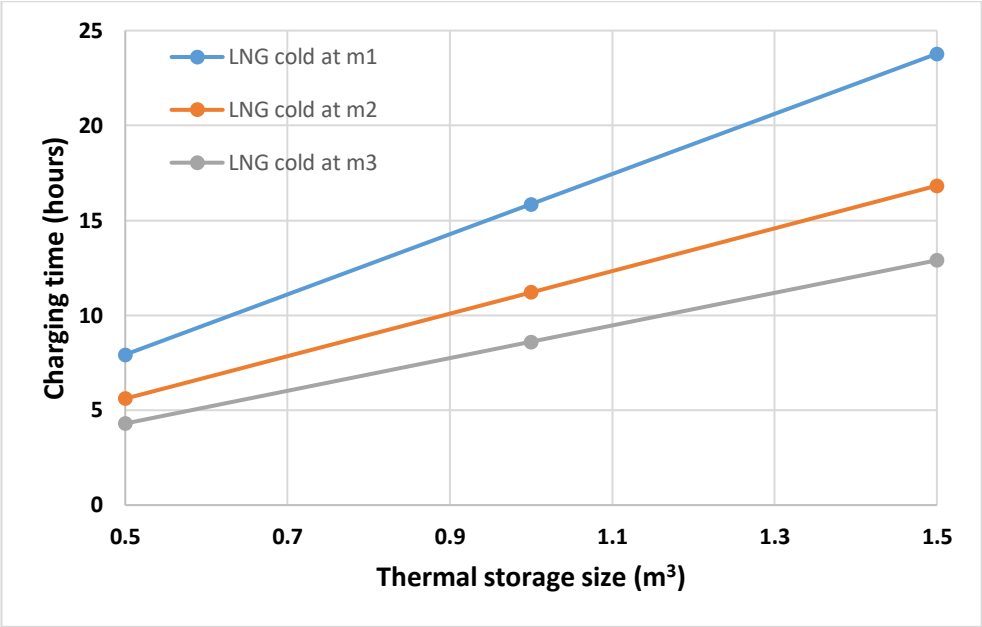

Figure 4: Storage size versus required charging time with LNG cold

The increased pressure in the LNG tank shows a reduction in the cold recovery potential. This is due to the high boiling temperature of methane at high pressures. High pressure also leads to a decrease in the density of fuel, which means less fuel in the same volume of the storage tank. Less amount of fuel can create issues for long journey fishing vessels. On the other hand, the high pressure of fuel can assist the medium or high-pressure engines by reducing the pressure lift in the pump or compressor. The cold recovery potential at different pressure levels in the tank is more visible at the maximum flow rate (m_3) of fuel, but the effect is small at a low flow rate (m_1). This is shown in Fig. 5.

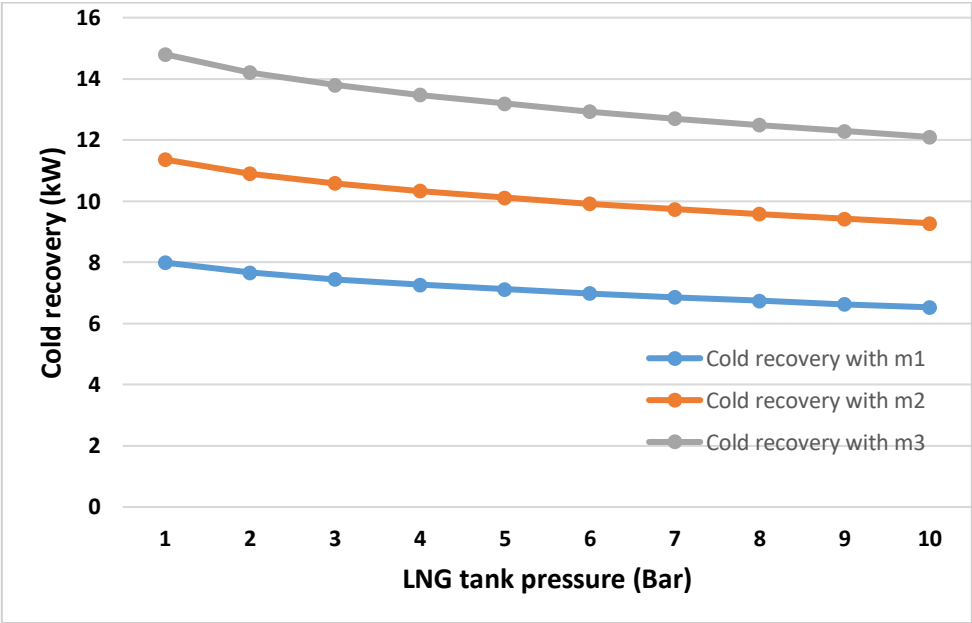

Figure 5: LNG tank pressure versus cold recovery potential

The compactness and robustness of the systems are very important on the fishing vessels. Each m^3 of space onboard costs a lot. Either it's the installation of LNG vaporizer, thermal storage tank, and LNG fuel tank, it should be a competitive choice in terms of size, investment, and sustainability. The life cycle and economic assessment are necessary before implementing any solution.

4.1. Future work

The cold recovery potential is sensitive to the fuel consumption of the engine, and the fuel consumption pattern is a dynamic factor. A small change during the trip leads to alter the fuel supply. More detailed data is a need for full dynamics. The fuel flow varies a lot for different fishing vessels and fishing methods, which makes it difficult to generalize the technology.
LNG heat exchanger or LNG vaporizer is very important to design smartly. Refrigerant load and fuel supply to the engine are independent parameters. LNG superheat in the heat exchanger is difficult to control due to its independent behaviour. It is recommended to use a secondary circuit between the LNG cold box and the cold recovery application for better monitoring and safety of the system.
There is a potential to extend this work with another case study to the onboard processing of fish, mainly big trawlers. Onboard processing includes filleting and freezing of fish. Waste material (small pieces and bones) from fish filleting demands further processing to produce fish oil, fish meal, and other nutritional products. This waste material processing requires a lot of heat energy. Heat recovery from the flue gases of the engine, desuperheater of the refrigeration system and their integration with other arrangements can make the fishing vessels more sustainable, climate-friendly, and energy-efficient.

5. CONCLUSIONS

In this paper, an innovative approach for LNG cold recovery potential on a fishing vessel was carried out on the software Aspen HYSYS V10. As a first application, LNG cold was utilized for the sub-cooling of the refrigerant in the CO_2 refrigeration system. Results show an increment of COP by 8 % at maximum and 4.5 % at minimum cold recovery potential at a constant refrigeration load of 173 kW. Other potential applications, direct chilling of a fish tank, and thermal storage with LNG cold were also analysed. For the direct chilling of a fish tank, a small temperature difference in the heat exchanger was observed for chilling water. The results predict that the option is viable for small refrigeration loads. It is perceived that the size of thermal storage relies on the available LNG cold and the length of a fishing journey. Optimum design pressure of fuel in the LNG tank can save the space on the vessel and capital investment. Dynamic simulations of the complete fishing trip are requisite for precise prediction of LNG cold applications.

ACKNOWLEDGEMENTS

The authors gratefully acknowledge the Research Council of Norway for the financial support for carrying out the present research [NFR project No. 294662, CoolFish and NFR project No. 257632, HighEFF].

REFERENCES

Jafarzadeh, S., Paltrinieri, N., Utne I. B., Ellingsen, H., 2017. LNG-fuelled fishing vessels. A systems engineering approach, Transportation Research Part D 50, 202–222.

Norwegian Ministry of climate and environment, 2018. Norway's seventh national communication under the framework convention on climate change. https://www.regjeringen.no/contentassets/52d65a62e2474bafa21f4476380cffda/t-1563e.pdf.

Sihvonen, J., 2018. CNG and LNG for vehicles and ships- the facts, a study by transport and environment. https://www.transportenvironment.org

Astolfi, M., Fantolini, A. M., Valenti, G., De Rinaldis, S., Inglese, L. D., Macchi, E., 2017. Cryogenic ORC to enhance the Efficiency of LNG regasification Terminals. Energy Procedia 129, 42–49.

Tan, H., Li, Y., Tuo, H., Zhou, M., Tian, B., 2010. Experimental study on liquid/solid phase change for cold energy storage of Liquefied Natural Gas (LNG) refrigerated vehicle, Energy, 35, 1927-1935.

Koo, J., Oh, S. R., Choi, Y. U., Jung, J. H., Park, K., 2019. Optimization of an organic Rankine cycle system for an LNG-powered ship. Energies 12 (10), 1933.

Gulbrandsen, O., 2012. Fuel saving for small fishing vessels. A manual. Rome. http://www.fao.org/3/i2461e/i2461e.pdf

Pelagic trawler, charisma, Skipsteknisk 2003. https://www.skipsteknisk.no/product_sheet.aspx?type=4&menu=29&id=229.

Nordtvedt, T. S., Widell, K. N., 2019. Chilling of pelagic fish onboard Norwegian fishing vessels. The 25th IIR international congress of refrigeration, Montreal, Canada, ICR/IIR, 2924-2931.

PlusICE range- Phase Change Materials, 2018. PCM products LTD. http://www.pcmproducts.net/files/E%20range-2018.pdf.

Arteconi, A., Fiaschi, D., Cioccolanti, L., Bartolini, C. M., Polonara, F., 2019. Liquefied natural gas cold recovery for heavy-duty vehicles smart management. The 25th IIR international congress of refrigeration, Montreal, Canada, ICR/IIR, 415-421.

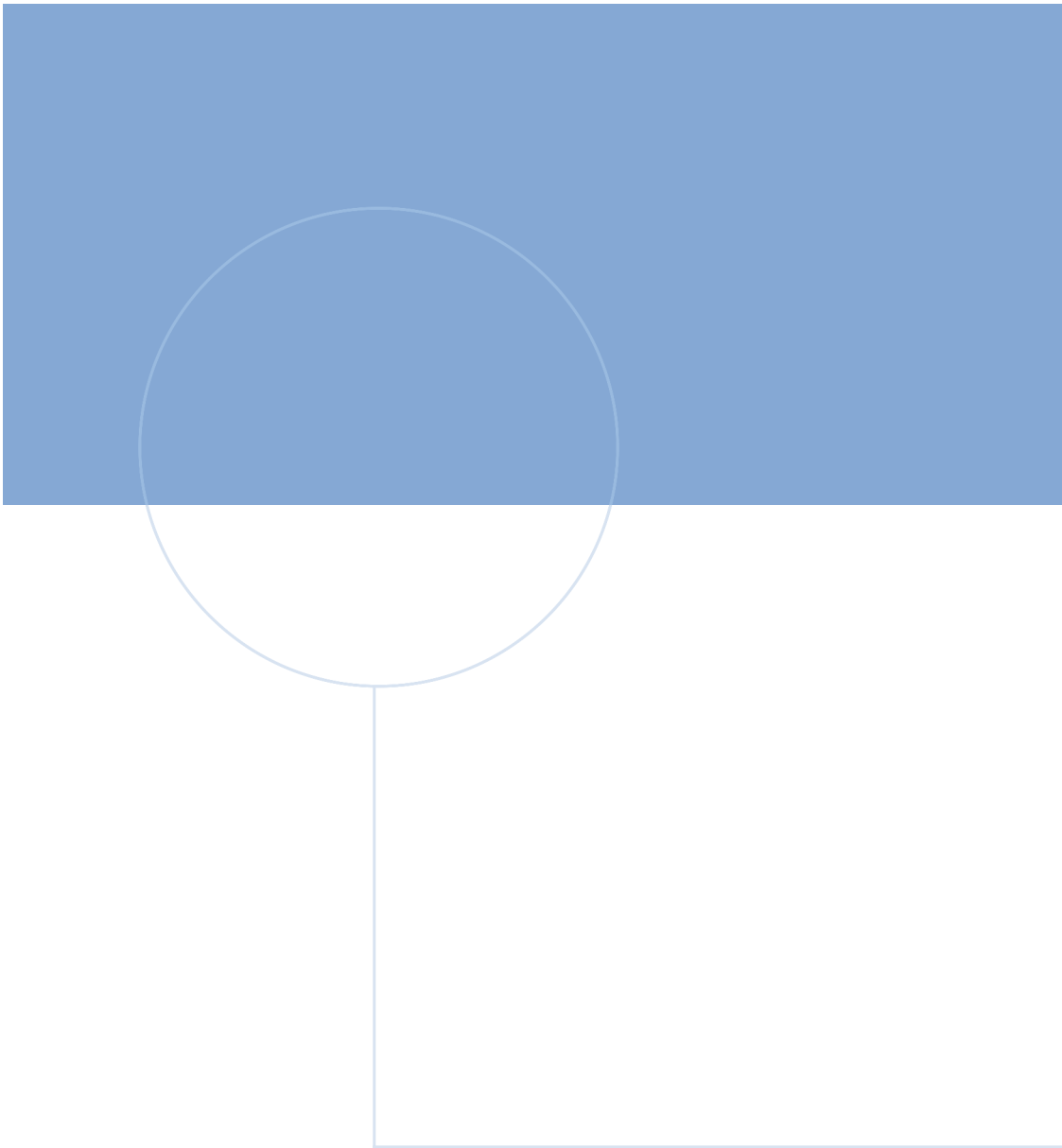

NTNU

Kunnskap for en bedre verden